

Cassini Ultraviolet Imaging Spectrograph
UVIS HSP

Ring Stellar Occultation Atlas

Volume 8: Rev 246 – Rev 288

Version: 1.3
May 31, 2018

Table of Contents

The table lists all occultations in this volume, including the star name, rev number, indication of ingress (I) or egress (E), date of the occultation, duration of the occultation, radial range coverage and elevation angle of the star.

Occultations are presented chronologically in the order they were observed. To keep the file size of this atlas manageable, it is presented in multiple volumes, each one covering a subset of the occultations.

Introduction

Over the course of the Cassini mission, the High Speed Photometer (HSP) of the Ultraviolet Imaging Spectrograph (UVIS) observed 170 occultations of stars by Saturn's rings. Details on the UVIS instrument can be found in Esposito et al. (1998, 2004). Information on the handling of HSP ring occultation data as well as a summary of data calibration and reduction techniques for the first part of the Cassini mission are in Colwell et al. (2010). This document provides a tabular and visual overview of these stellar occultations.

Description of Data Products in the Atlas

The HSP data consist of a time series of measured photon counts. With the exception of observations of some faint stars where the background signal dominates or is a significant contribution, the measured signal is primarily due to starlight transmitted through the rings. The HSP integration times are 1, 2, 4, or 8 msec. The majority of occultations used a 1 msec integration period, with most of the rest at 2 msec. In this atlas the data are binned to 1 second.

The data are shown in two plots: (1) a plot spanning the range of 70,000 km to 150,000 km from Saturn for all occultations to allow direct comparison of signal and coverage on a single distance scale; and (2) a plot that shows the data zoomed to the radial range of coverage of the occultation.

Two additional geometry plots are included for each occultation: (1) the radial ring plane resolution of the occultation (in the frame of Saturn, not accounting for ring particle motion or diffraction); and (2) the value of ϕ , an angle measured in the ring plane in the counterclockwise sense from the outward radial vector at the measurement point to the direction to the star projected into the ring plane. Thus, an observation where the look vector to the star is tangent to the rings has $\phi=90$ degrees.

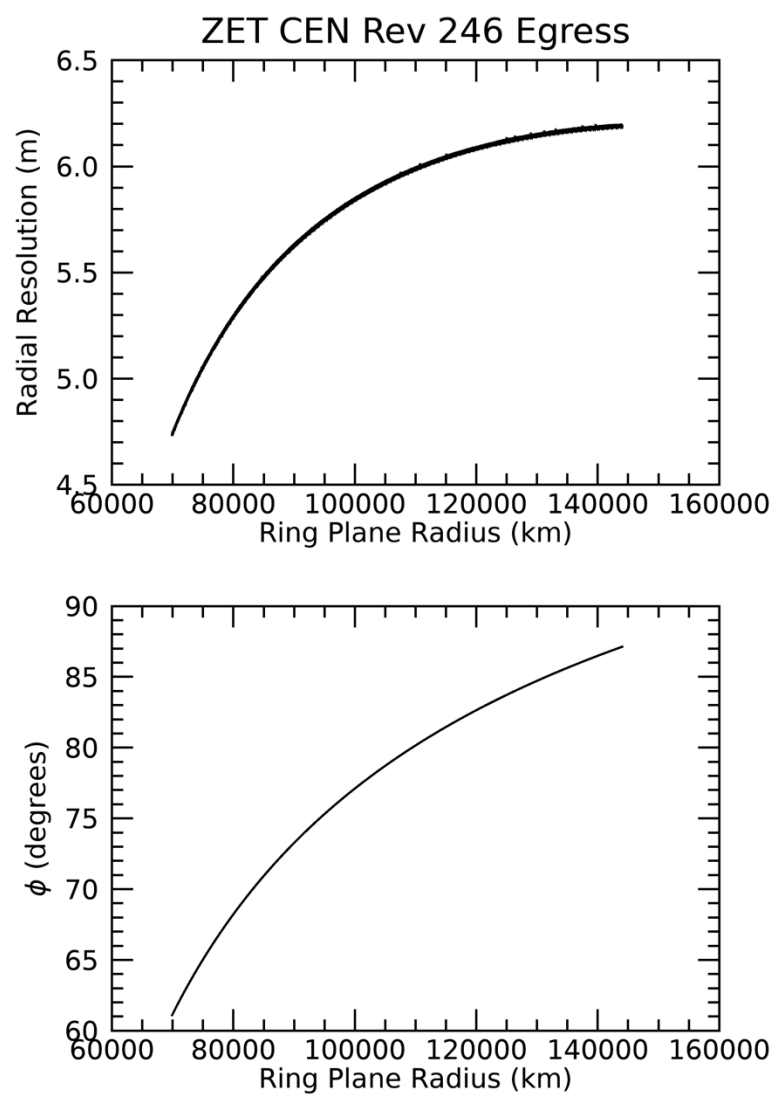
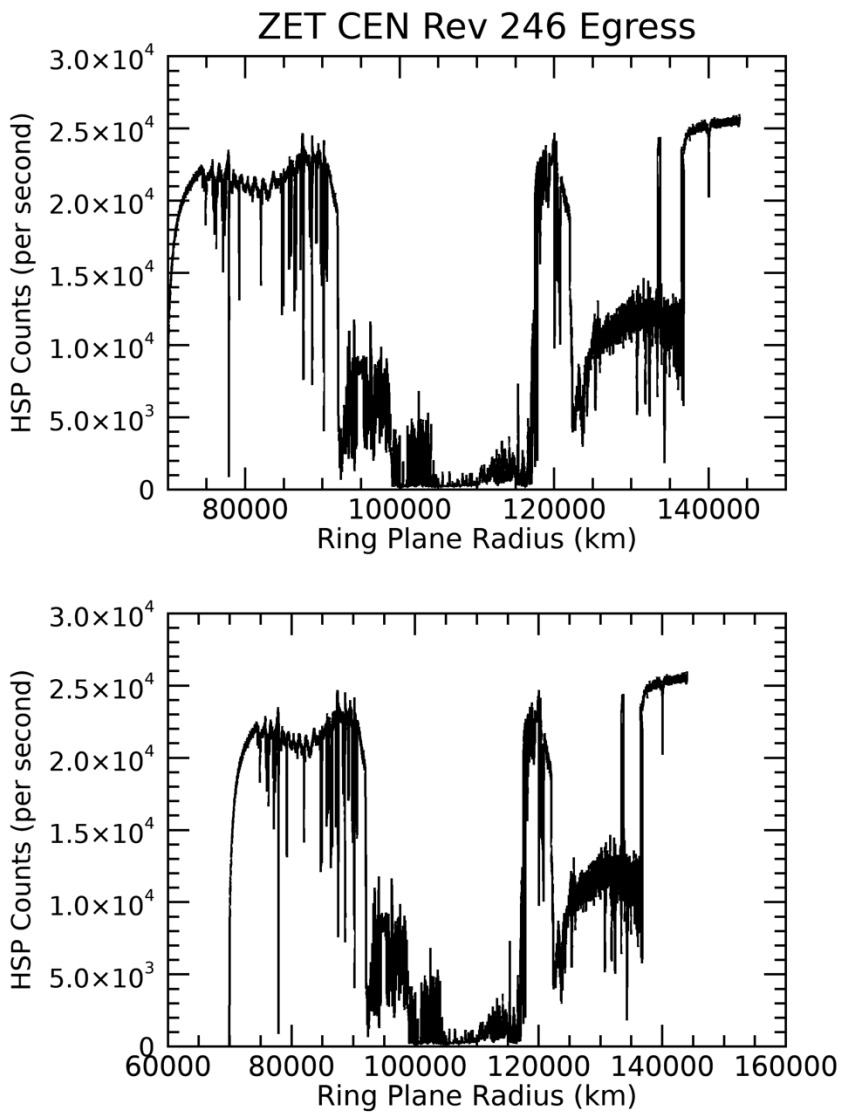
On the page following the data plots, a geometry visualization is shown at a time near the middle of the occultation. The position of the UVIS HSP field of view is labeled on each of these plots. Occultations that cut a chord across the rings, are presented here as separate "Ingress" and "Egress" occultations, referring to the portion of the occultation where the observation point is approaching or receding from Saturn, respectively. Some geometry visualizations are missing and will be included in the next revision of this volume.

Document assembled by Joshua Colwell, UVIS Co-Investigator, University of Central Florida, with the assistance of Stephanie Eckert Grant, Richard Jerousek, and Tina Notrika, UCF.

References

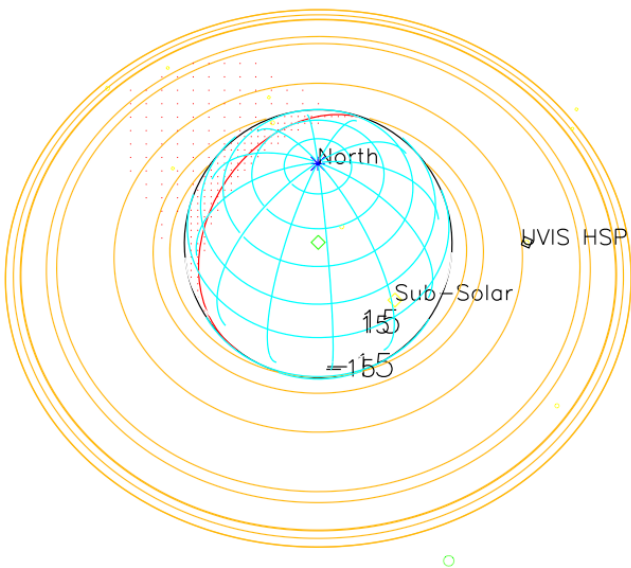
1. Colwell, J. E., L. W. Esposito, D. Pettis, M. Sremčević, R. G. Jerousek, E. T. Bradley 2010. Cassini UVIS Stellar Occultation Observations of Saturn's Rings. *Astron. J.* **140**, 1569-1578, doi:10.1088/0004-6256/140/6/1569.
2. Esposito, L. W., J. E. Colwell, and W. E. McClintock 1998. Cassini UVIS Observations of Saturn's Rings. *Planet. Space Sci.* **46**, 1221-1235.
3. Esposito, L. W., C. A. Barth, J. E. Colwell, G. M. Lawrence, W. E. McClintock, A. I. F. Stewart, H. U. Keller, , A. Korth, H. Lauche, M. Festou, A. L. Lane, C. J. Hansen, J. N. Maki, R. A. West, H. Jahn, R. Reulke, K. Warlich, D. E. Shemansky, and Y. L. Yung 2004. The Cassini Ultraviolet Imaging Spectrograph Investigation. *Space Sci. Rev.* **115**, 299-361.

Star		Rev	Ing/Eg	Year/Day	B	Φ	Radius	Duration (min)
ζ	CEN	246	E	2016-296	53.6	61.1- 87.1	69910-144020	213.7
ε	SGR	247	E	2016-306	37.9	247.5-209.2	131510-165889	108.3
ε	SGR	247	I	2016-306	37.9	271.1-247.5	143101-131510	60.2
κ	SCO	247	E	2016-306	43.4	241.7-228.0	108397-111491	33.4
κ	SCO	247	I	2016-306	43.4	284.0-241.7	145116-108397	123.8
α	LUP	248	E	2016-315	53.9	108.0-113.1	72487-146613	165.2
λ	SCO	248	E	2016-315	41.7	241.9-219.1	87541- 94808	45.3
λ	SCO	248	I	2016-315	41.7	295.8-241.9	146529- 87541	146.8
β	CRU	253	I	2016-353	65.2	257.0-253.0	142423- 75438	120
α	PAV	254	I	2016-360	56.6	300.8-273.8	146924-121523	55.5
β	CRU	262	I	2017-052	65.2	258.9-253.9	147992- 68616	140.3
η	CMA	265	I	2017-072	27	135.4-108.7	137822-113583	173
β	CRU	267	I	2017-087	65.2	257.6-256.4	90601- 76140	25
α	CMA	272	E	2017-120	13.5	95.0- 49.7	101028-143371	235.7
α	CMA	272	I	2017-120	13.5	141.1- 95.0	145340-101028	242
α	CMA	274	E	2017-133	13.5	72.5- 30.0	67816-151660	259.7
ε	CMA	276	E	2017-147	26	96.9- 38.4	78383-146397	348.8
ε	CMA	276	I	2017-147	26	98.7- 96.9	78418- 78383	6.5
γ	ORI	276	E	2017-149	-11.2	81.6-144.8	67895-149909	192.8
γ	ORI	276	I	2017-149	-11.2	77.8- 81.6	68048- 67895	6.6
ε	ORI	277	E	2017-156	-3.5	87.5-133.5	110402-158694	67.4
ε	ORI	277	I	2017-156	-3.5	41.4- 87.5	159146-110402	67.8
ζ	ORI	277	E	2017-156	-2.7	88.2-133.2	100633-142173	46.3
ζ	ORI	277	I	2017-156	-2.7	35.5- 88.2	165925-100633	60.9
κ	ORI	279	E	2017-171	5.2	92.8- 56.6	135211-167521	99.8
κ	ORI	279	I	2017-171	5.2	129.9- 92.8	169592-135211	103.3
κ	ORI	280	E	2017-177	5.2	92.8- 51.7	113448-150437	99.7
κ	ORI	280	I	2017-177	5.2	133.5- 92.8	149618-113448	98.5
α	CMA	281	E	2017-178	13.5	278.8-340.5	72322-151777	319.1
α	CMA	281	I	2017-178	13.5	218.3-278.8	146547- 72322	304.6
κ	ORI	281	E	2017-184	5.2	92.8- 39.2	91253-153745	125
κ	ORI	281	I	2017-184	5.2	146.6- 92.8	154310- 91253	125.7
α	CMA	282	E	2017-185	13.5	279.2-331.6	92210-150458	285.6
α	CMA	282	I	2017-185	13.5	228.6-279.2	145050- 92210	268.8
κ	CMA	282	E	2017-186	29.3	68.0- 35.3	66132-126671	221.7
κ	CMA	283	E	2017-193	29.3	51.0- 37.3	71928-103079	104.2
β	ORI	288	E	2017-228	3.1	91.8- 31.7	80553-161530	84.1
β	ORI	288	I	2017-228	3.1	152.5- 91.8	164278- 80553	86
δ	ORI	288	E	2017-227	-4.5	268.4-214.9	93906-158115	91
δ	ORI	288	I	2017-227	-4.5	321.8-268.4	157199- 93906	90.2



.TETHYS

.MIMAS



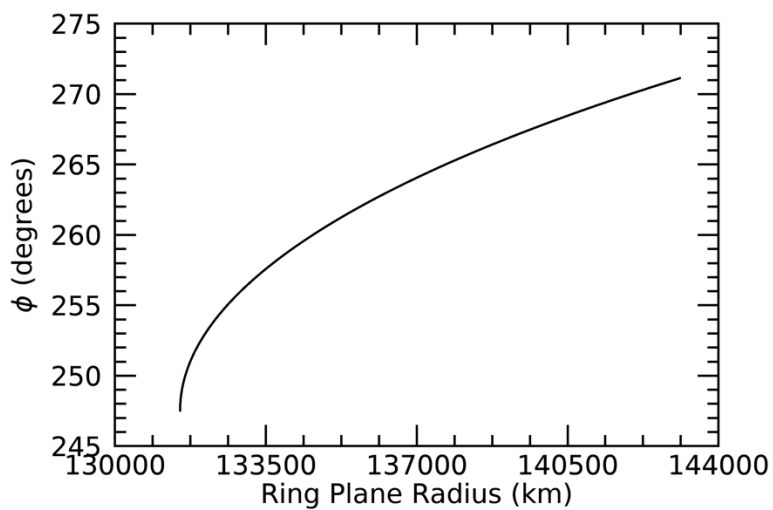
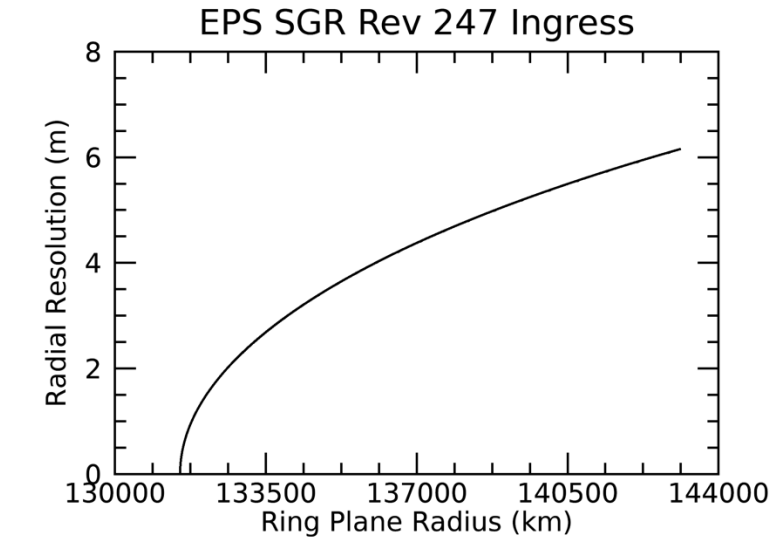
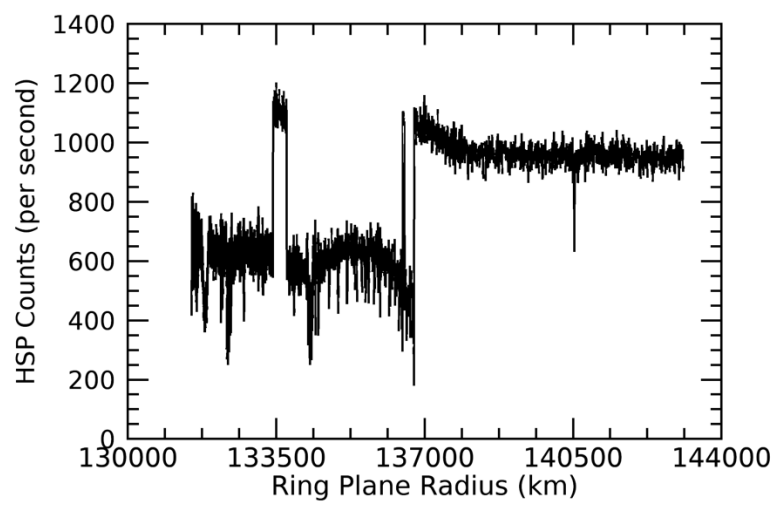
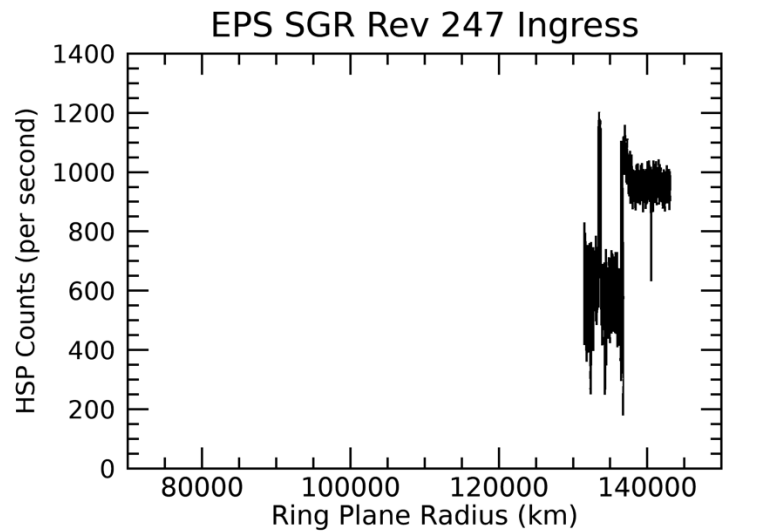
2016-296T08:53:00.000 607098.37 km

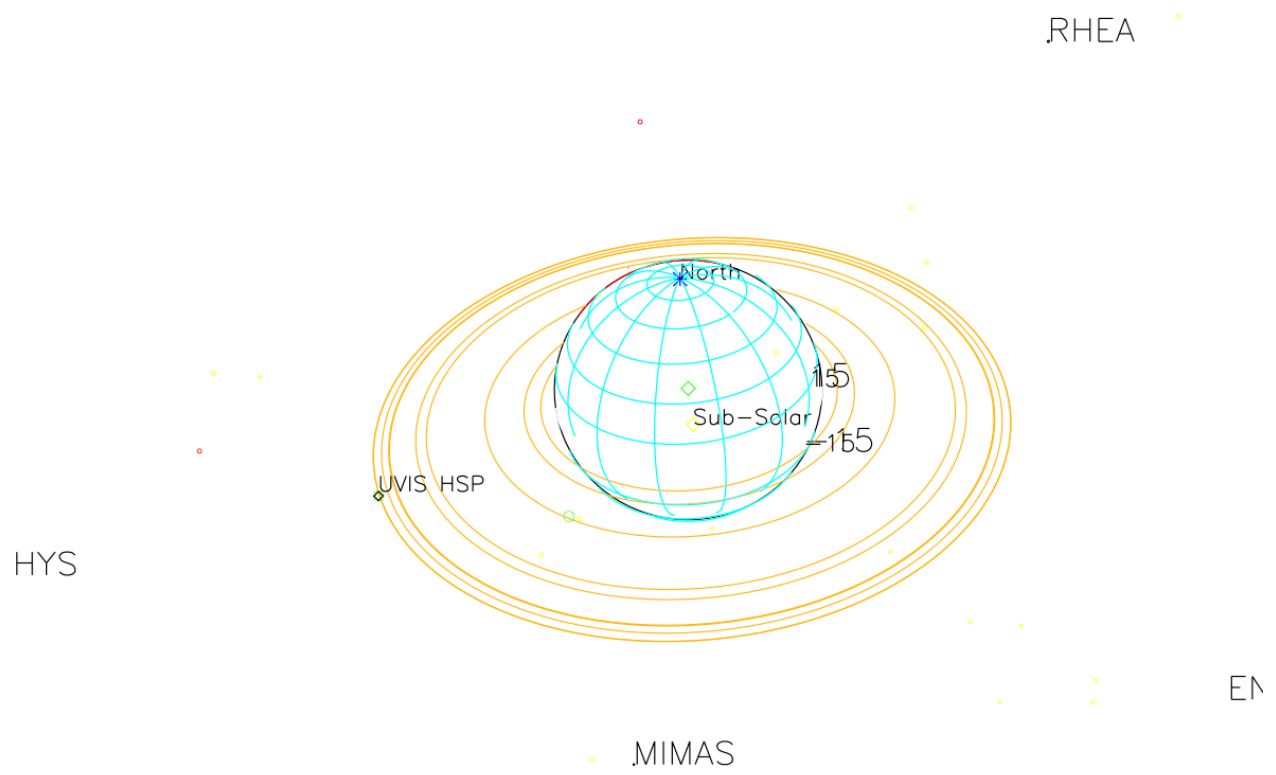
Target RA/dec: 221.97, -48.04

Subsolar lat/lon: 22.12, -90.68

Sub-s/c lat/lon: 49.32, -126.40

ENCELADUS



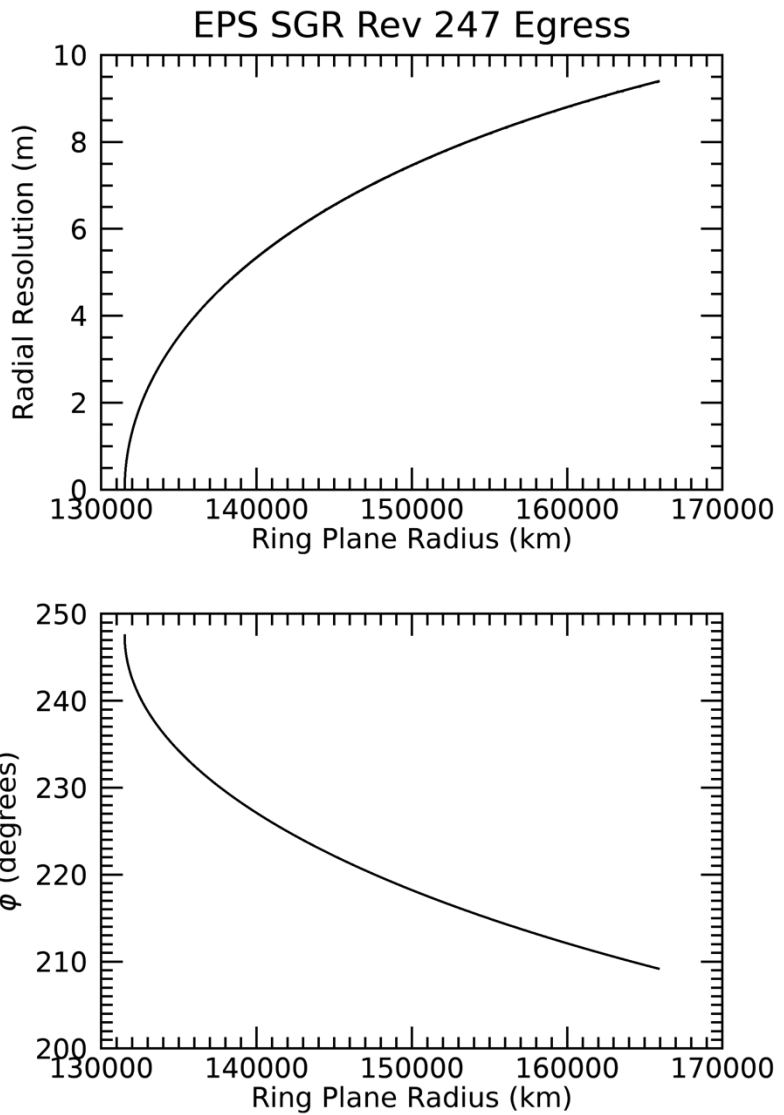
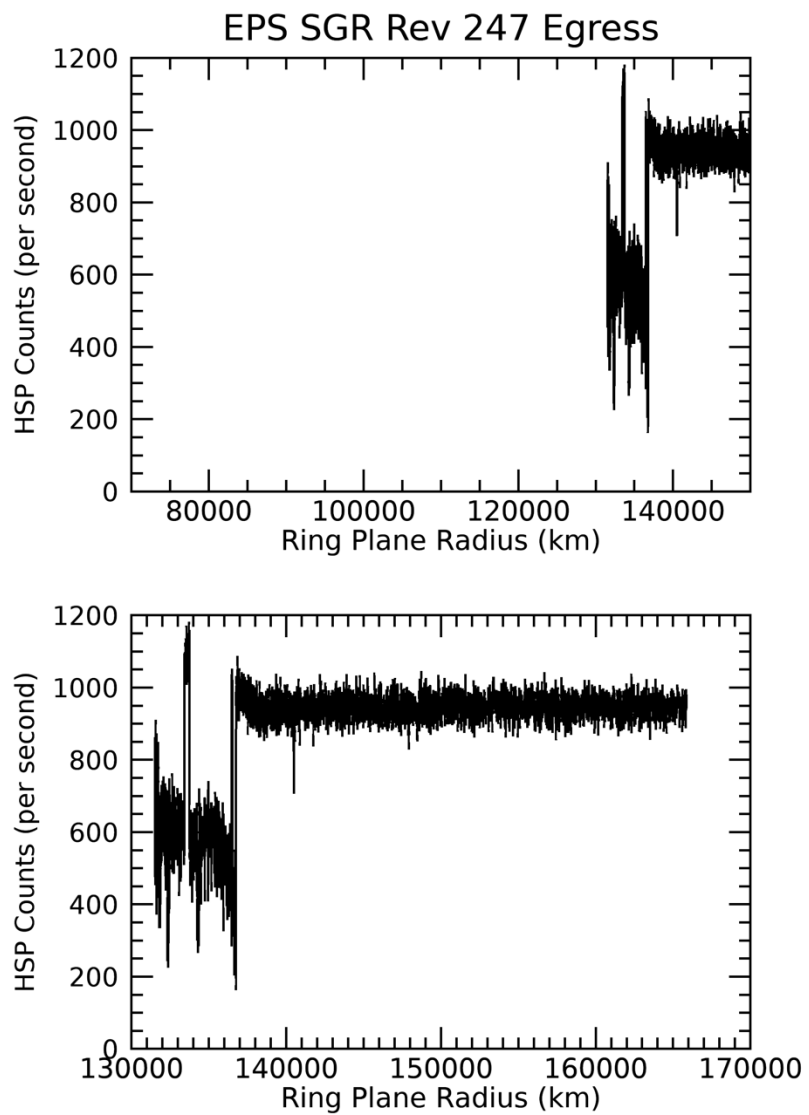


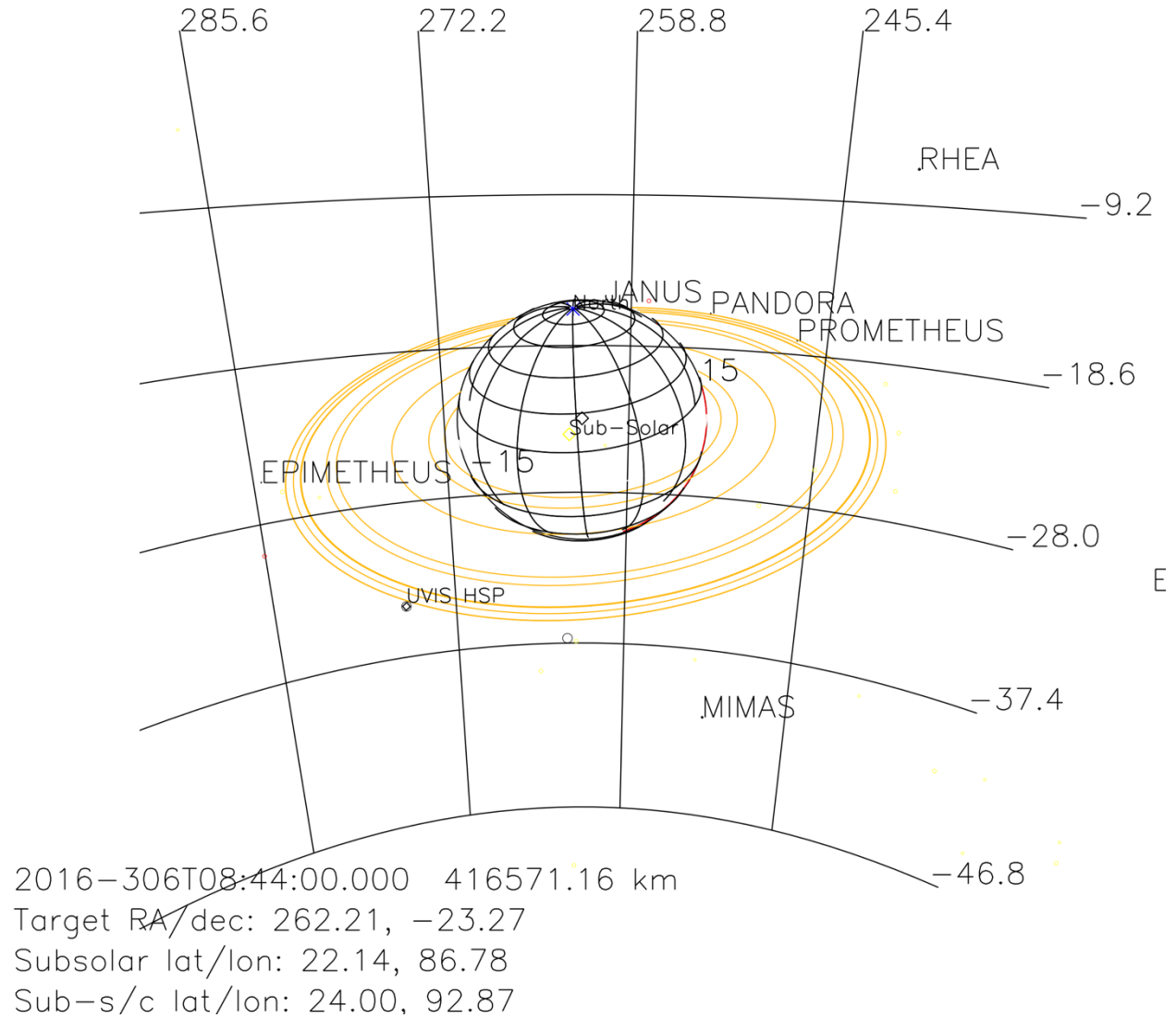
2016-306T07:14:00.000 445956.71 km

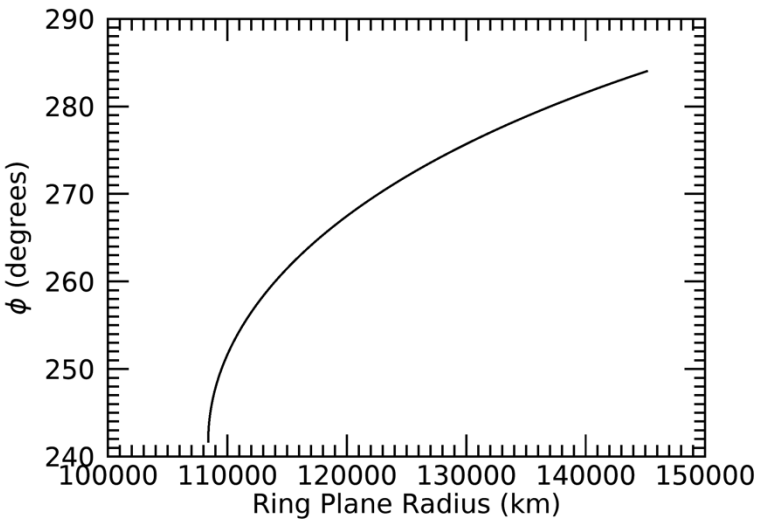
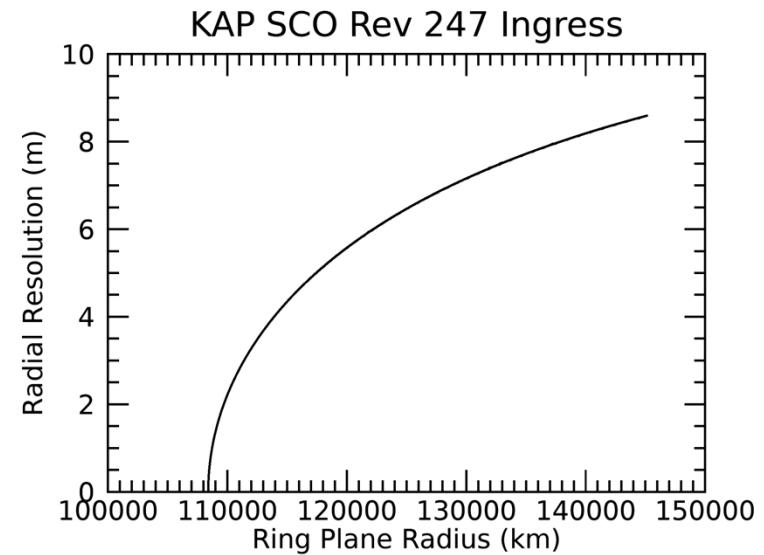
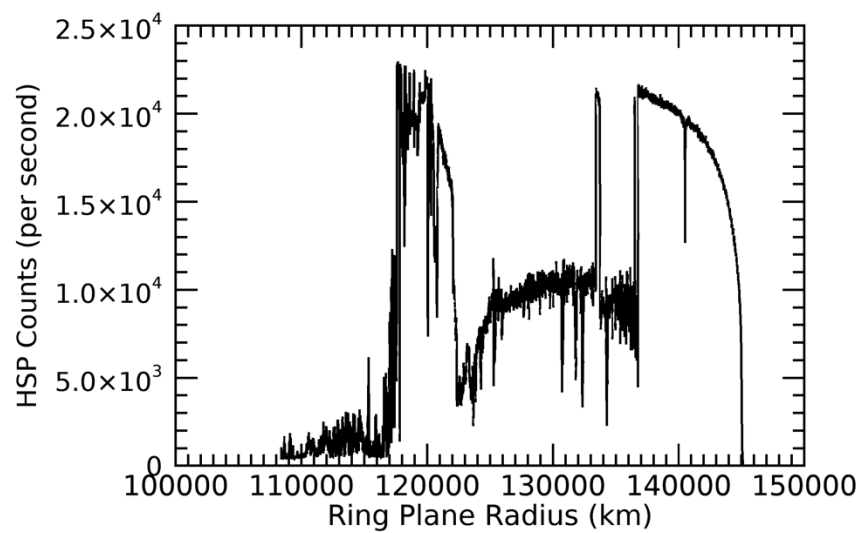
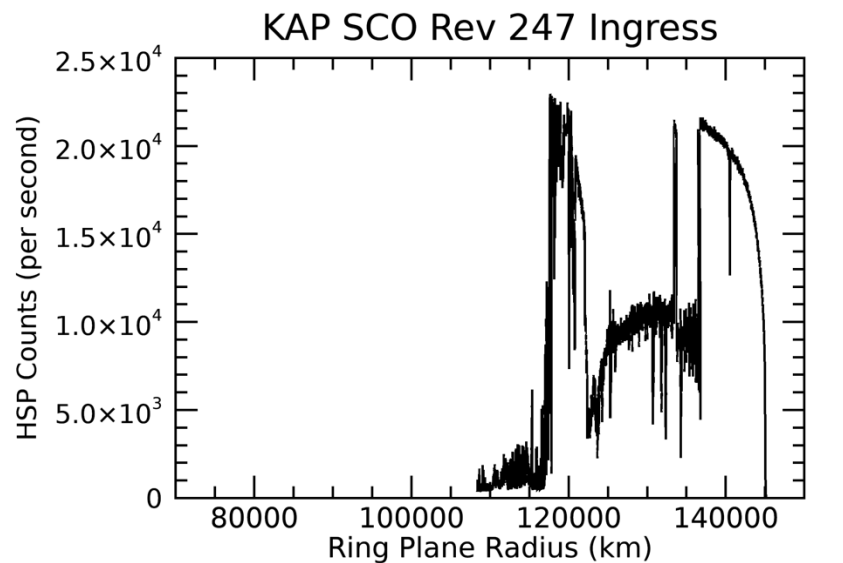
Target RA/dec: 254.78, -30.30

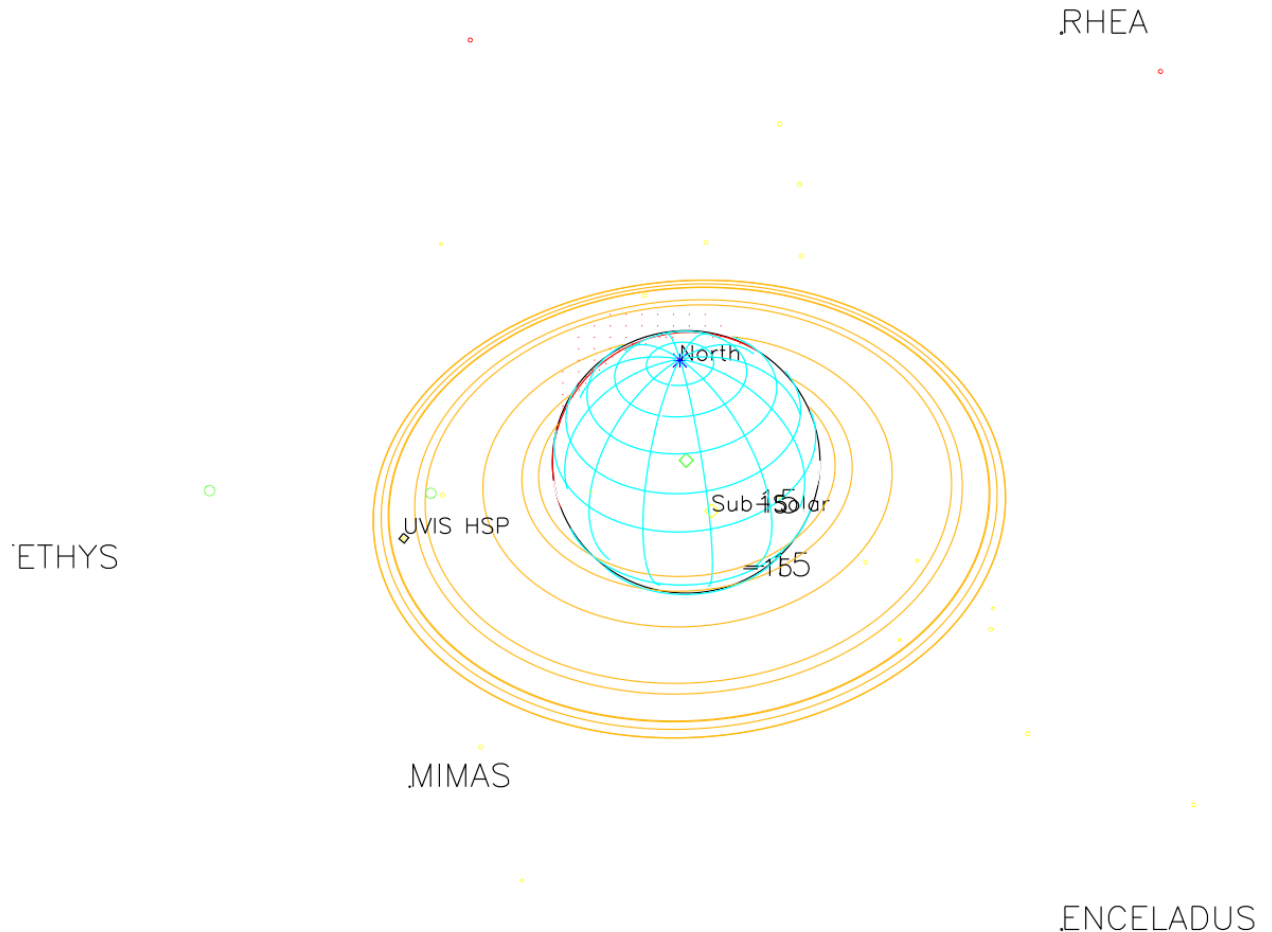
Subsolar lat/lon: 22.14, 137.46

Sub-s/c lat/lon: 30.85, 136.43







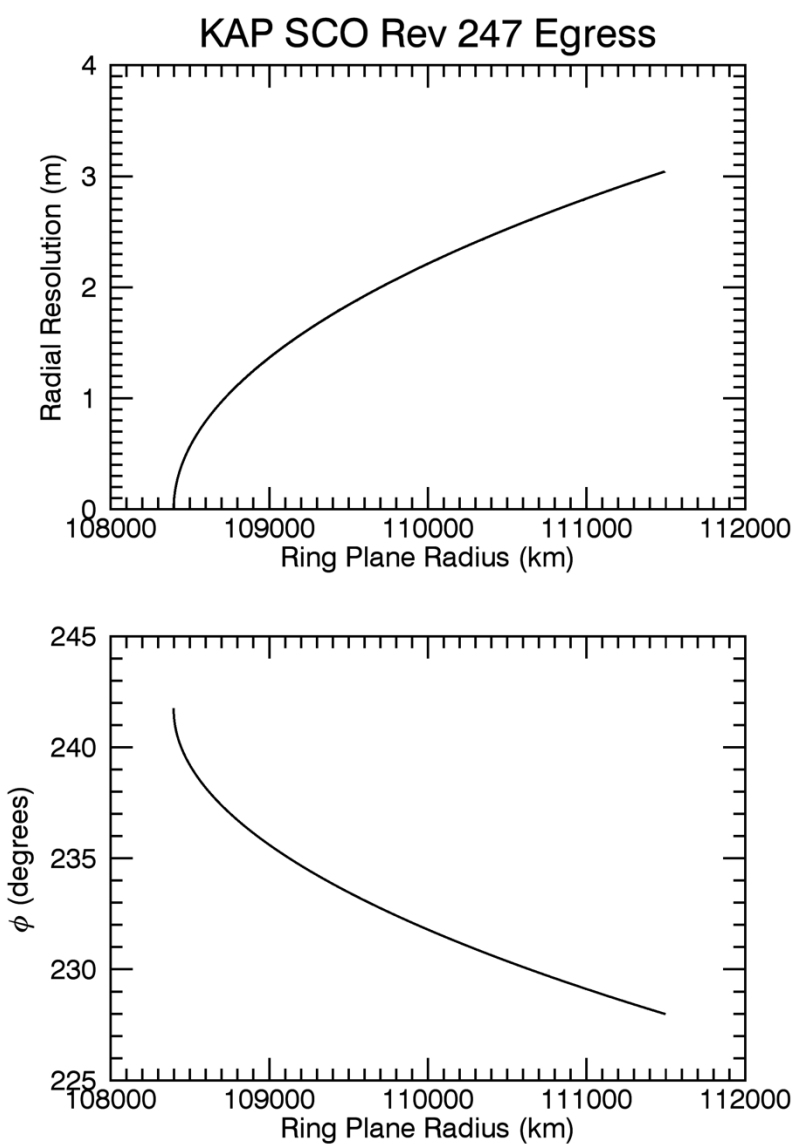
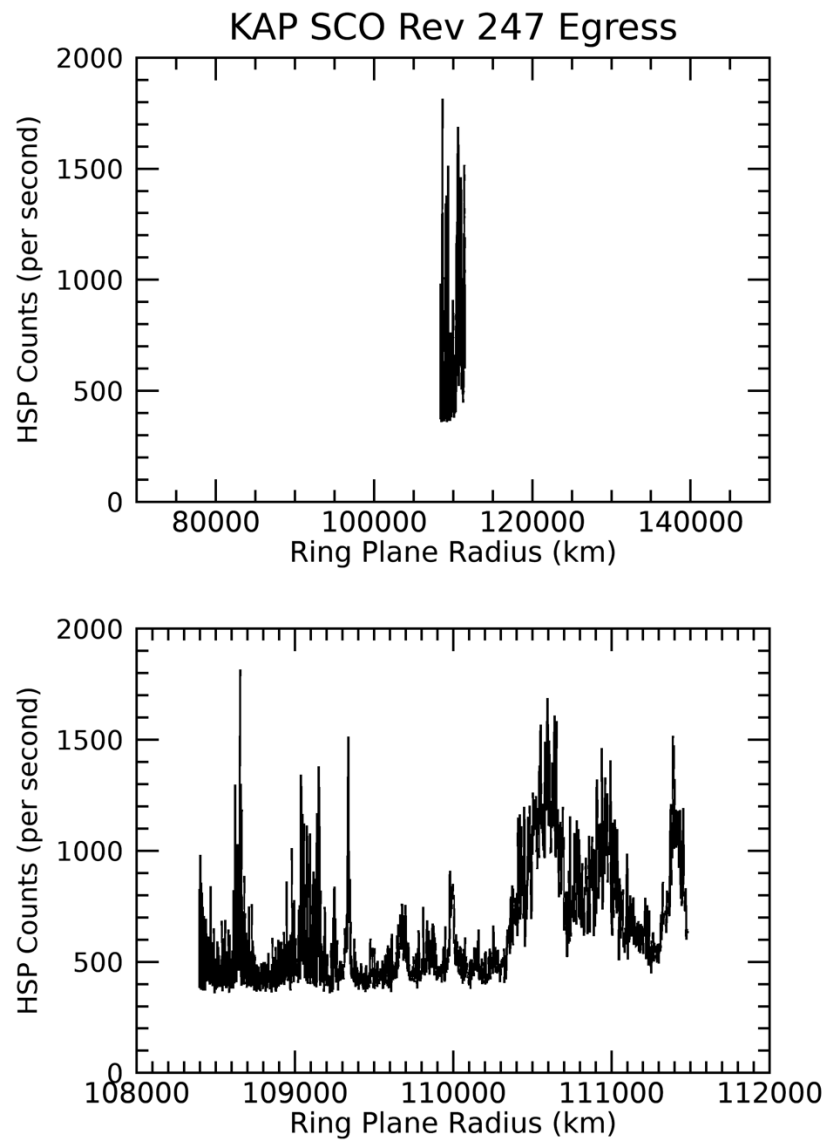


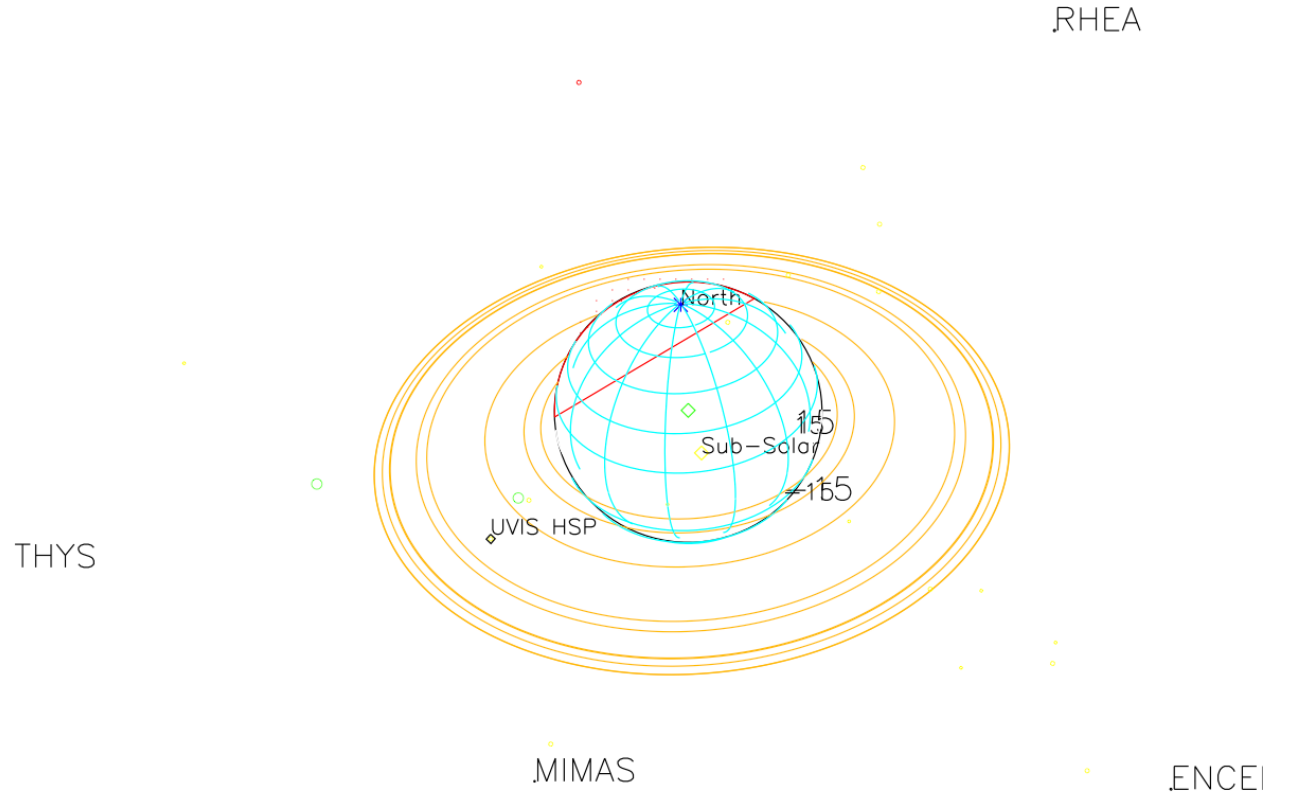
2016-306T05:04:00.000 484307.39 km

Target RA/dec: 246.45, -36.65

Subsolar lat/lon: 22.14, -149.35

Sub-s/c lat/lon: 37.28, -158.69



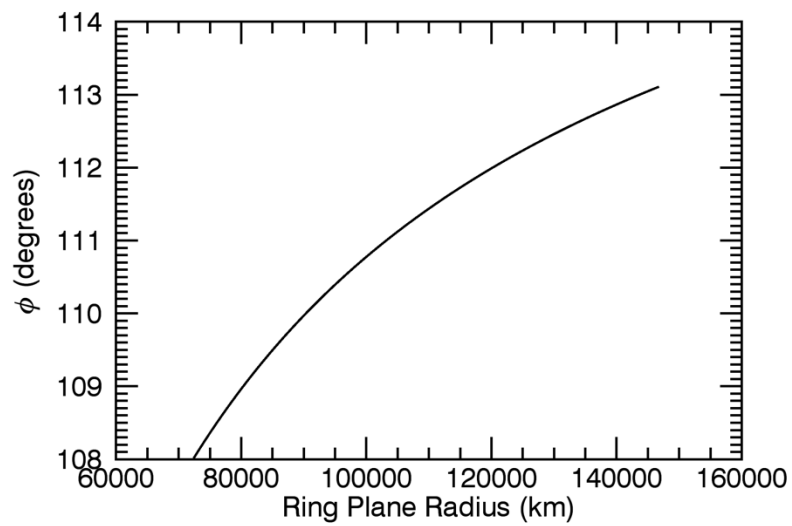
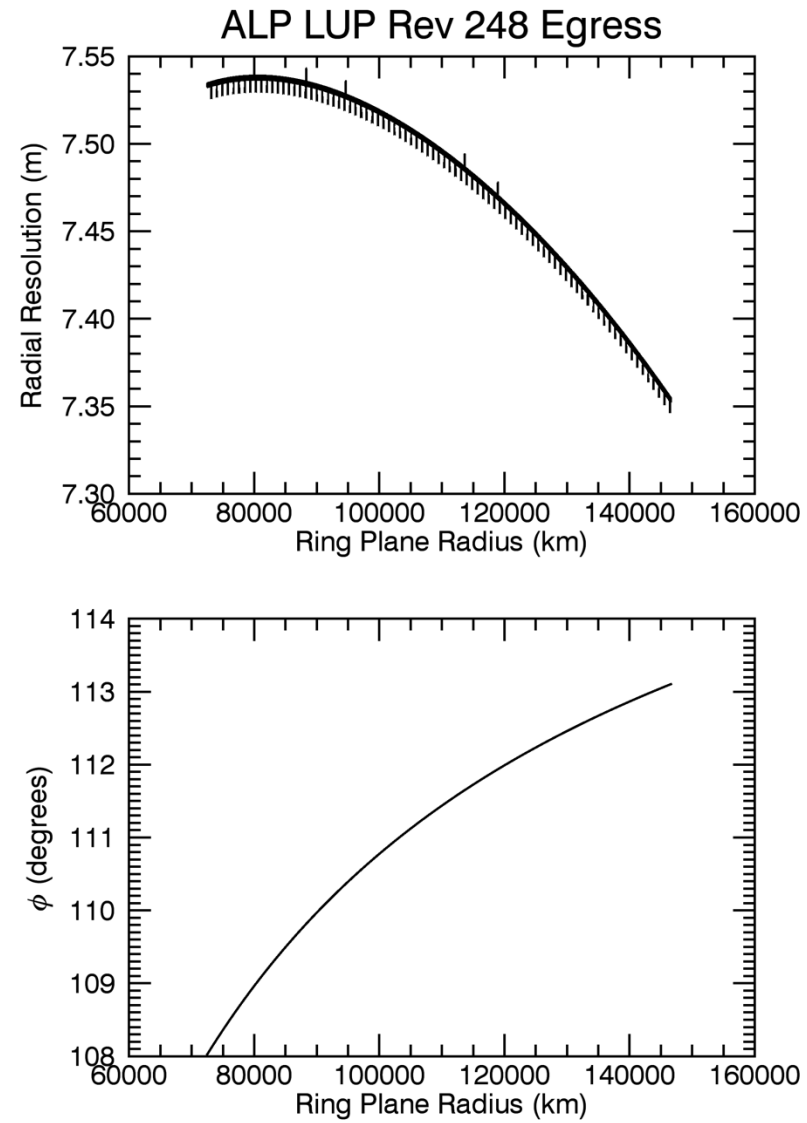
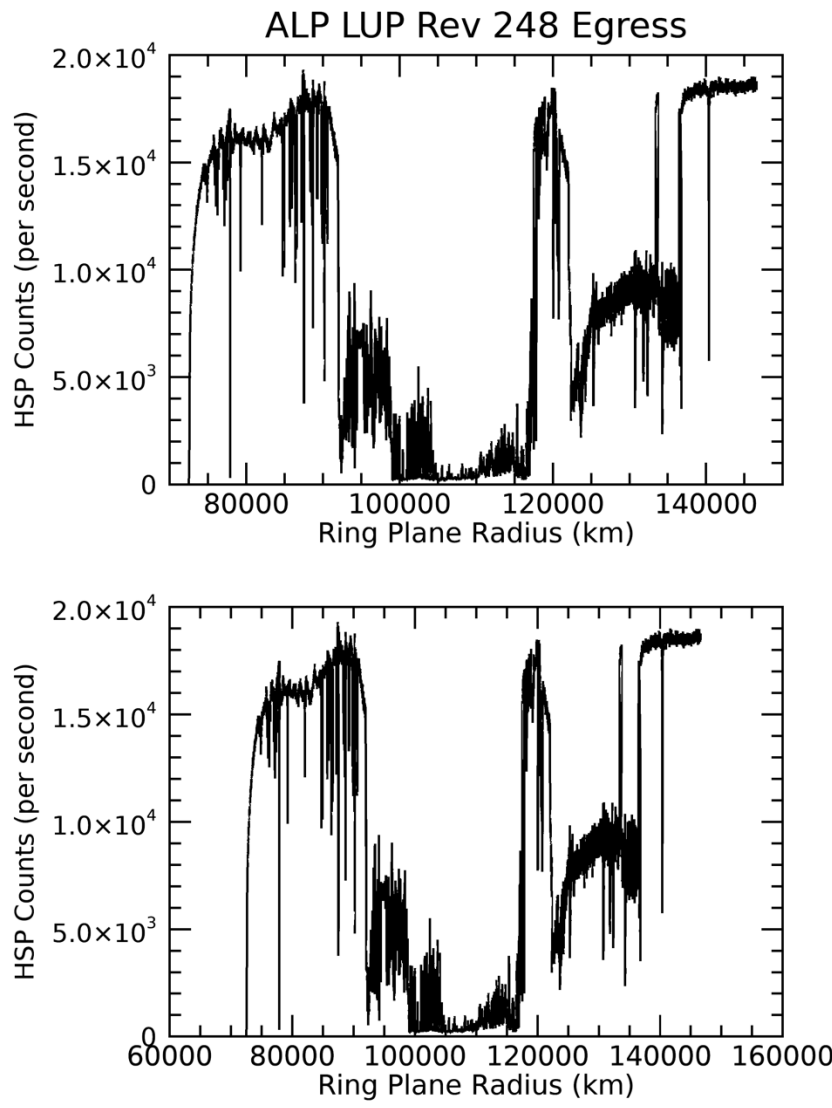


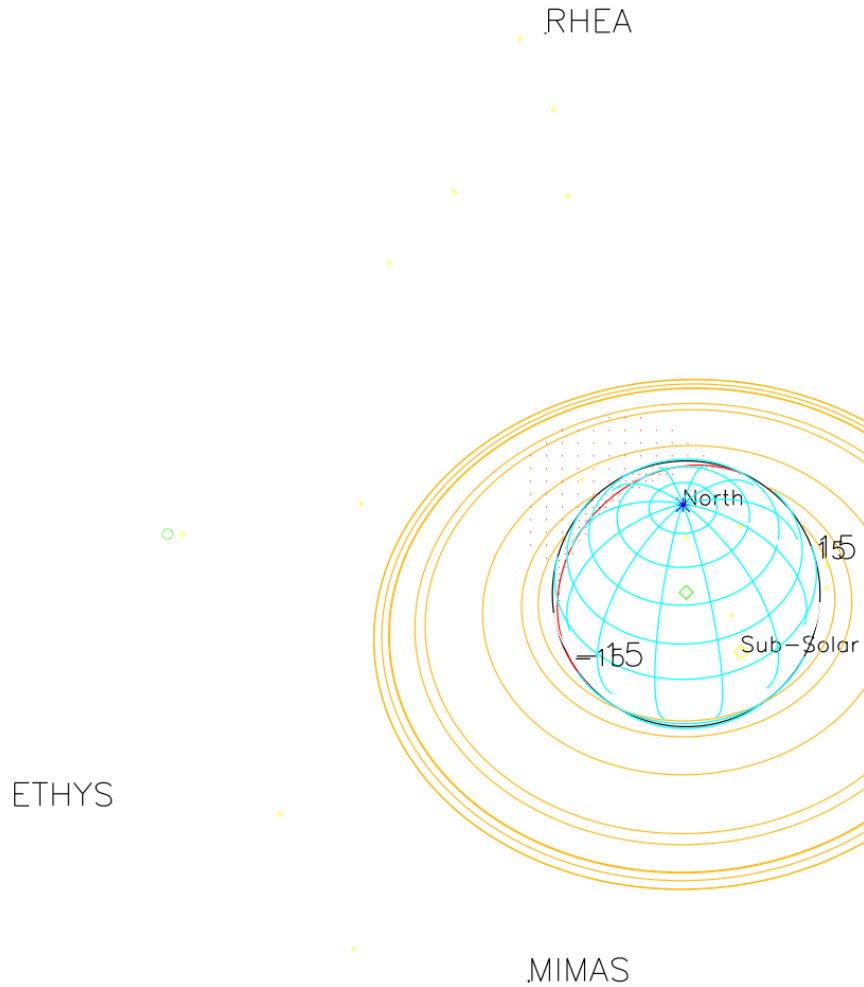
2016-306T06:23:00.000 460781.26 km

Target RA/dec: 251.49, -32.98

Subsolar lat/lon: 22.14, 166.17

Sub-s/c lat/lon: 33.54, 161.91



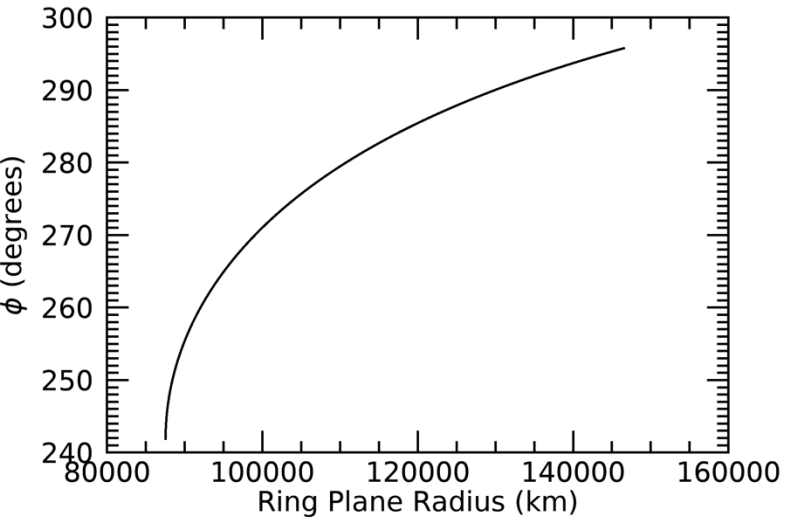
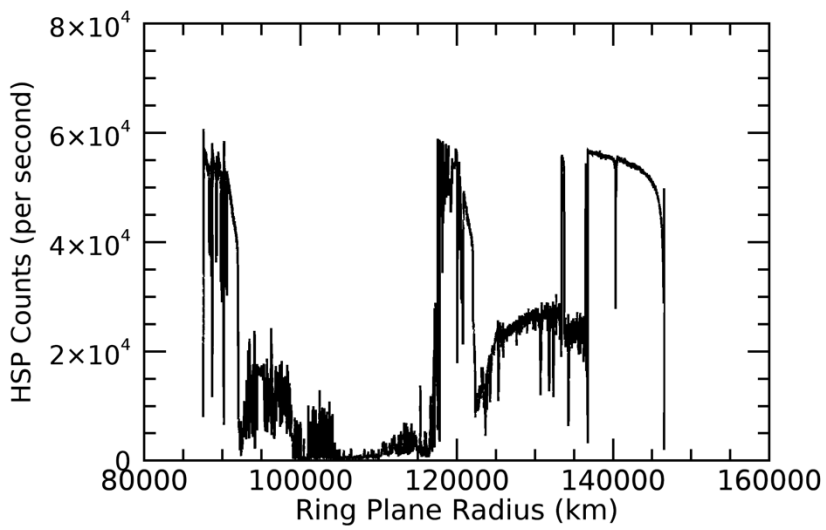
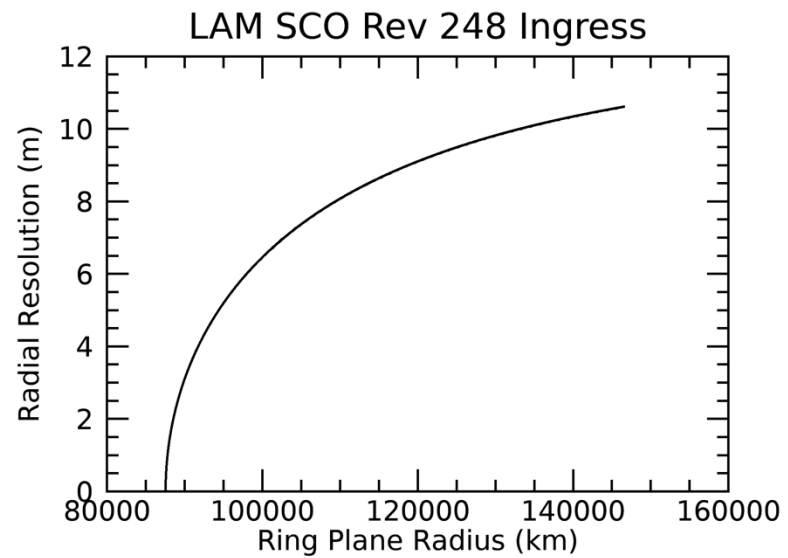
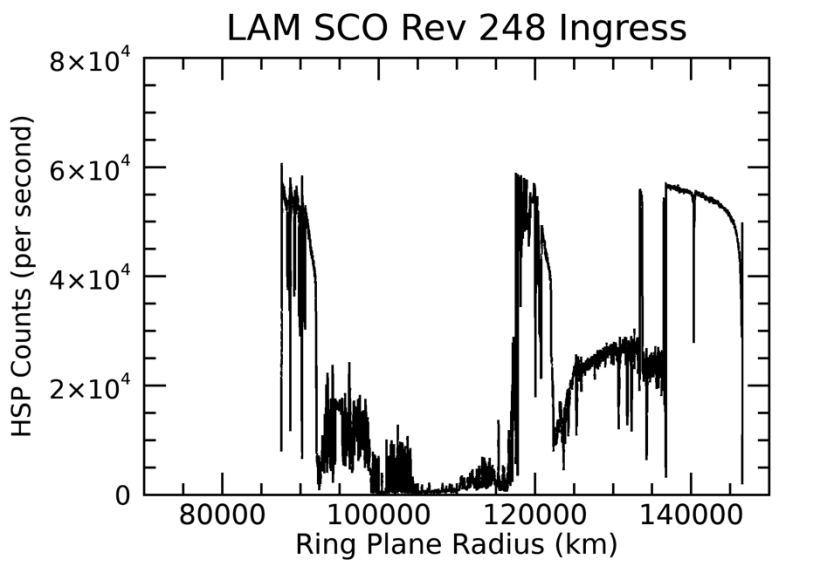


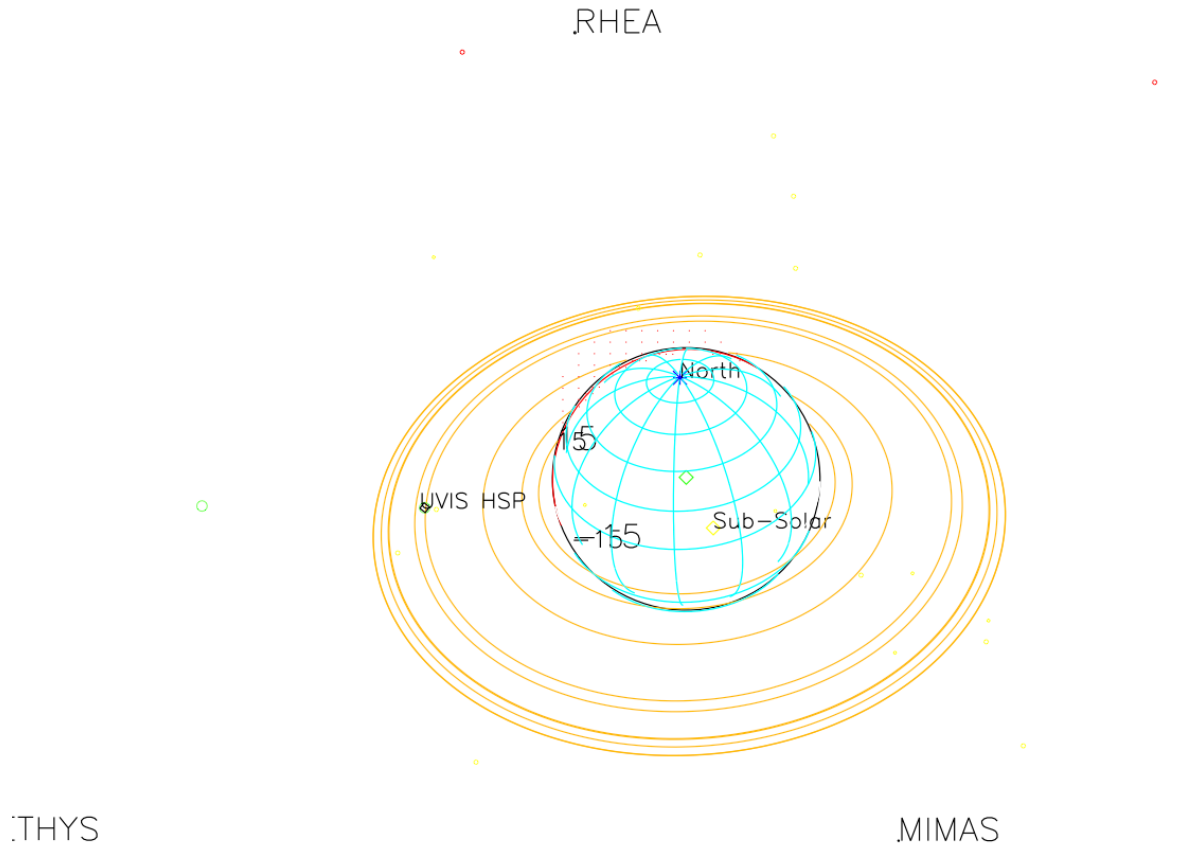
2016-315T15:17:00.000 546186.33 km

Target RA/dec: 233.73, -43.69

Subsolar lat/lon: 22.15, 128.67

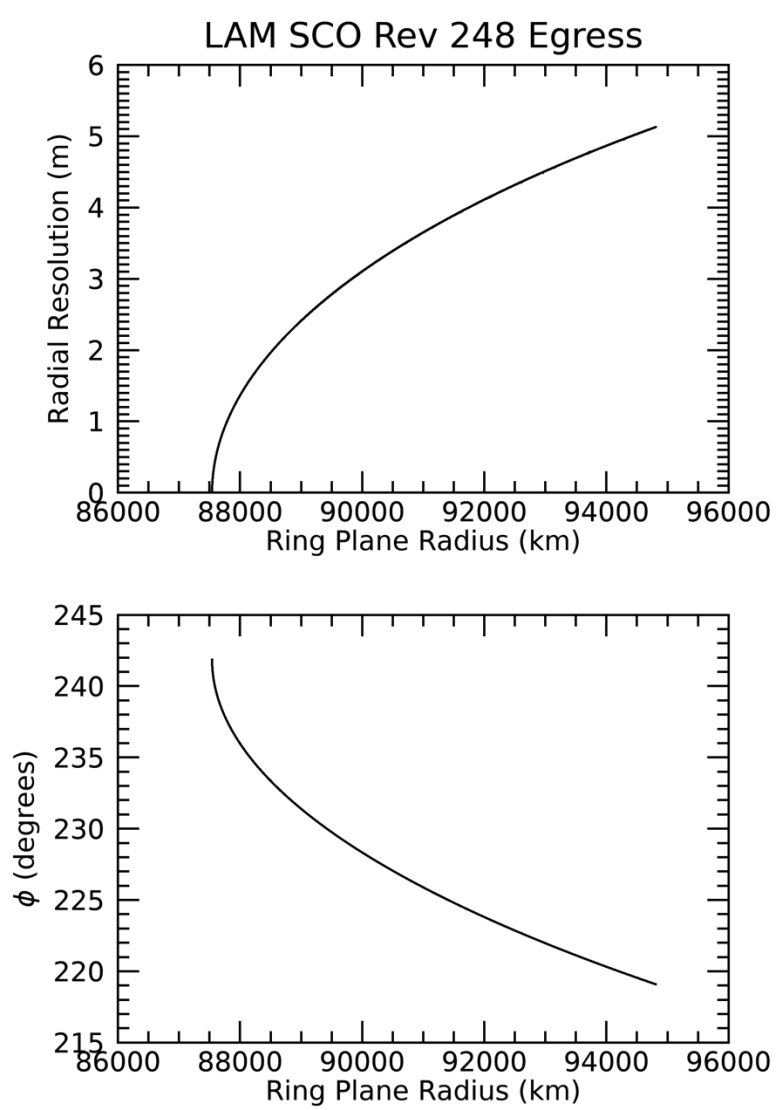
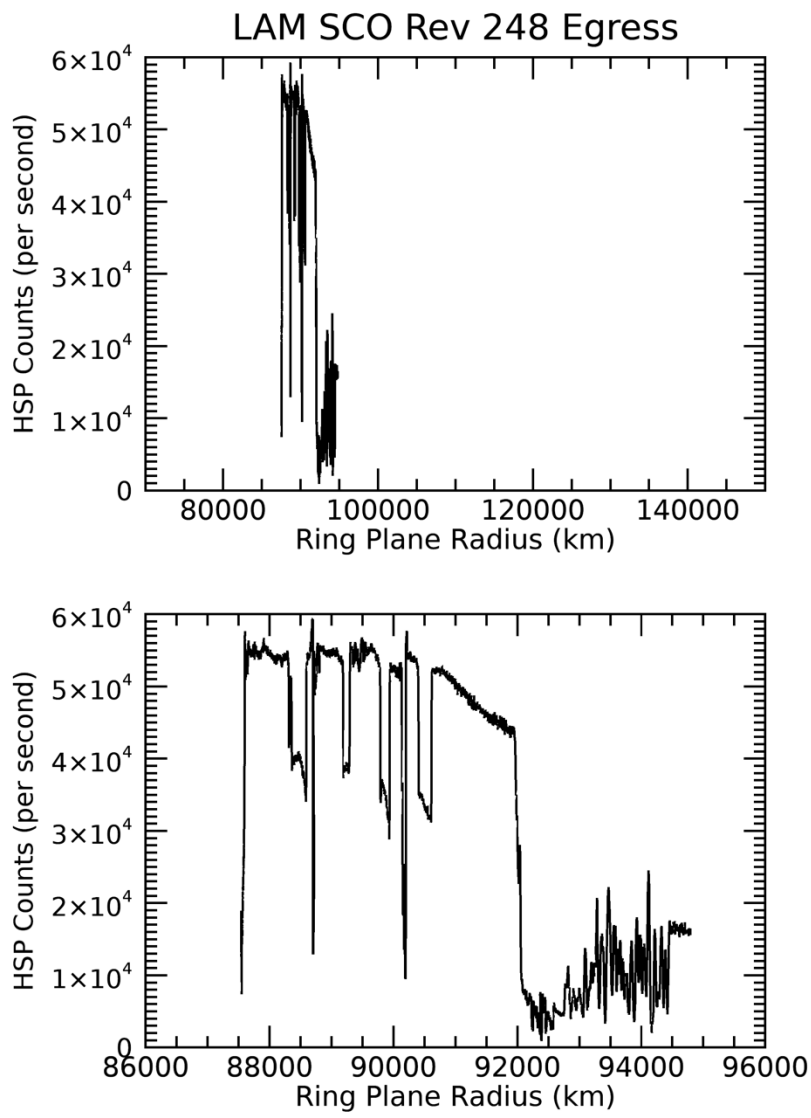
Sub-s/c lat/lon: 44.71, 105.52





2016-315T18:35:00.000 485670.61 km
Target RA/dec: 246.10, -36.83
Subsolar lat/lon: 22.15, 17.19
Sub-s/c lat/lon: 37.48, 7.16

ENCELADUS°

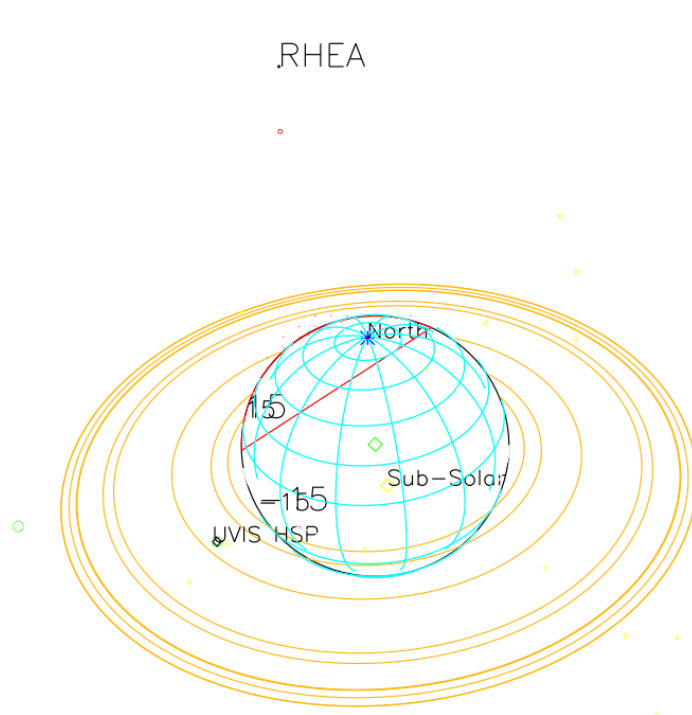


TYS

RHEA

MIMAS

ENCELADUS

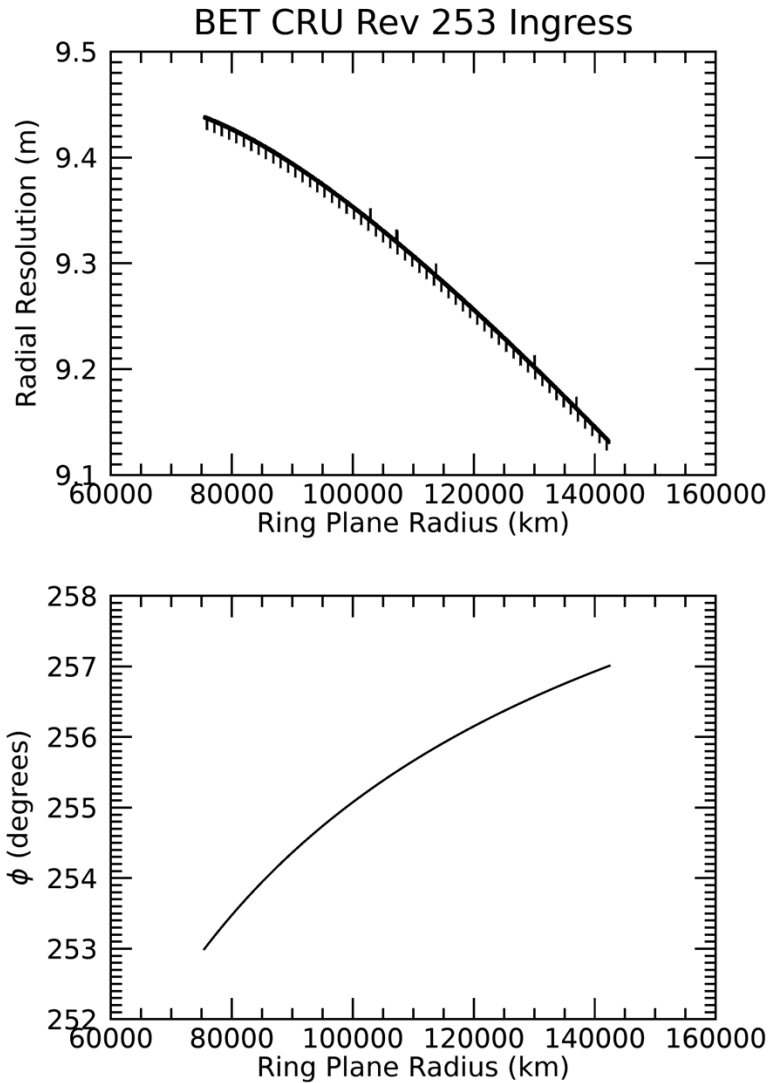
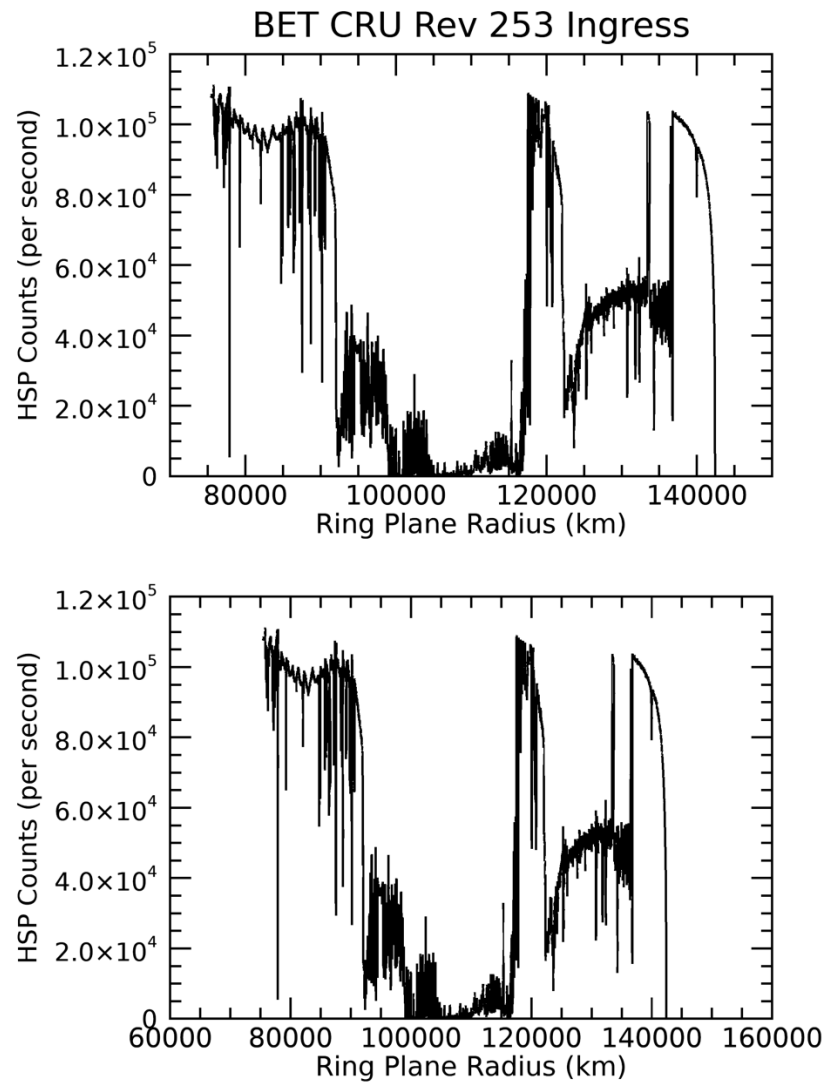


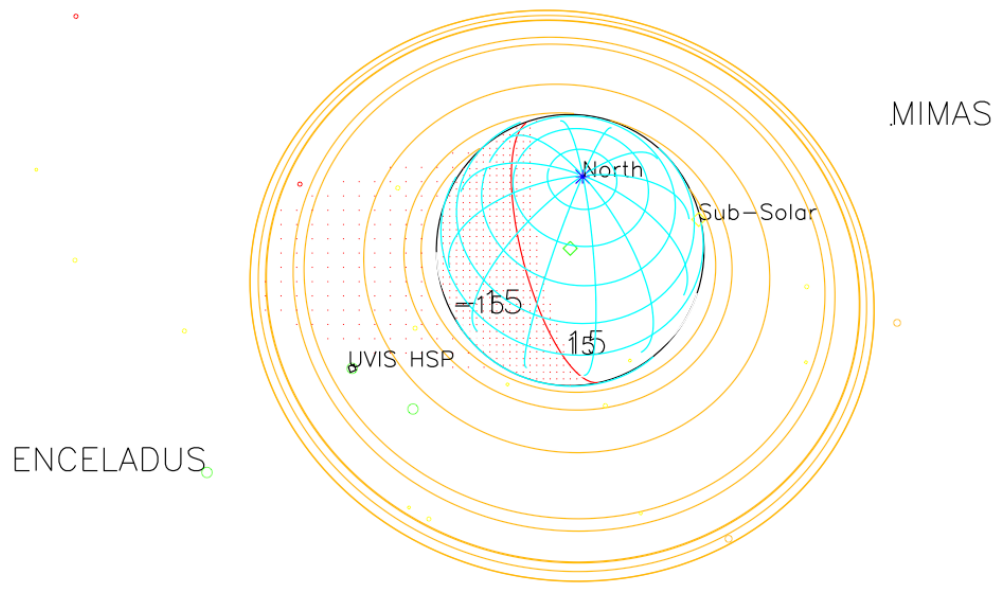
2016-315T20:11:00.000 457105.74 km

Target RA/dec: 252.22, -32.35

Subsolar lat/lon: 22.15, -36.86

Sub-s/c lat/lon: 32.90, -40.72



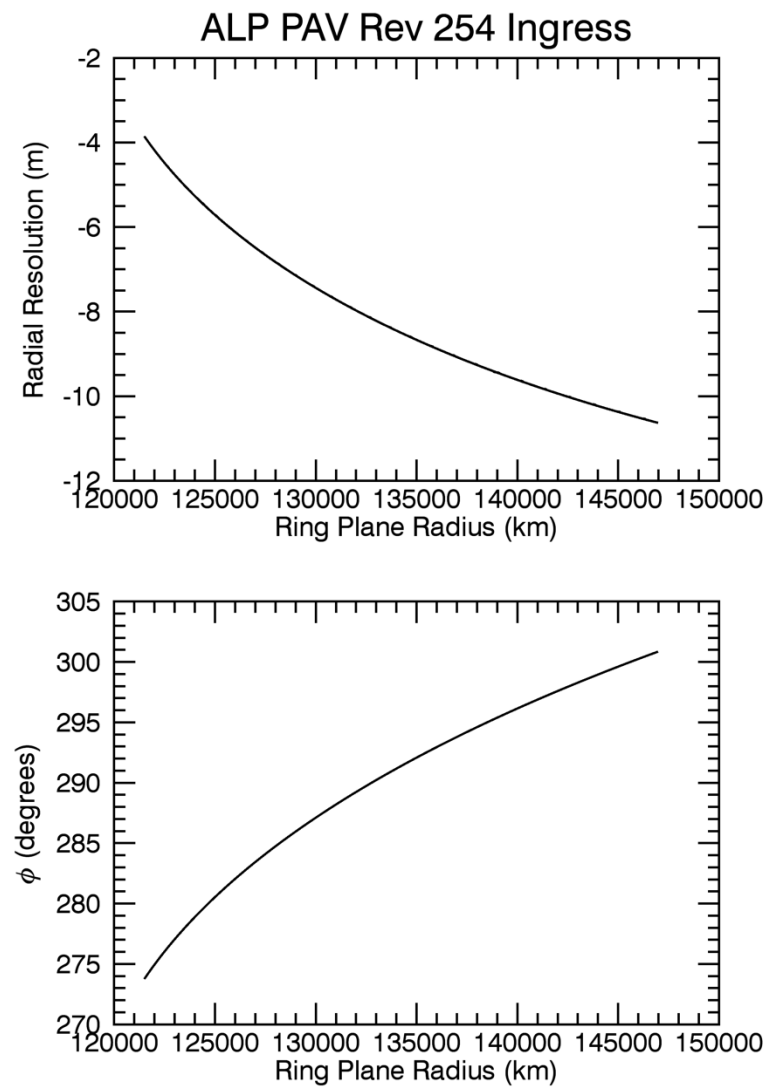
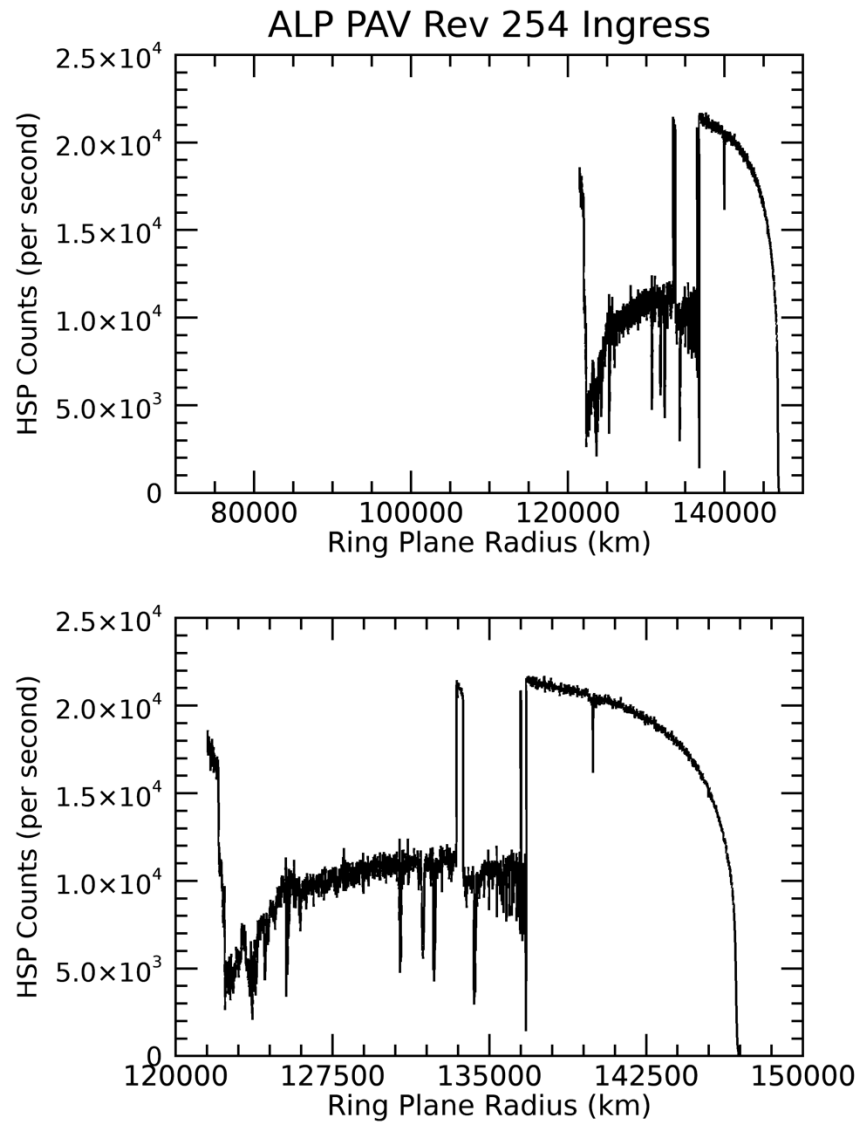


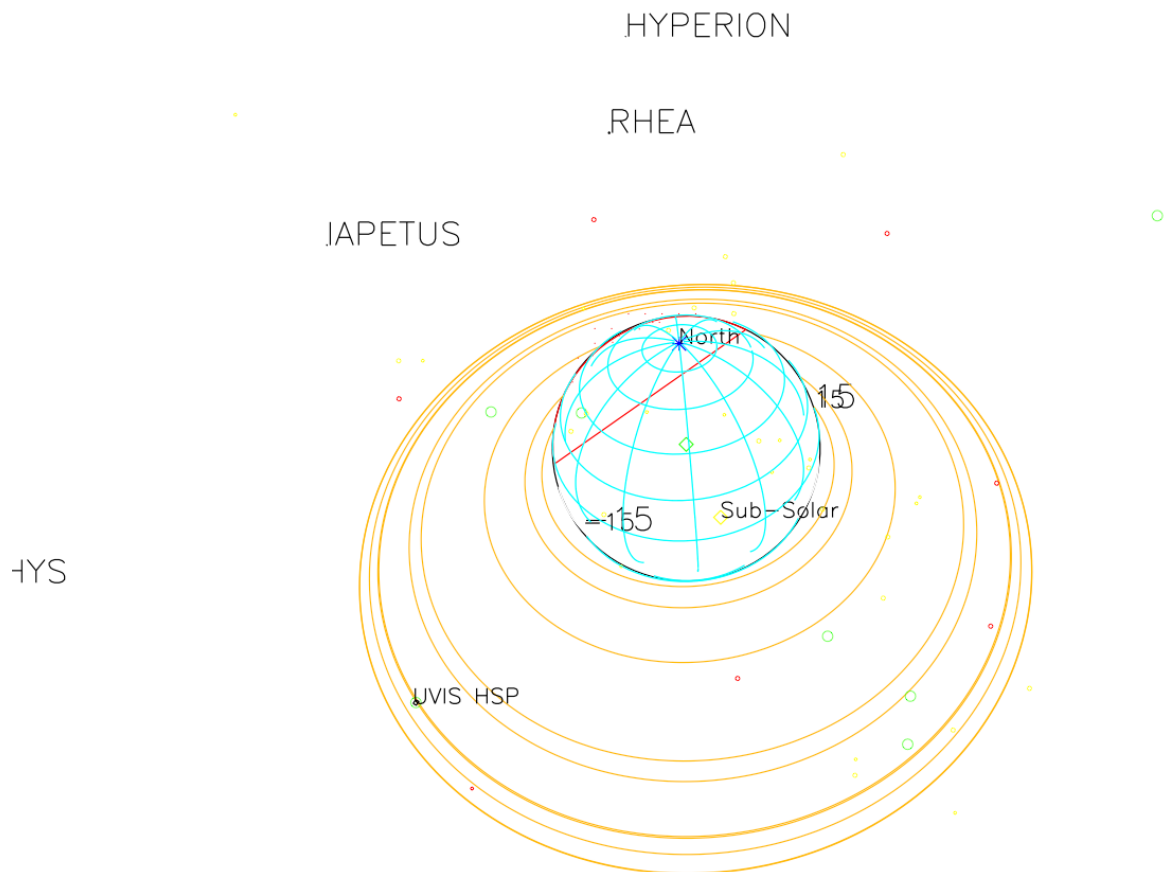
2016-353T12:11:00.000 428319.86 km

Target RA/dec: 165.61, -55.40

Subsolar lat/lon: 22.20, 24.51

Sub-s/c lat/lon: 54.02, -78.29



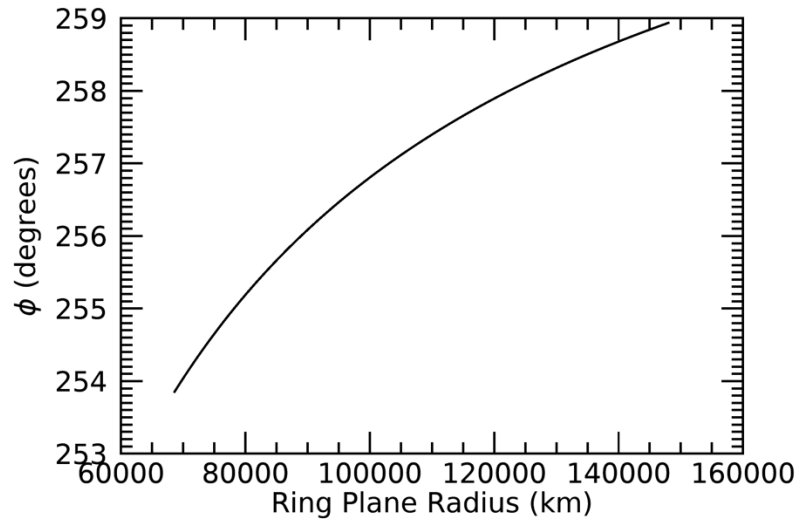
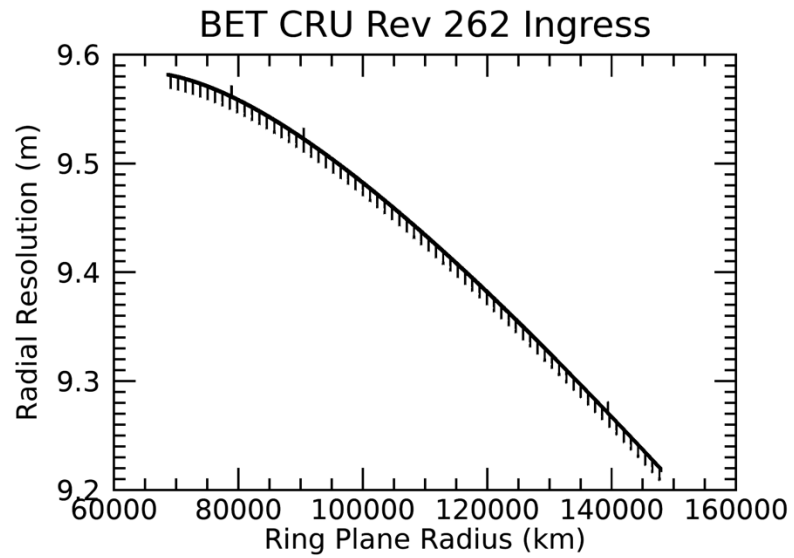
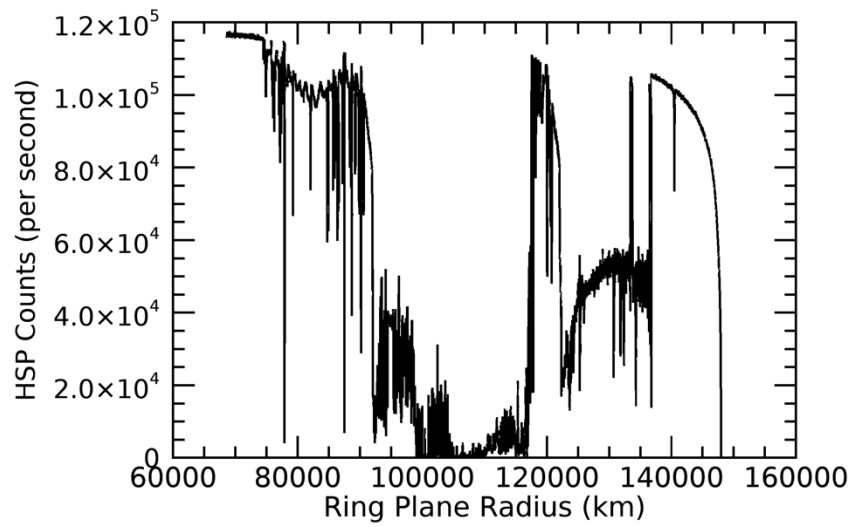
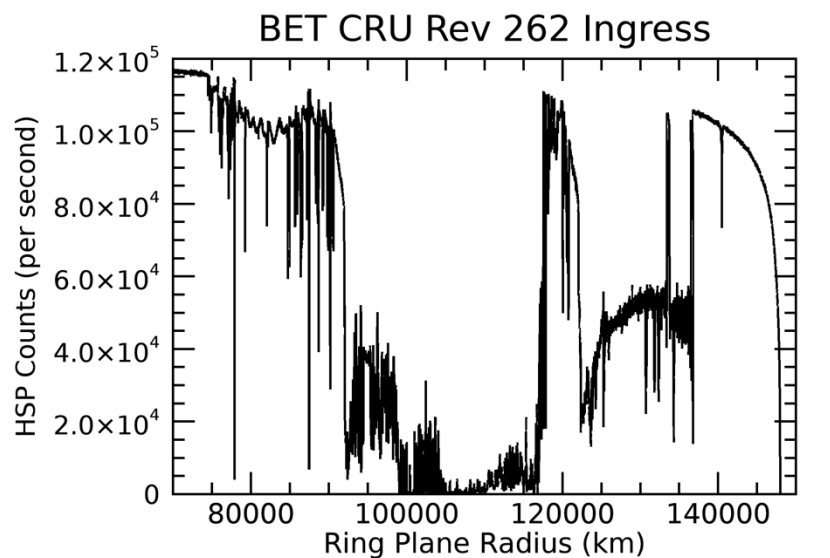


2016-360T23:08:00.000 204339.58 km

Target RA/dec: 246.40, -42.29

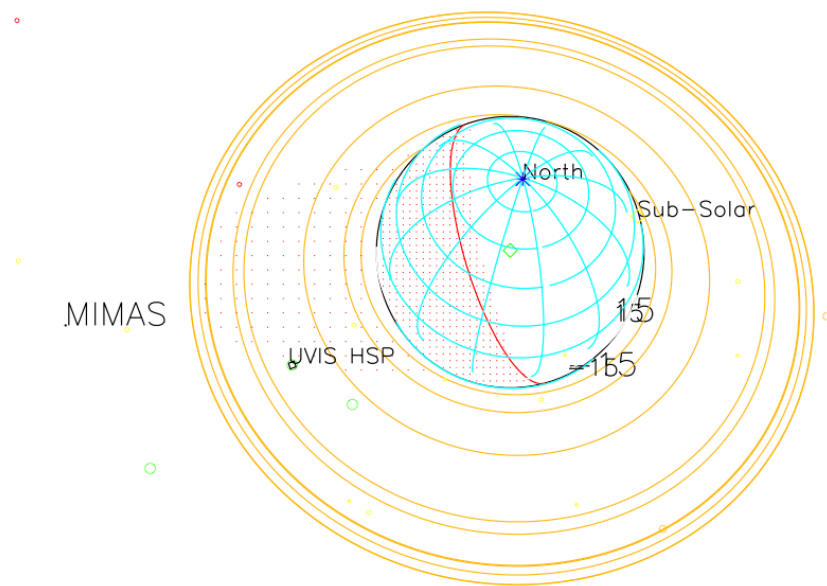
Subsolar lat/lon: 22.21, 99.27

Sub-s/c lat/lon: 43.79, 88.58



RHEA

DIC

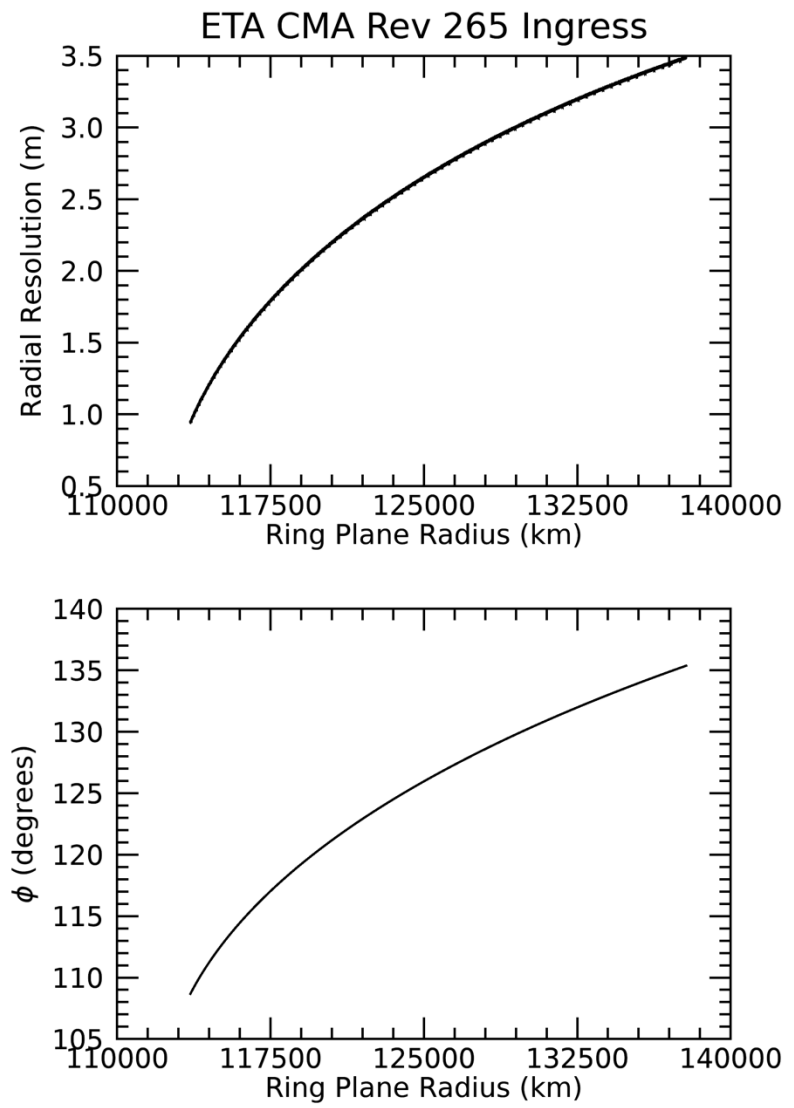
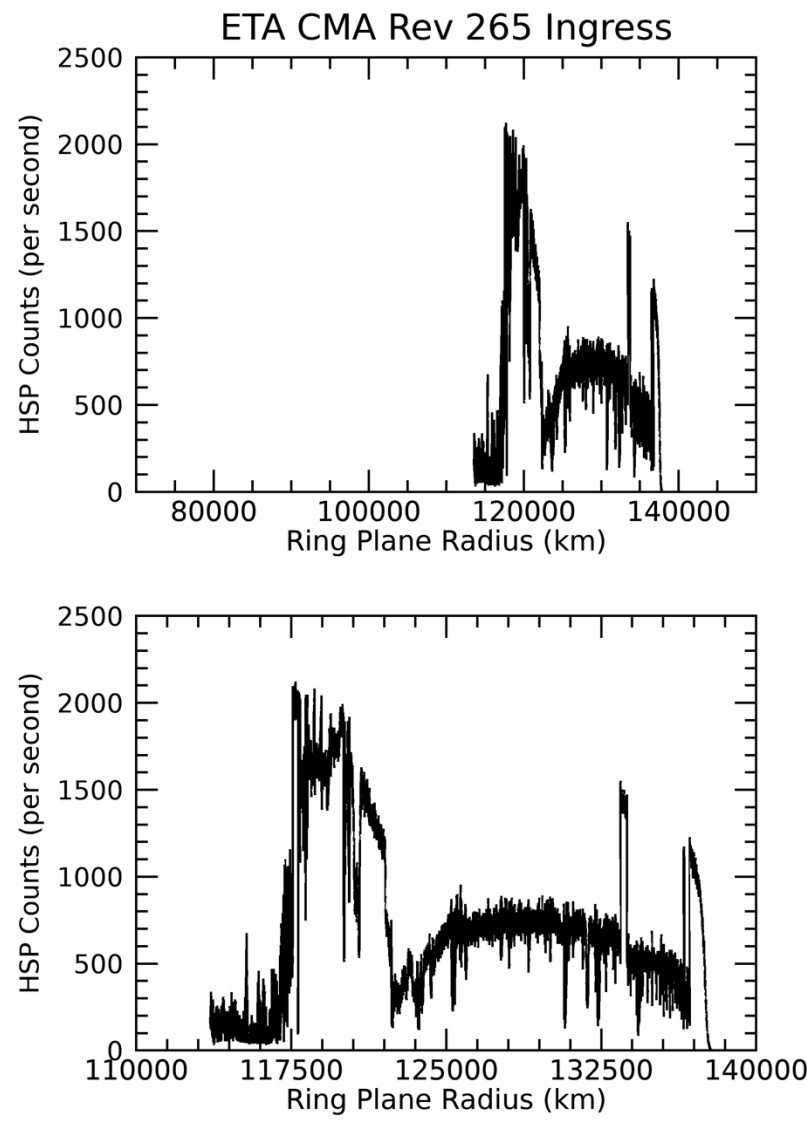


2017-052T00:59:00.000 420686.80 km

Target RA/dec: 165.12, -56.9° CELADUS

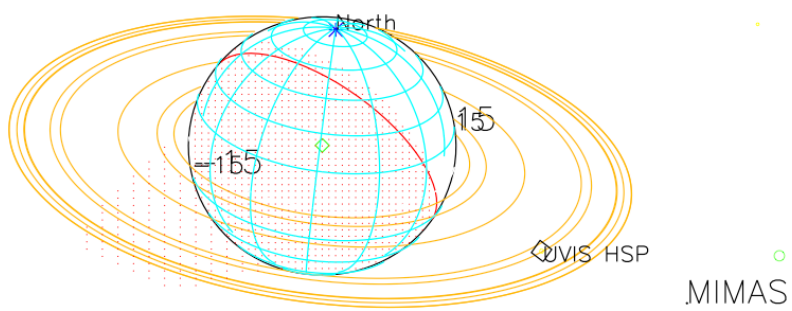
Subsolar lat/lon: 22.25, -96.56

Sub-s/c lat/lon: 54.28, 157.83



TITAN

ENCELADUS



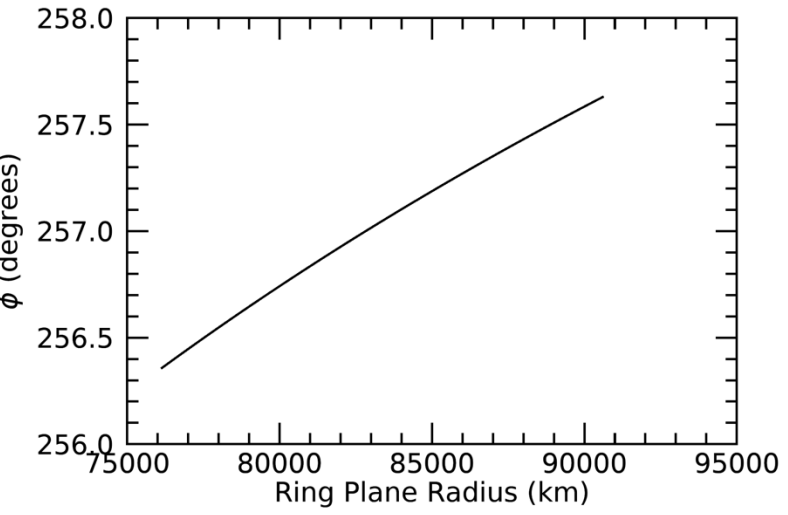
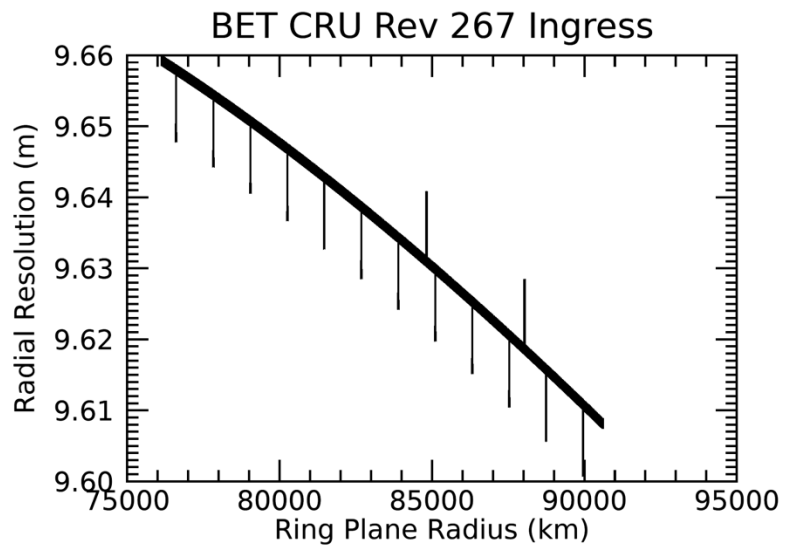
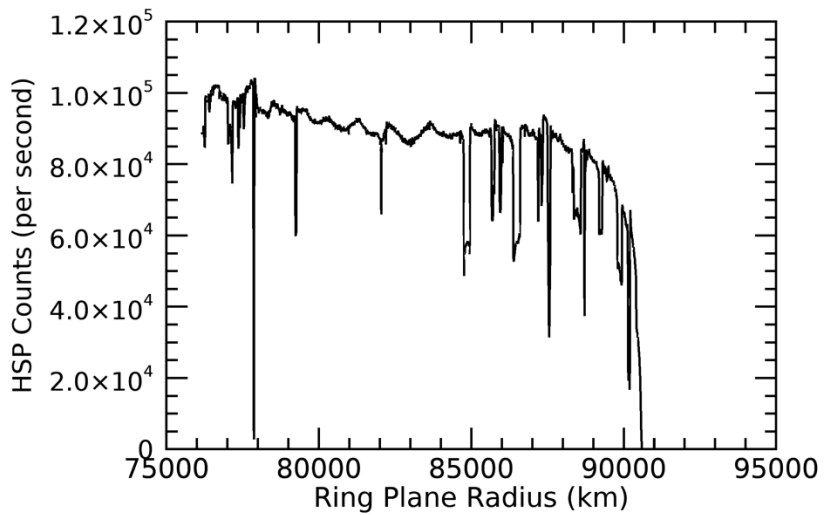
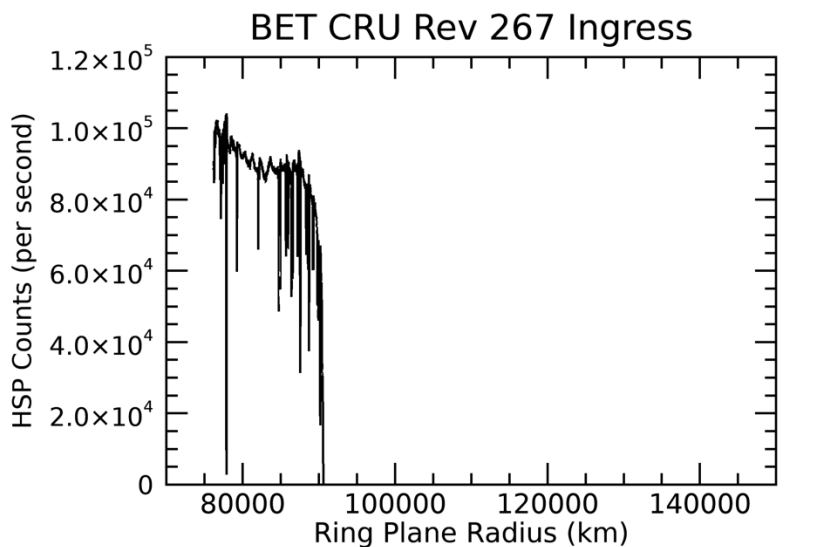
TETHYS

2017-072T01:14:00.000 1079483.0 km

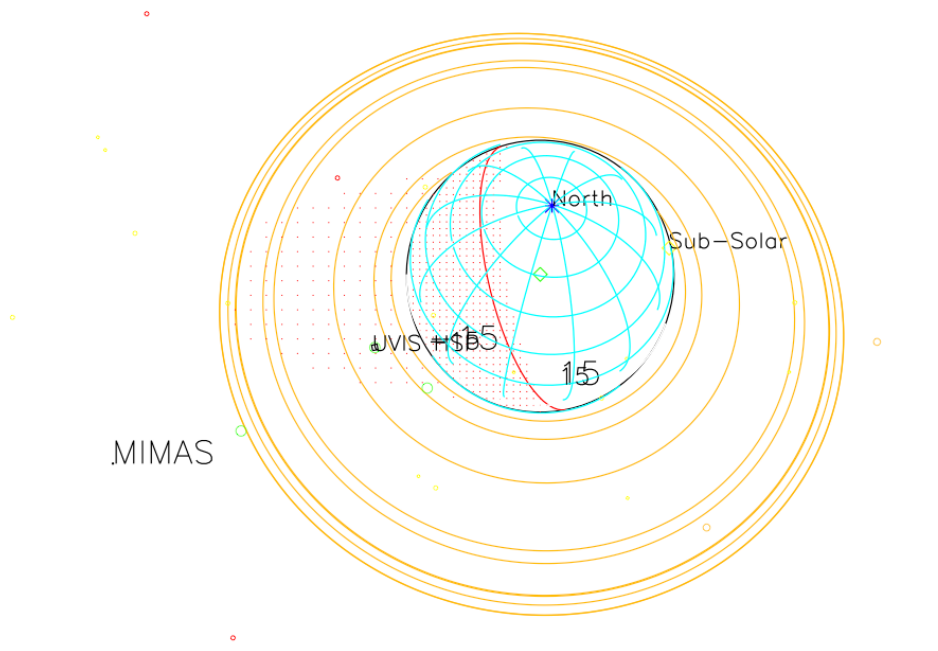
Target RA/dec: 117.03, -27.02

Subsolar lat/lon: 22.27, -120.19

Sub-s/c lat/lon: 21.27, 91.09



DIONE



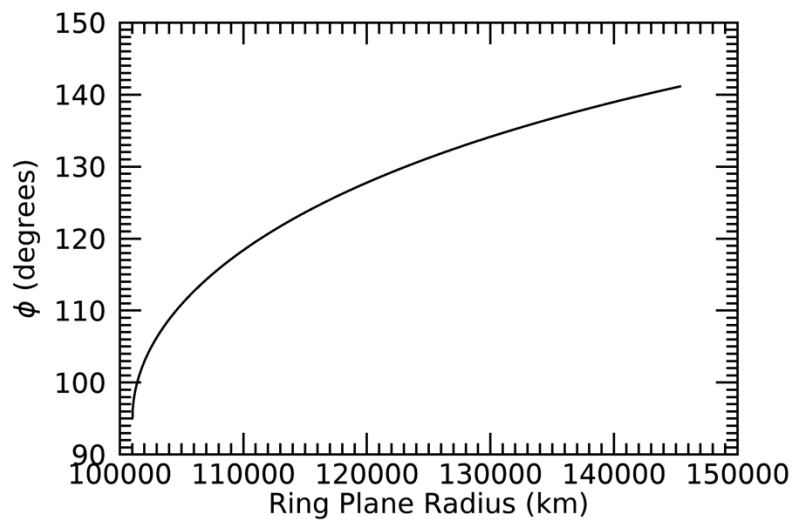
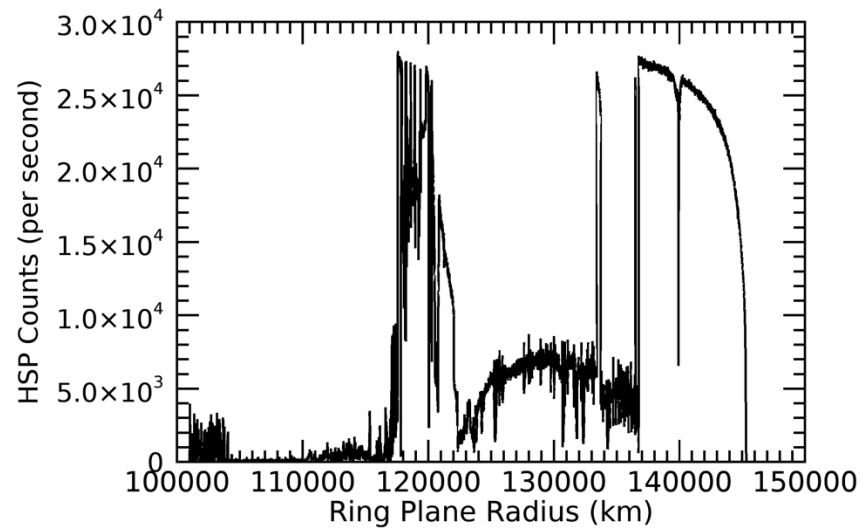
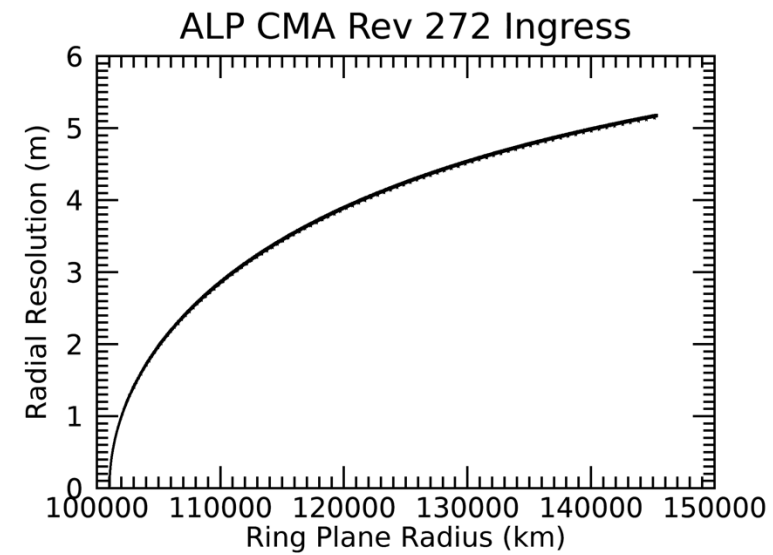
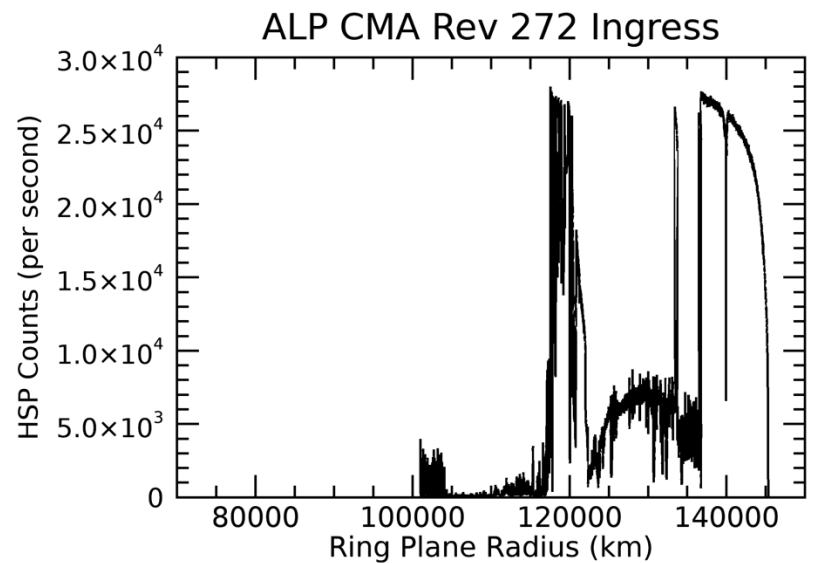
2017-087T21:38:00.000 392321.92 km

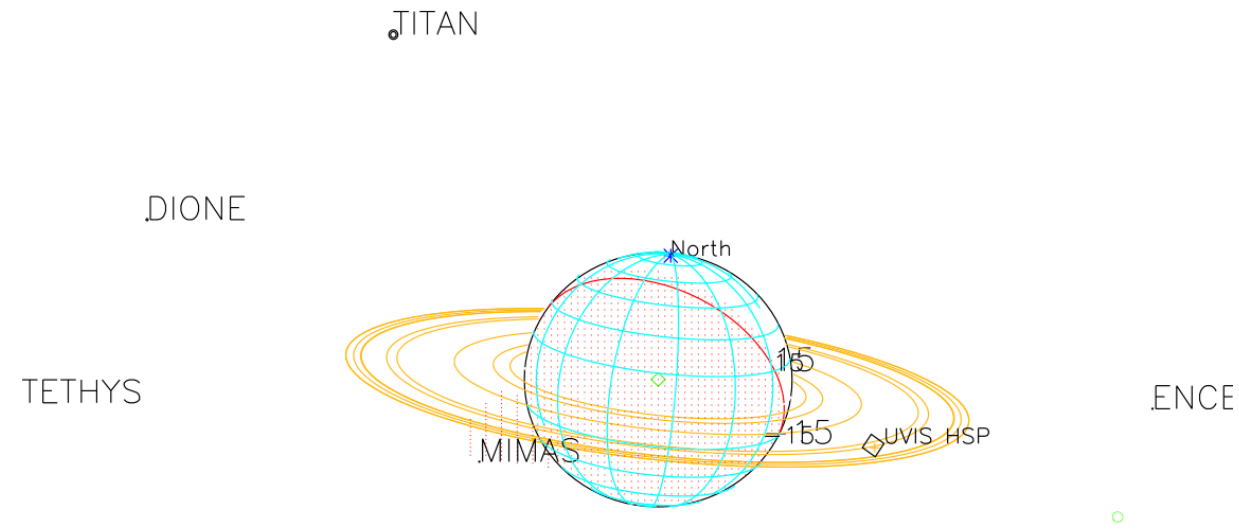
Target RA/dec: 170.10, -56.87

Subsolar lat/lon: 22.27, -10.76

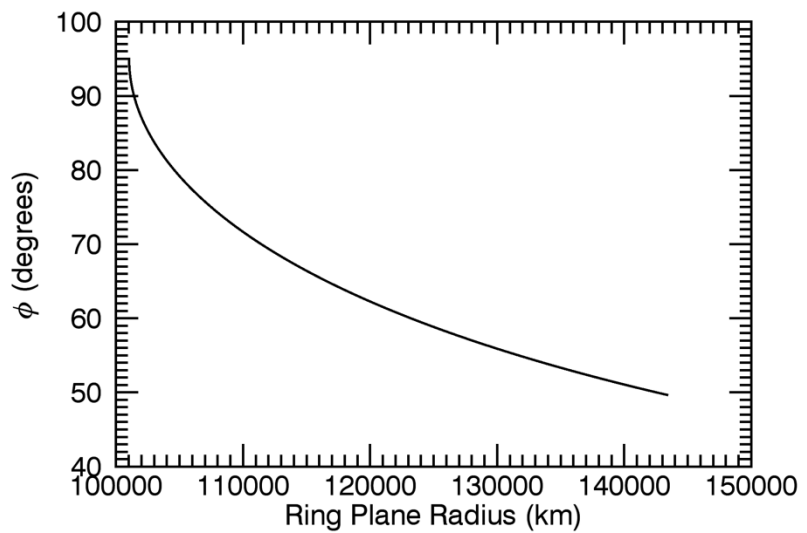
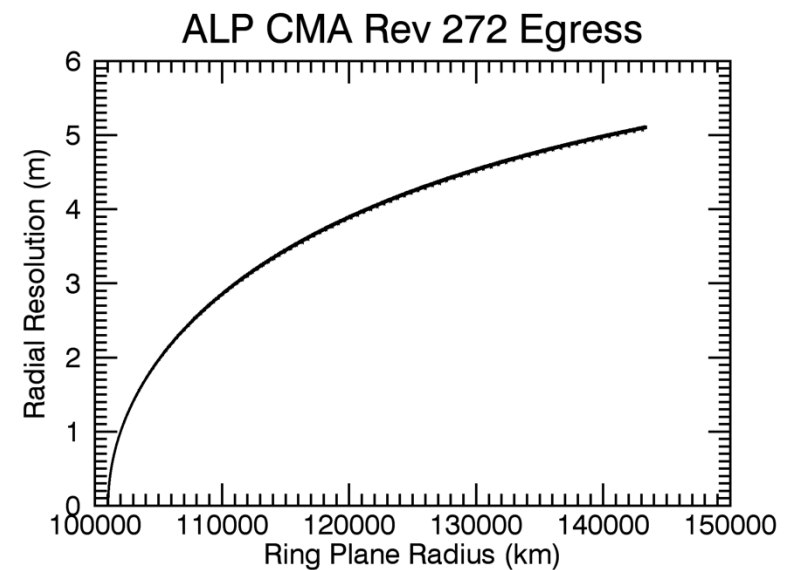
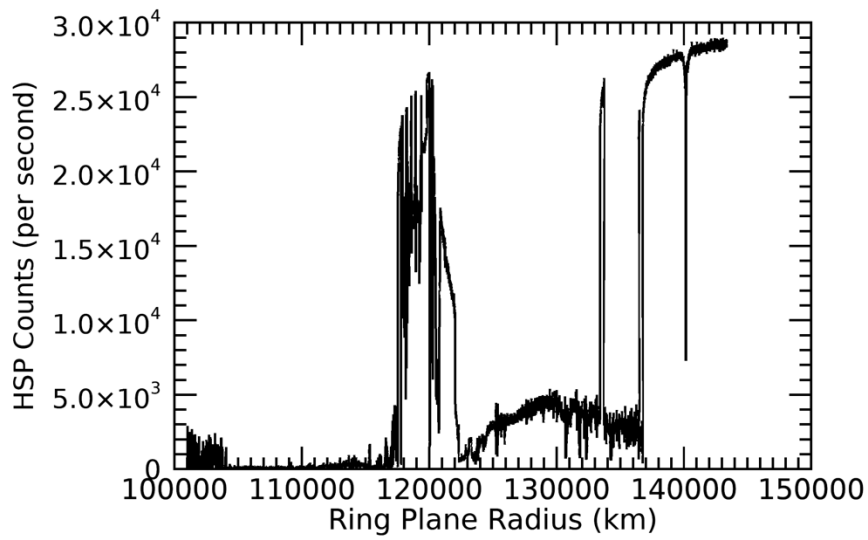
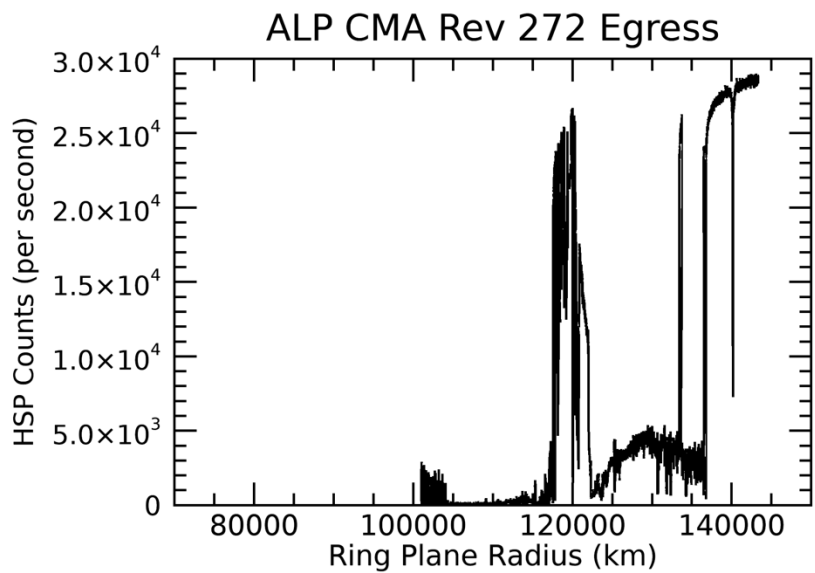
Sub-s/c lat/lon: 56.12, -112.59

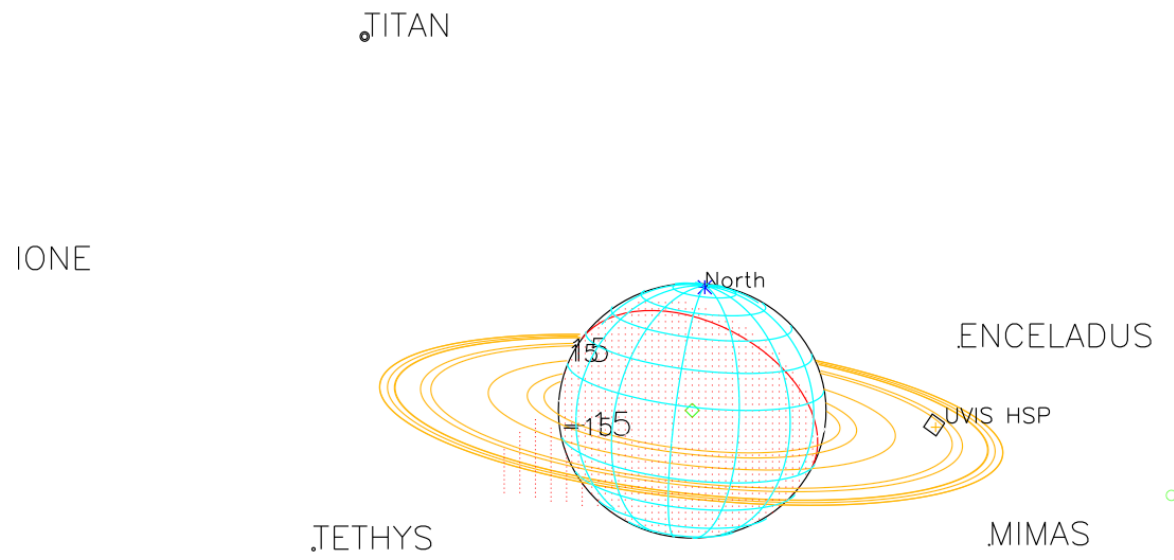
ENCELADUS





2017-120T19:39:00.000 1160503.4 km
Target RA/dec: 106.31, -15.32
Subsolar lat/lon: 22.28, -58.82
Sub-s/c lat/lon: 10.39, 141.71



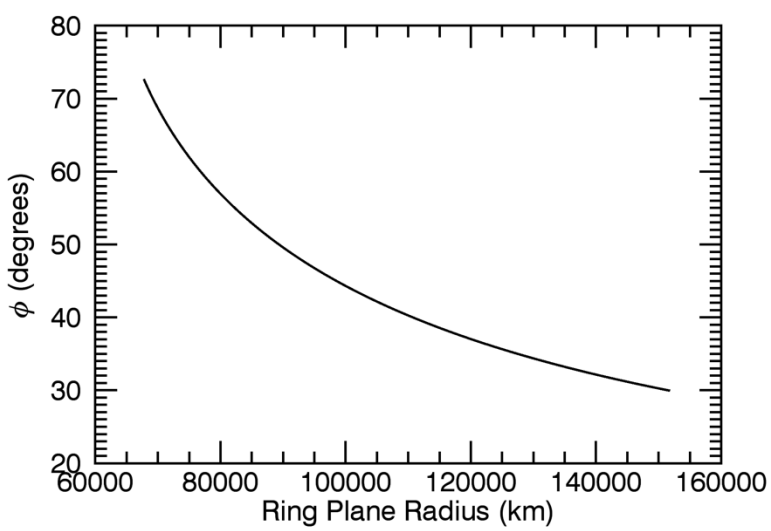
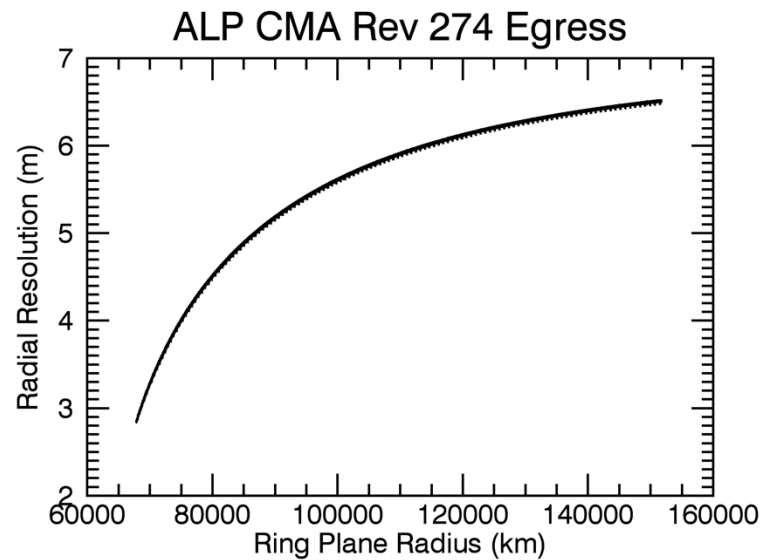
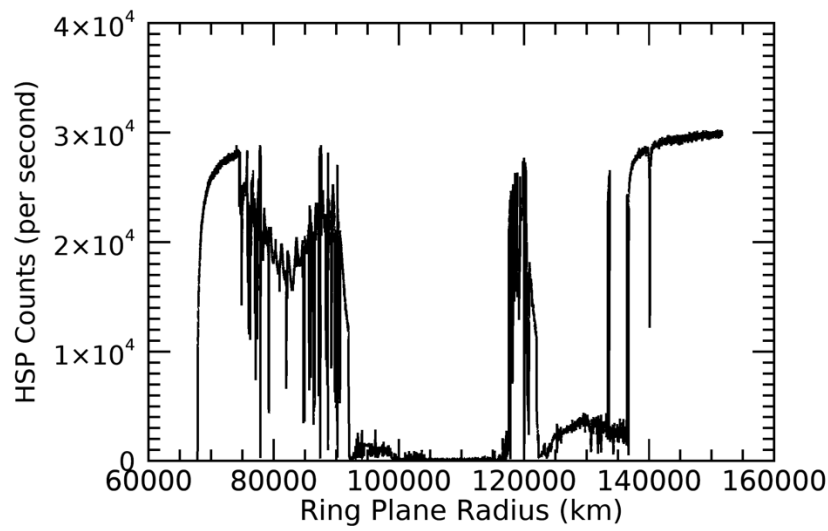
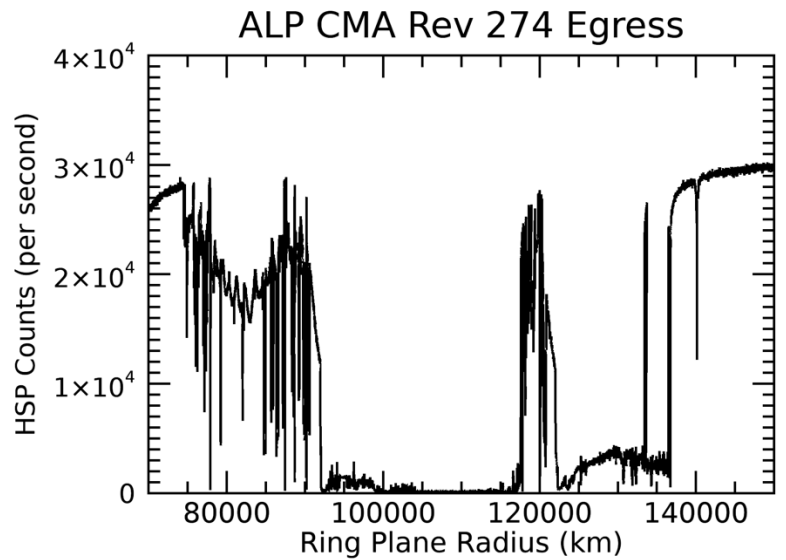


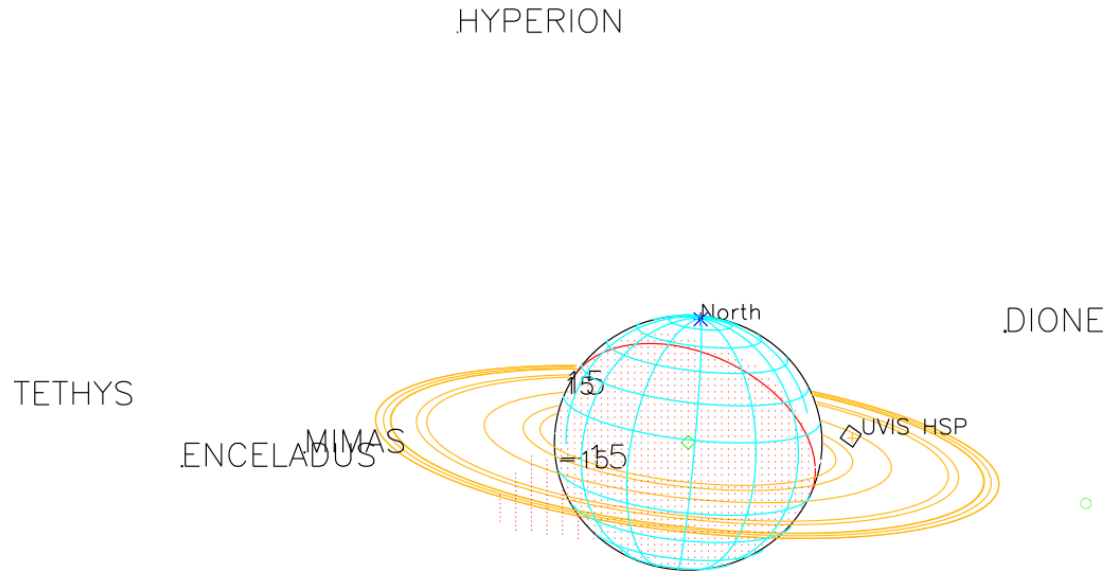
2017-120T23:38:00.000 1125022.8 km

Target RA/dec: 107.11, -16.43

Subsolar lat/lon: 22.28, 166.61

Sub-s/c lat/lon: 11.39, 7.80



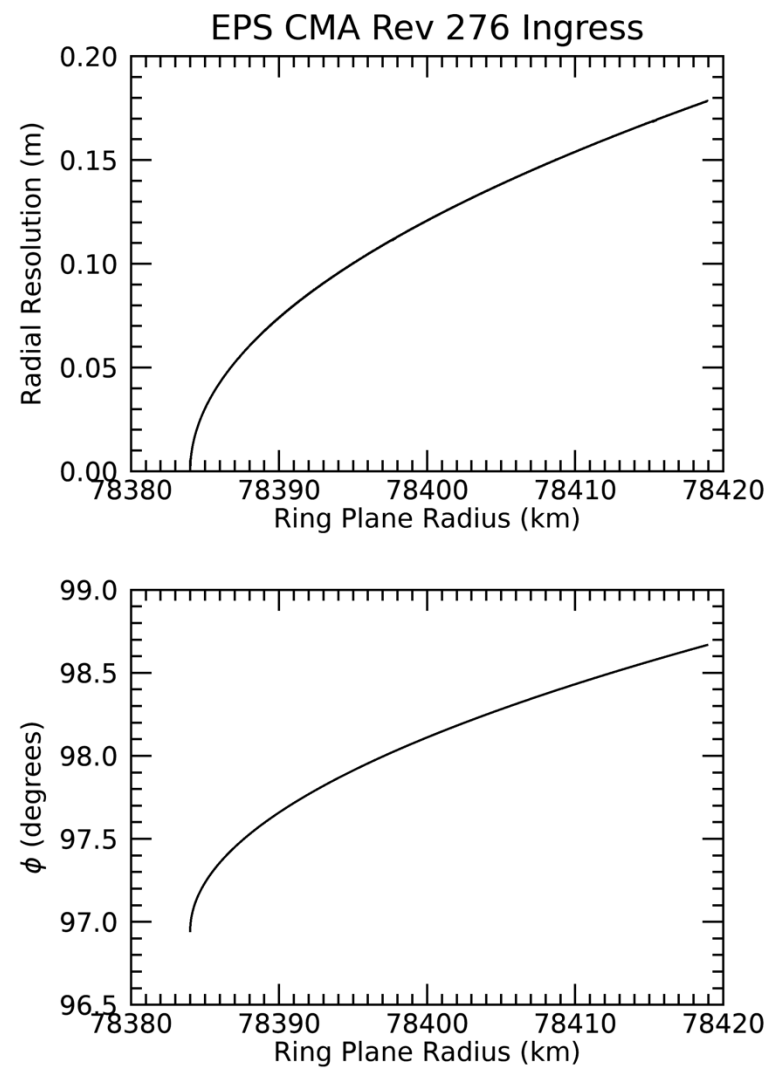
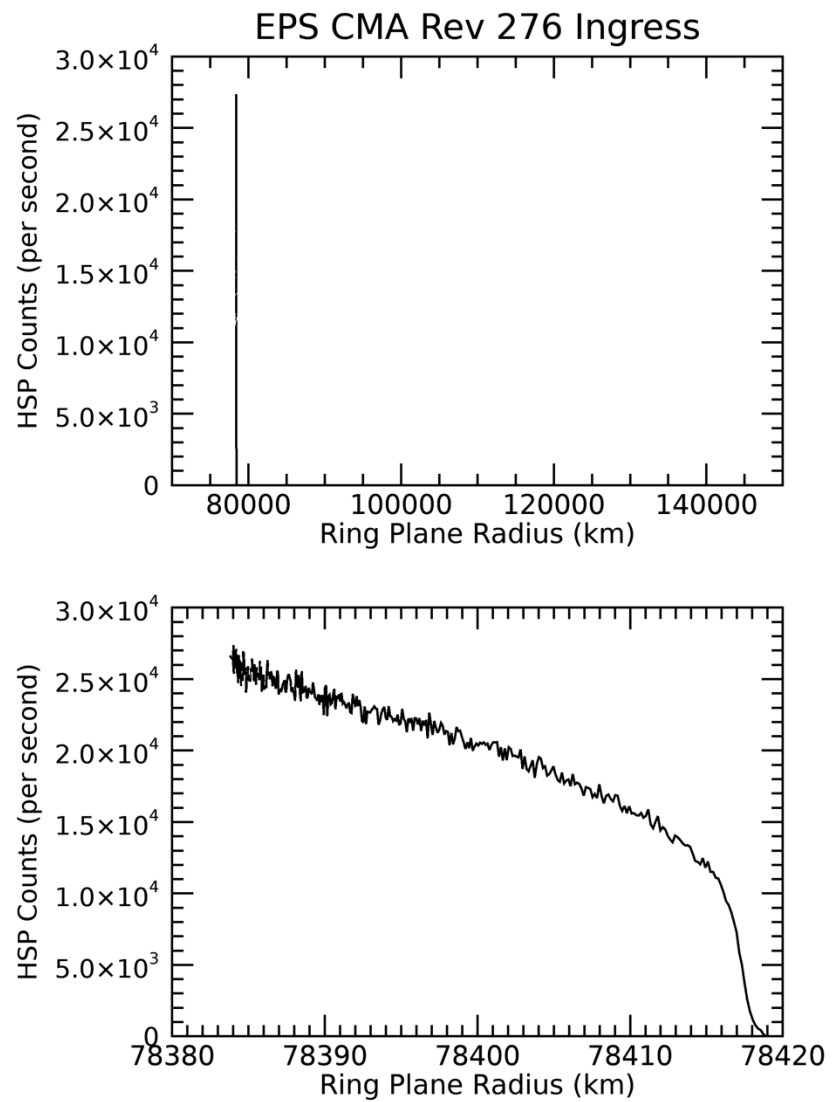


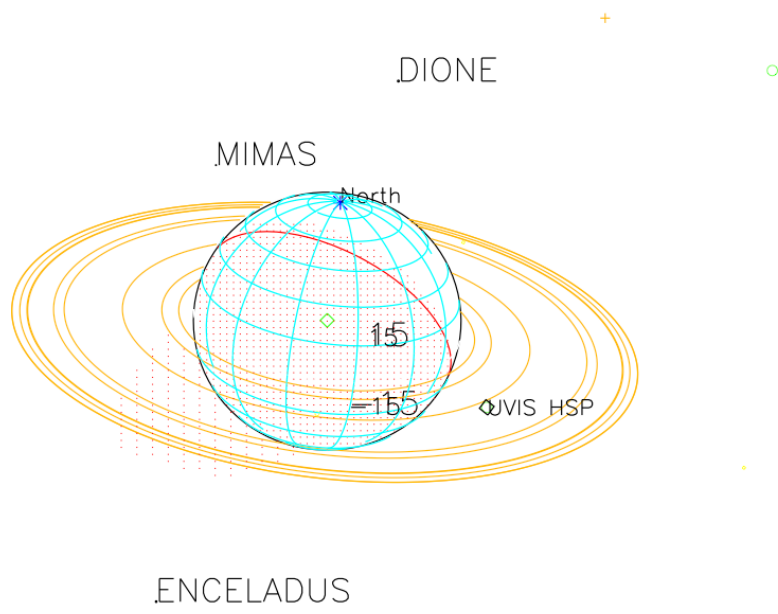
2017-133T21:49:00.000 1121506.0 km

Target RA/dec: 105.23, -16.85

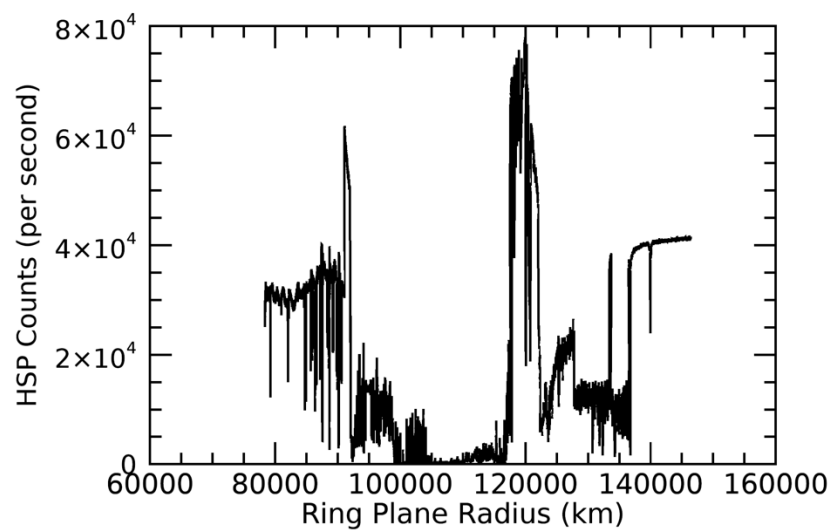
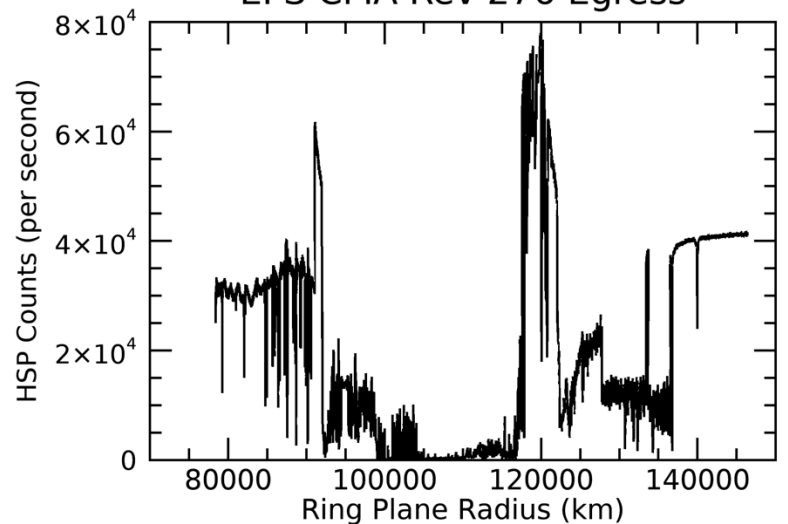
Subsolar lat/lon: 22.28, 128.10

Sub-s/c lat/lon: 11.58, -33.03

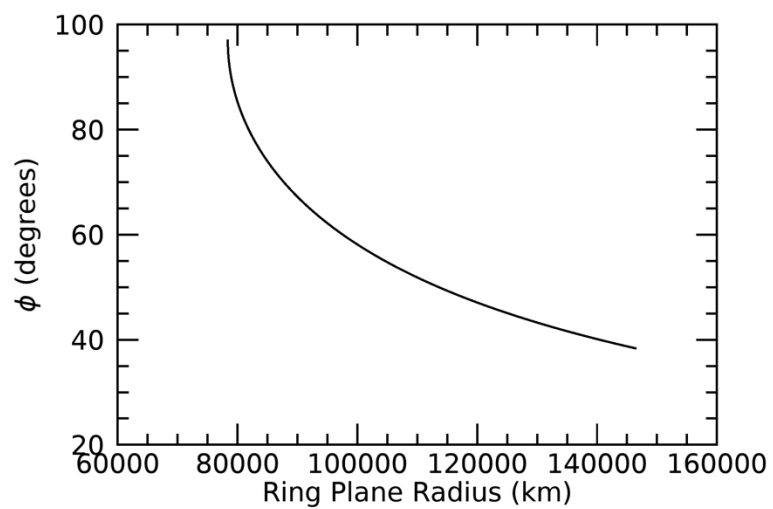
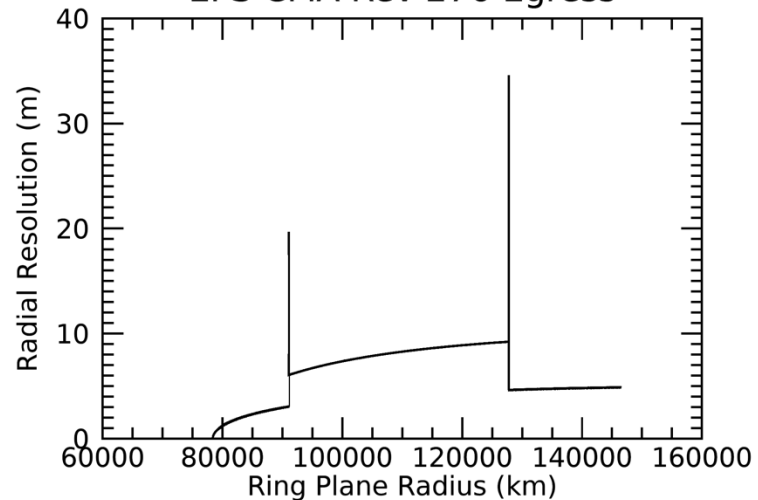


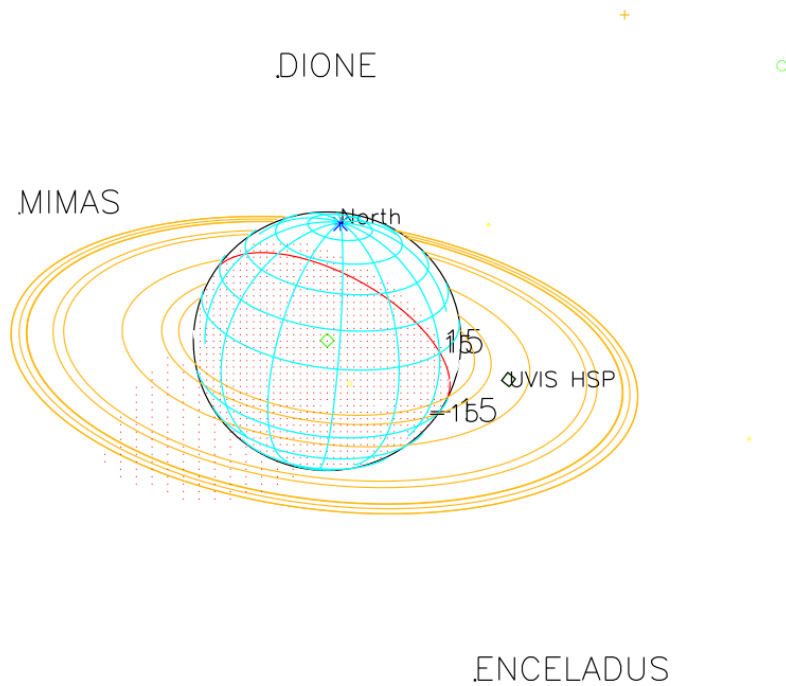


EPS CMA Rev 276 Egress

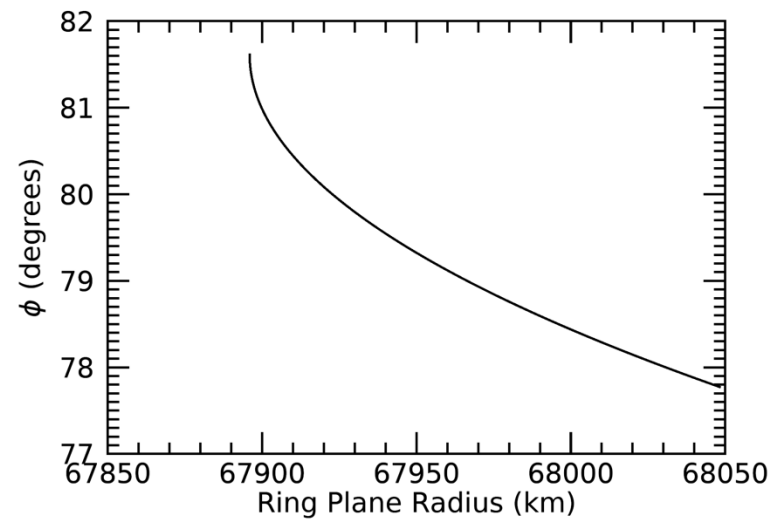
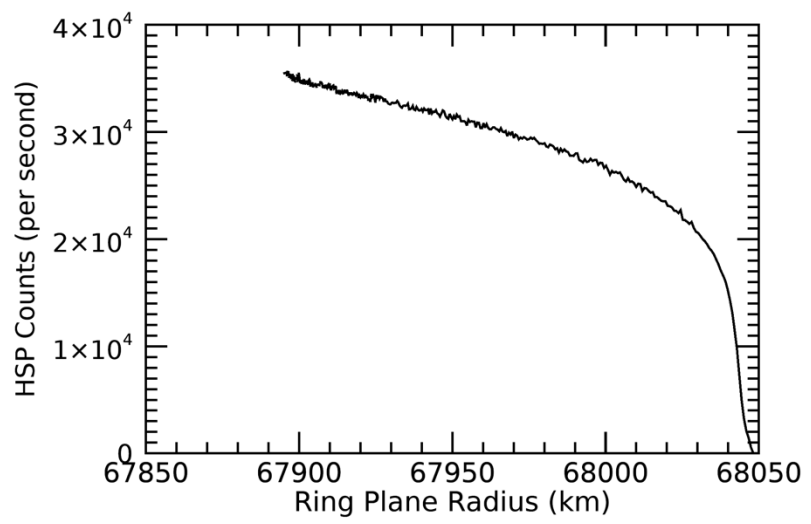
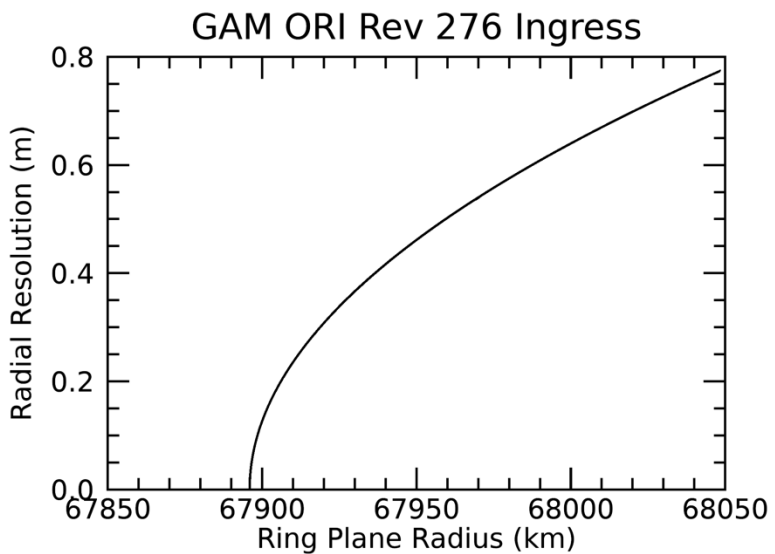
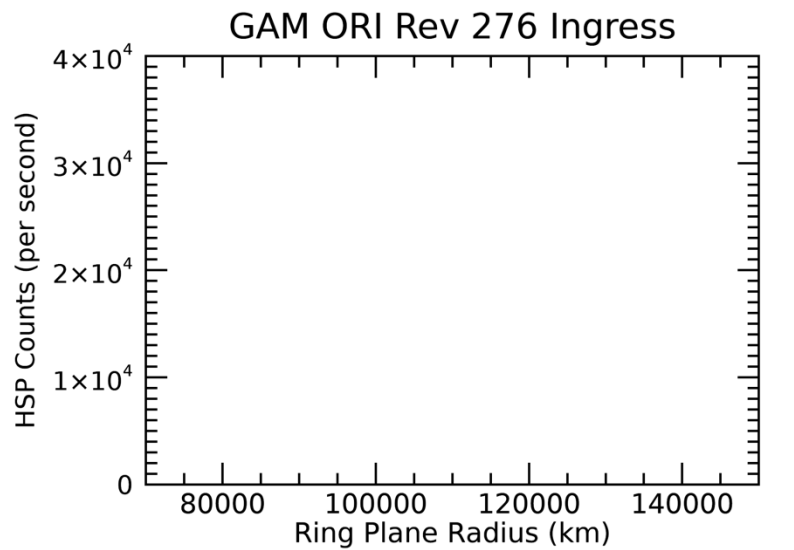


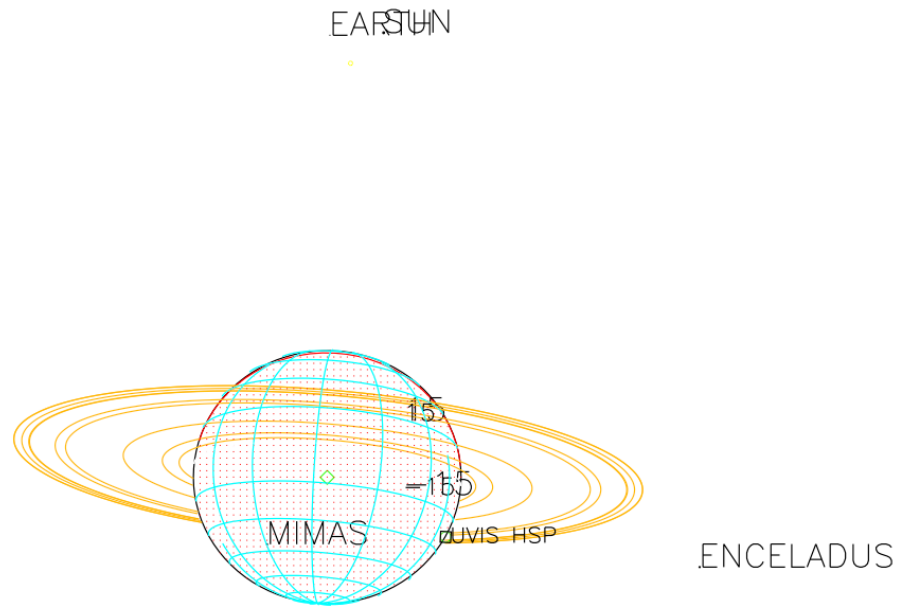
EPS CMA Rev 276 Egress





2017-147T21:44:00.000 733769.72 km
Target RA/dec: 111.94, -27.84
Subsolar lat/lon: 22.28, -59.74
Sub-s/c lat/lon: 21.61, 143.91



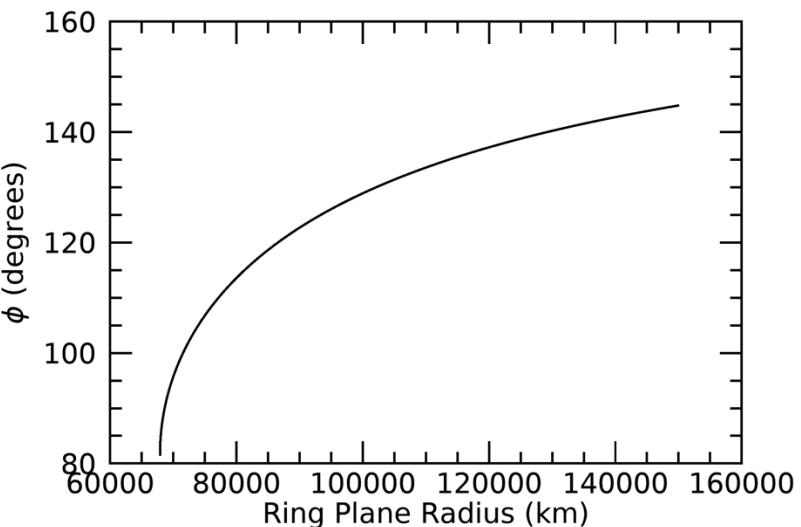
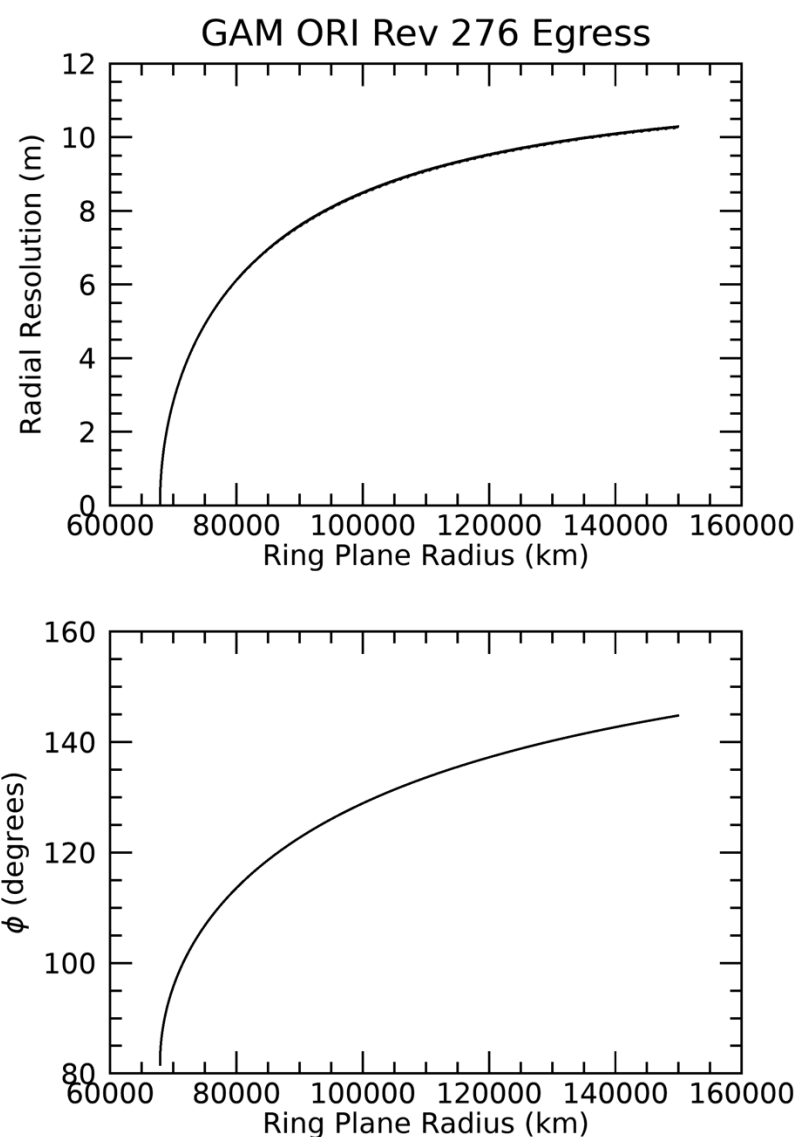
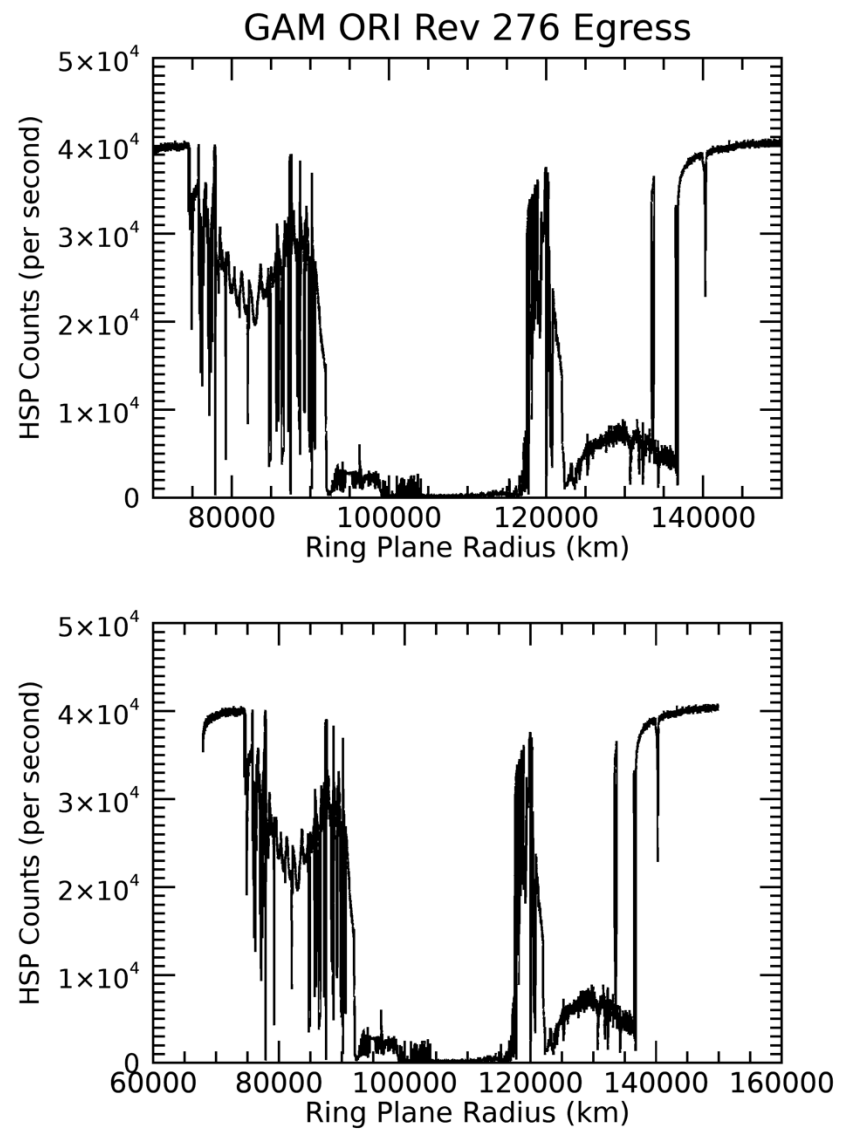


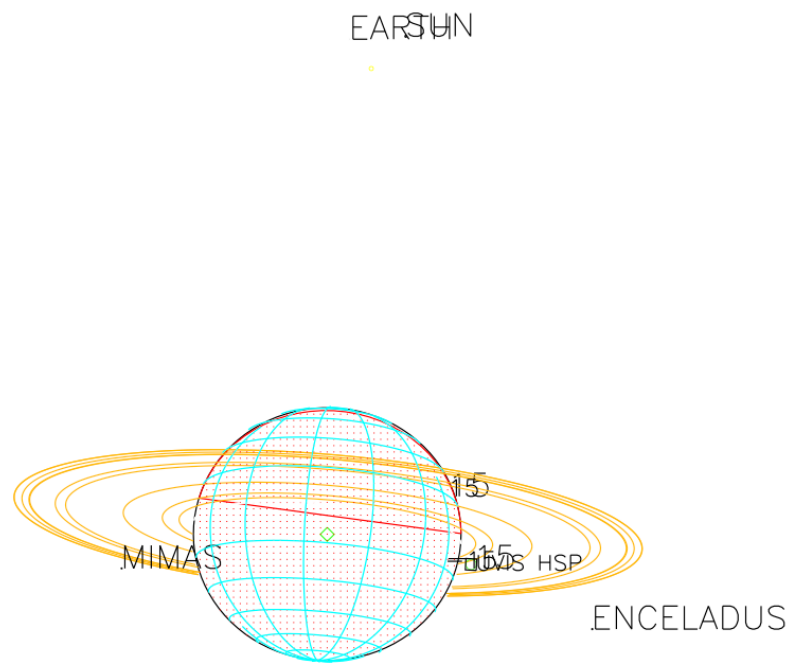
2017-149T14:26:00.000 781827.32 km

Target RA/dec: 85.22, 8.25

Subsolar lat/lon: 22.28, 5.35

Sub-s/c lat/lon: -10.64, -173.87



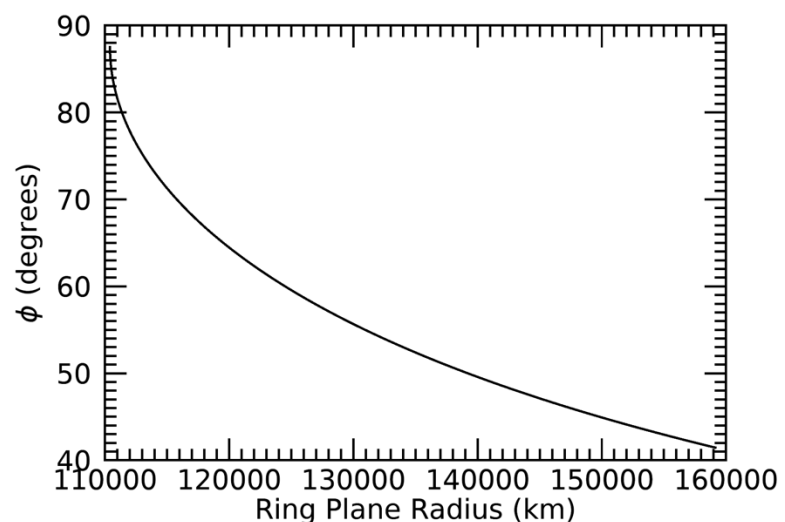
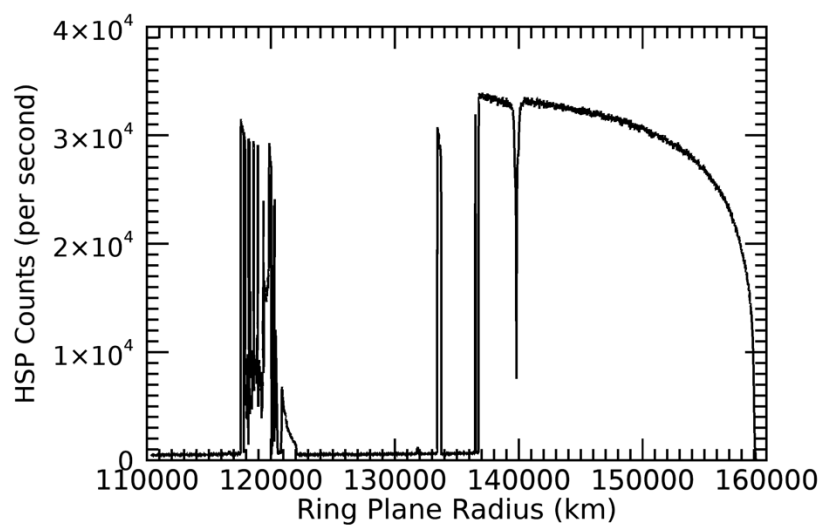
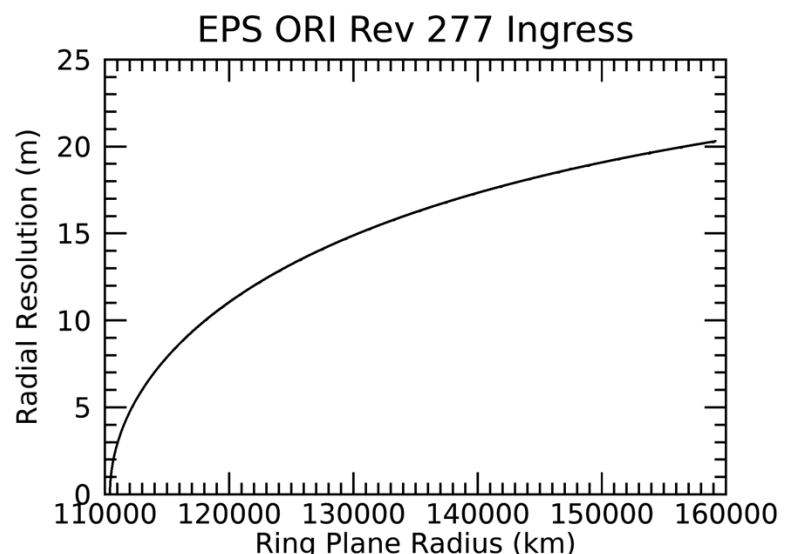
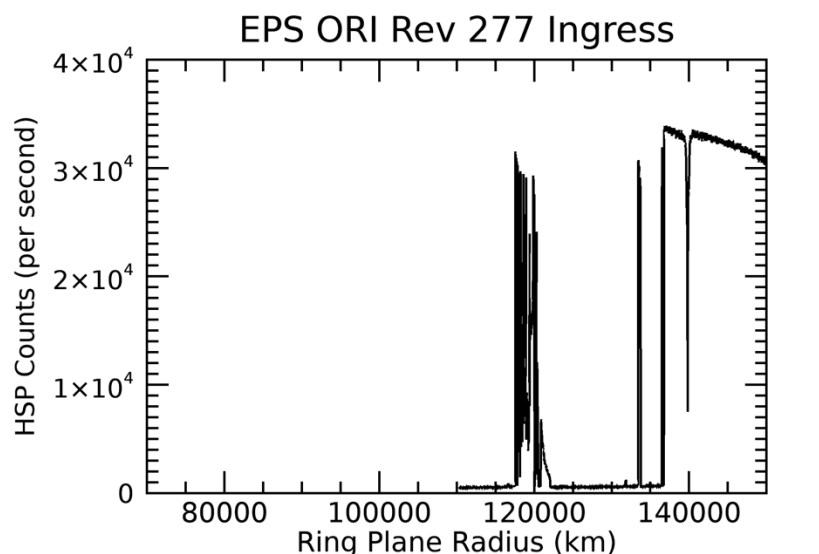


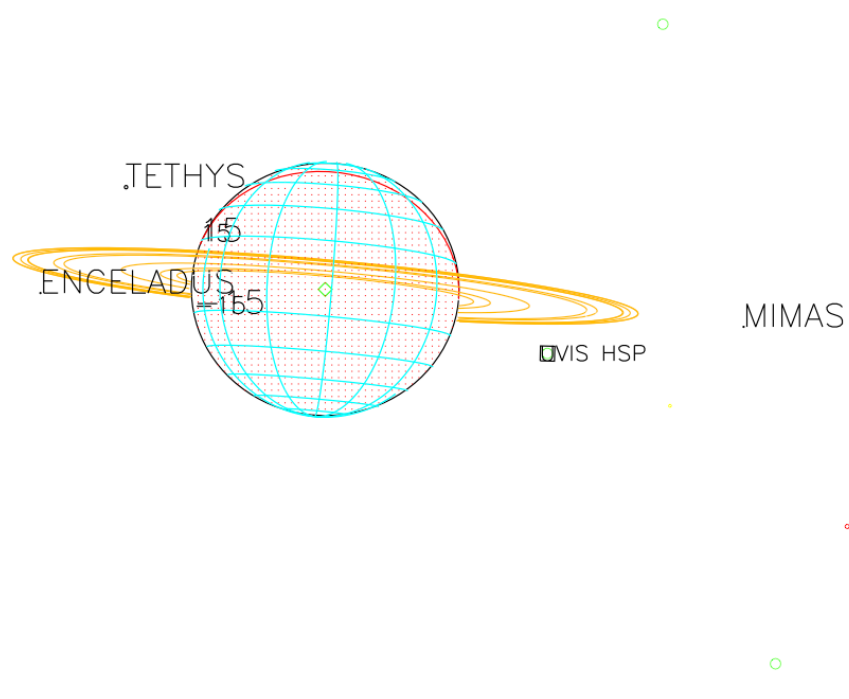
2017-149T16:06:00.000 815292.06 km

Target RA/dec: 85.87, 7.28

Subsolar lat/lon: 22.28, -50.95

Sub-s/c lat/lon: -9.78, 130.40



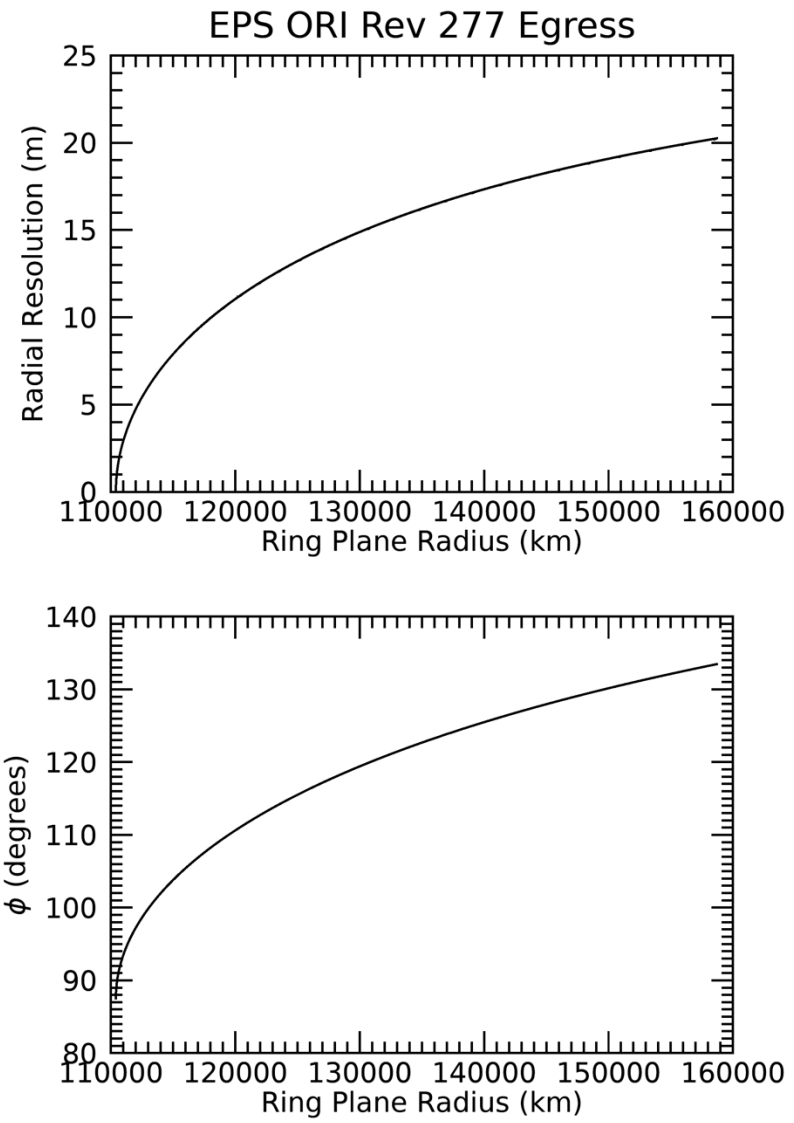
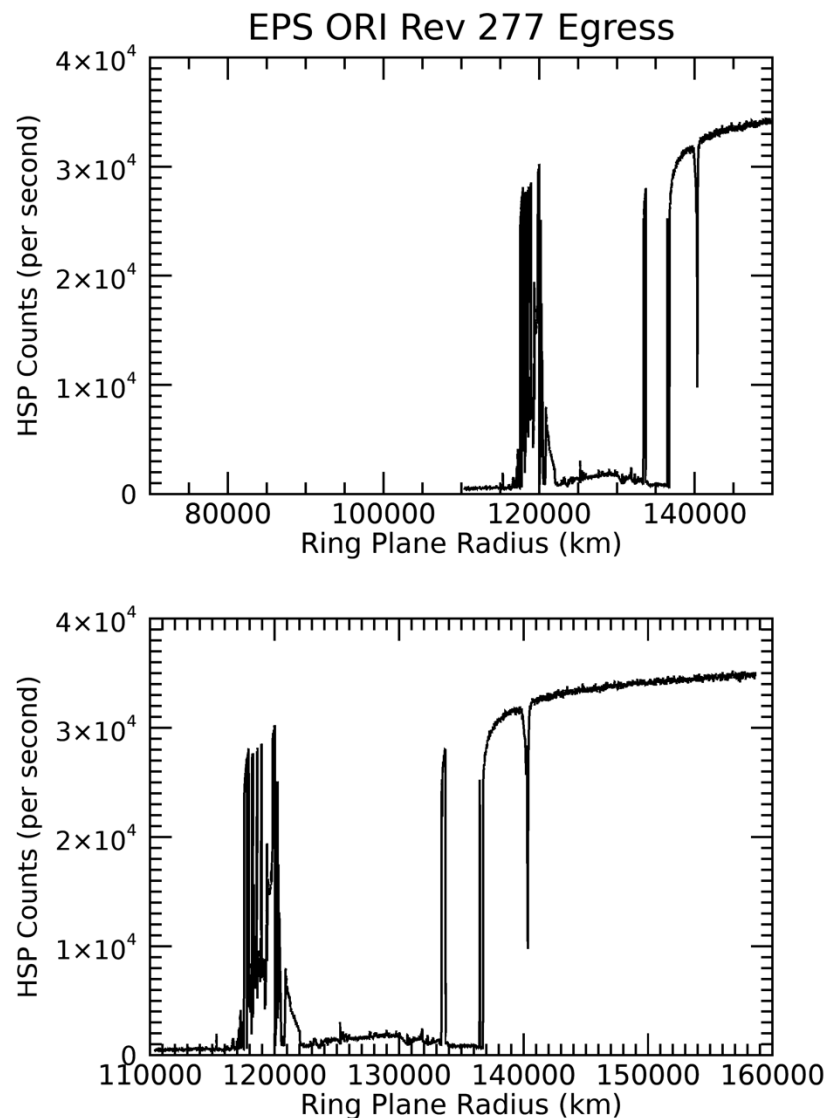


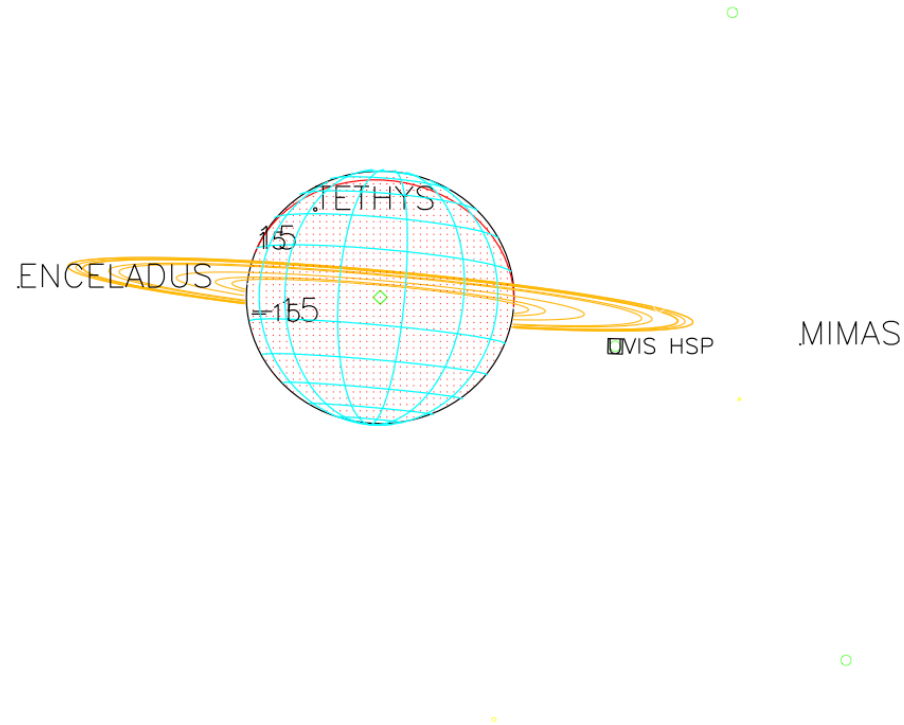
2017-156T19:58:00.000 1064808.4 km

Target RA/dec: 89.43, 0.28

Subsolar lat/lon: 22.28, -96.89

Sub-s/c lat/lon: -3.73, 87.21



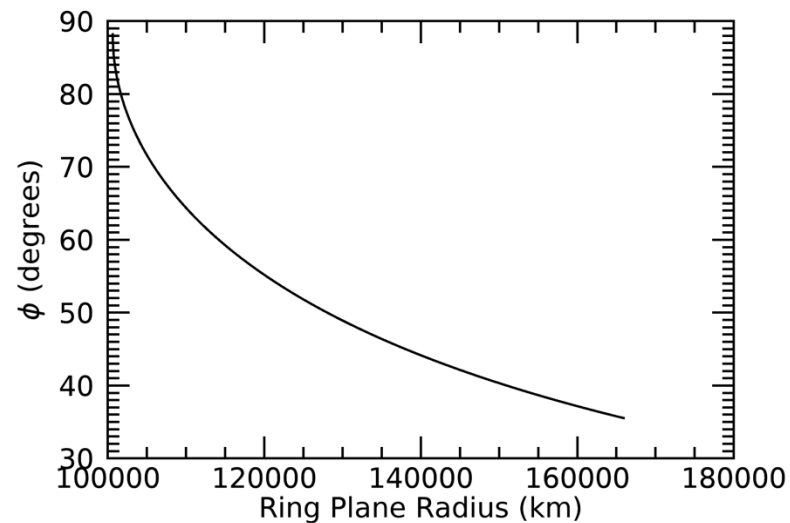
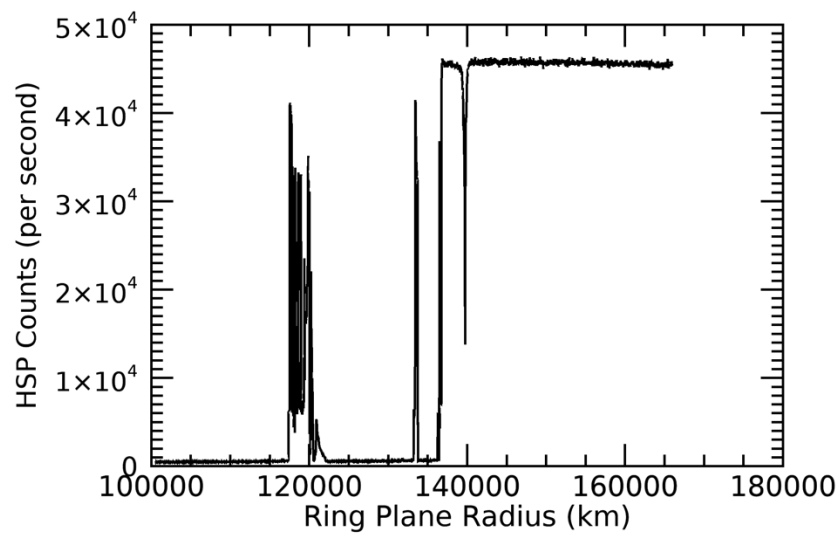
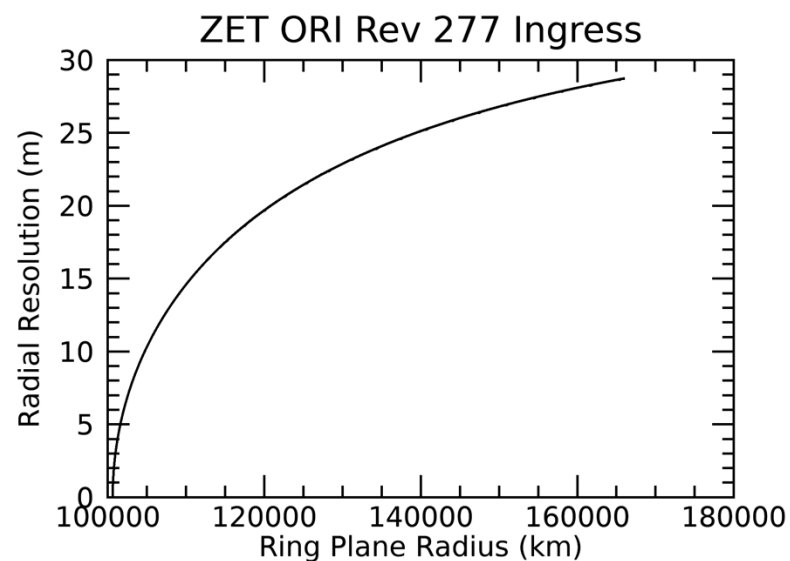
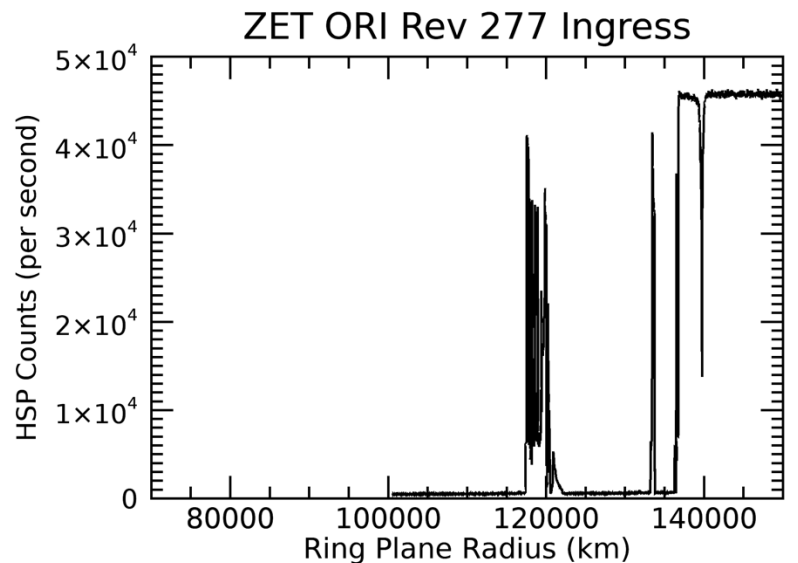


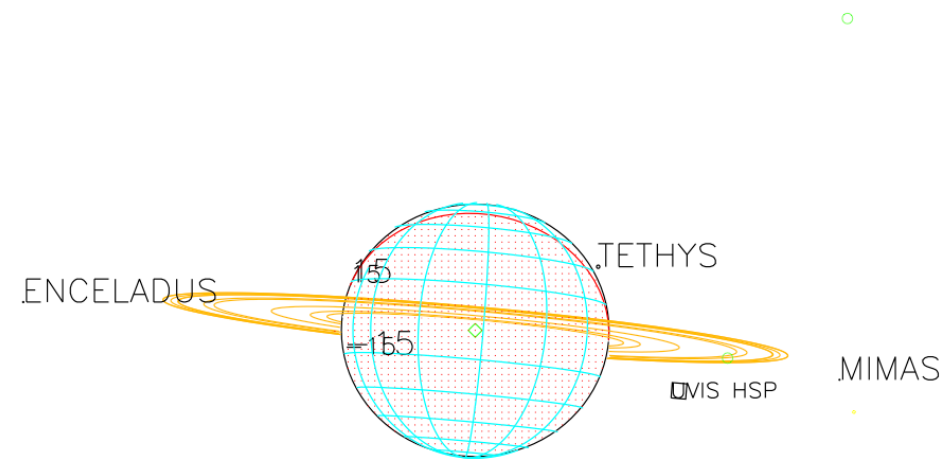
2017-156T21:06:00.000 1077819.7 km

Target RA/dec: 89.67, -0.09

Subsolar lat/lon: 22.28, -135.17

Sub-s/c lat/lon: -3.41, 49.13



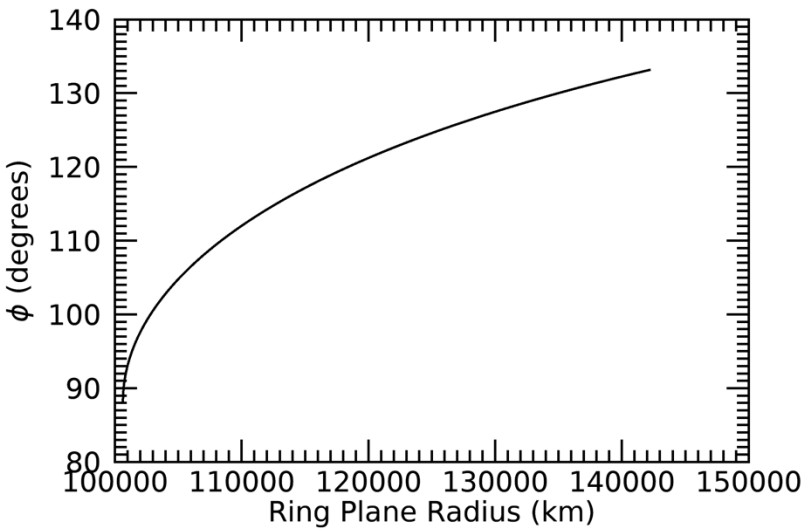
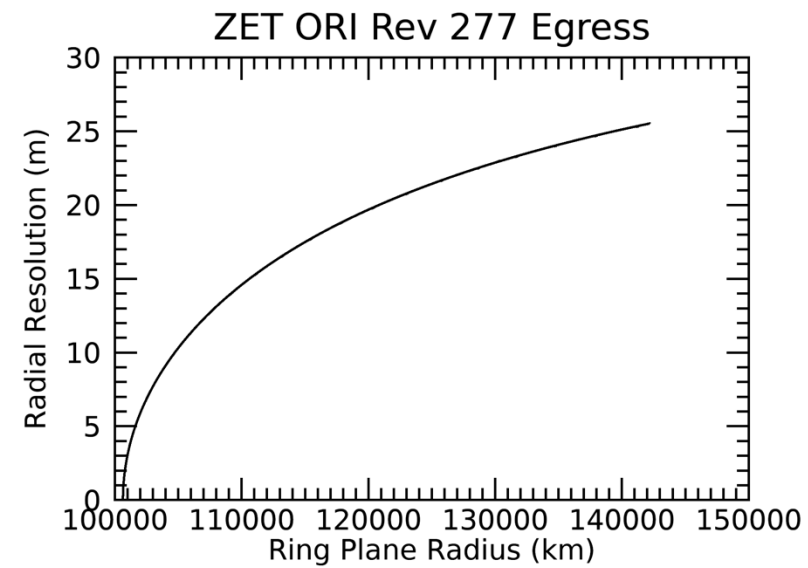
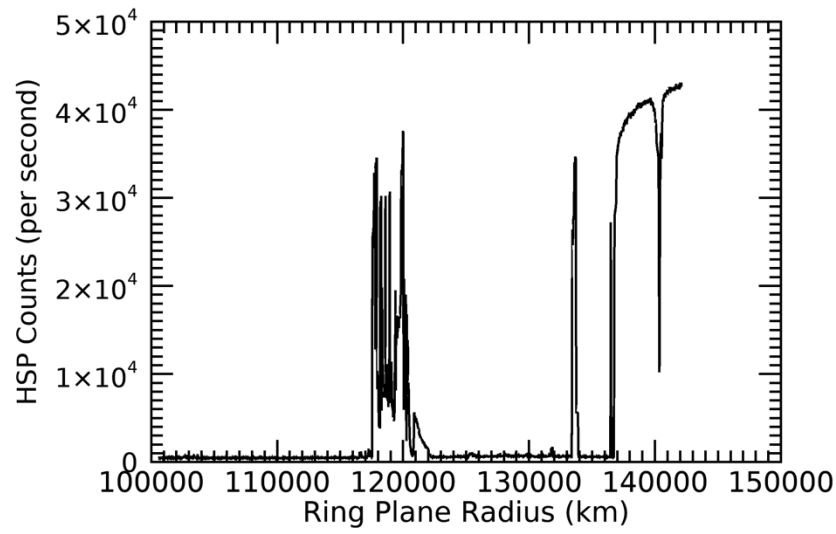
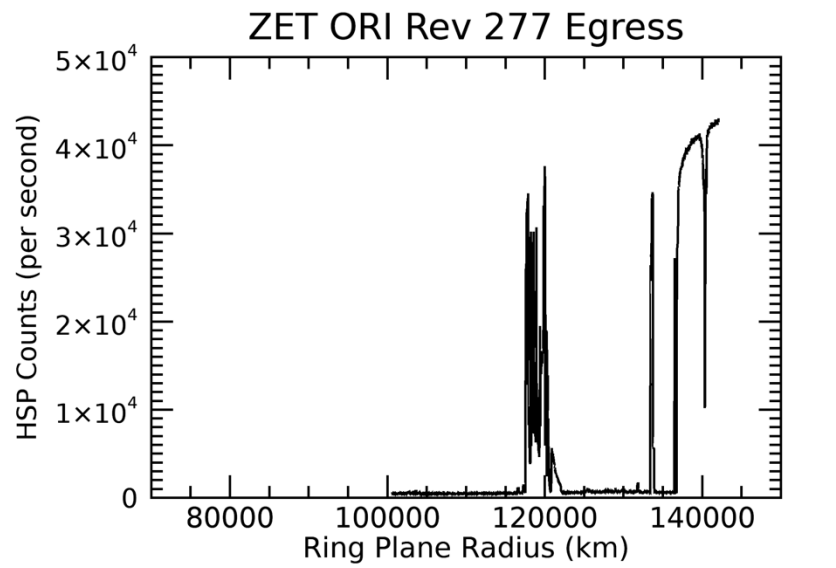


2017-156T22:40:00.000 1095014.8 km

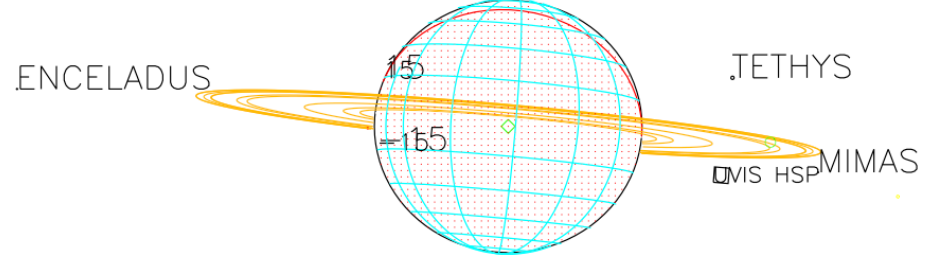
Target RA/dec: 89.99, -0.58

Subsolar lat/lon: 22.28, 171.90

Sub-s/c lat/lon: -2.98, -3.52



ONE

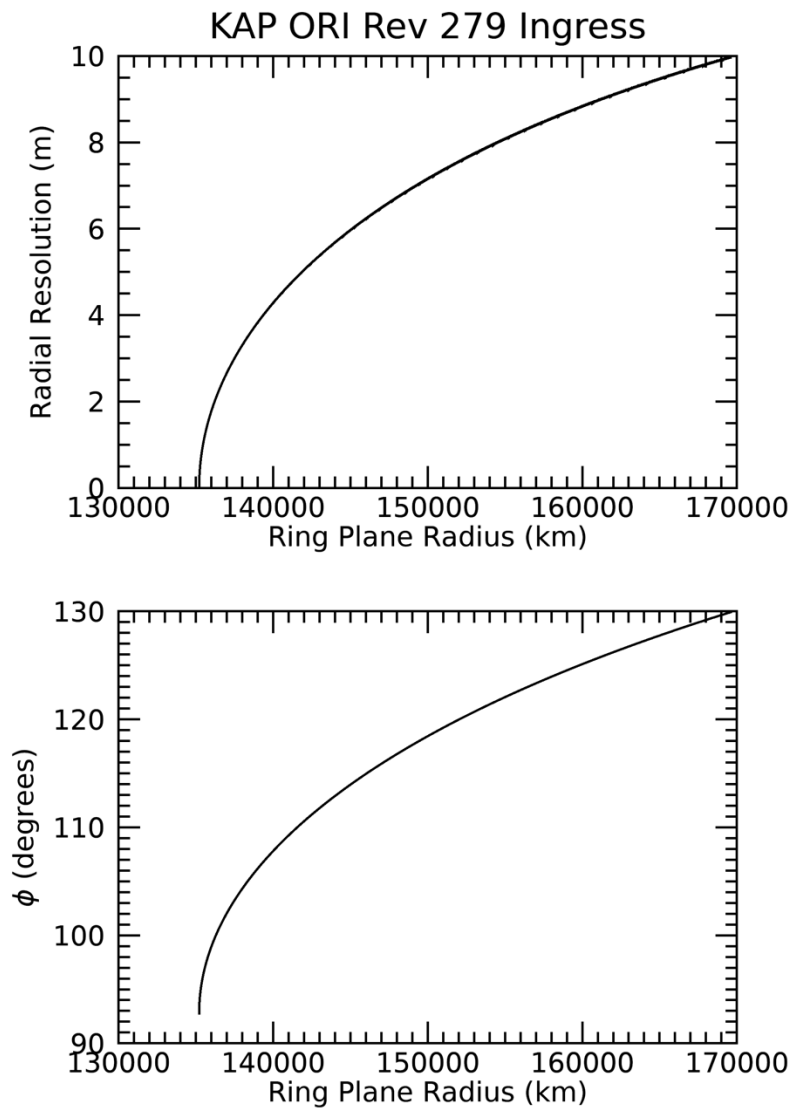
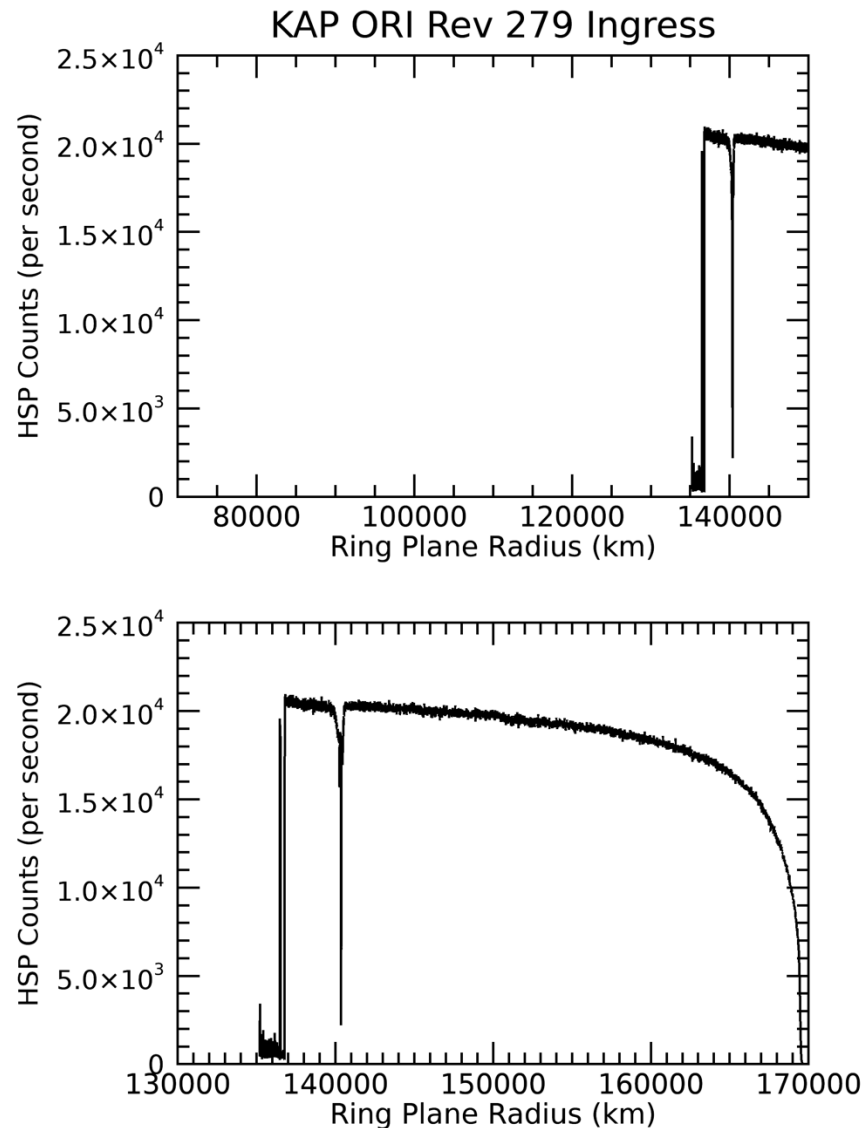


2017-156T23:33:00.000 1104314.1 km

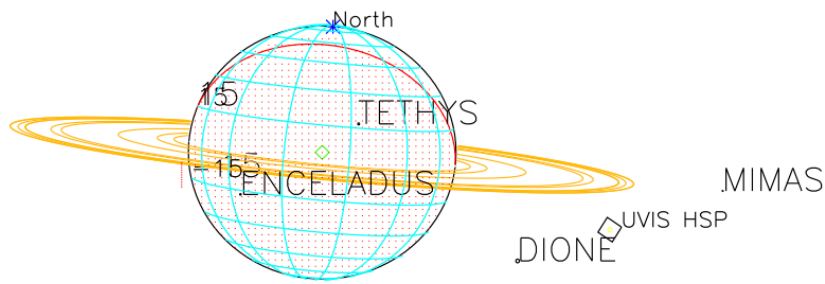
Target RA/dec: 90.17, -0.85

Subsolar lat/lon: 22.28, 142.06

Sub-s/c lat/lon: -2.74, -33.20



A



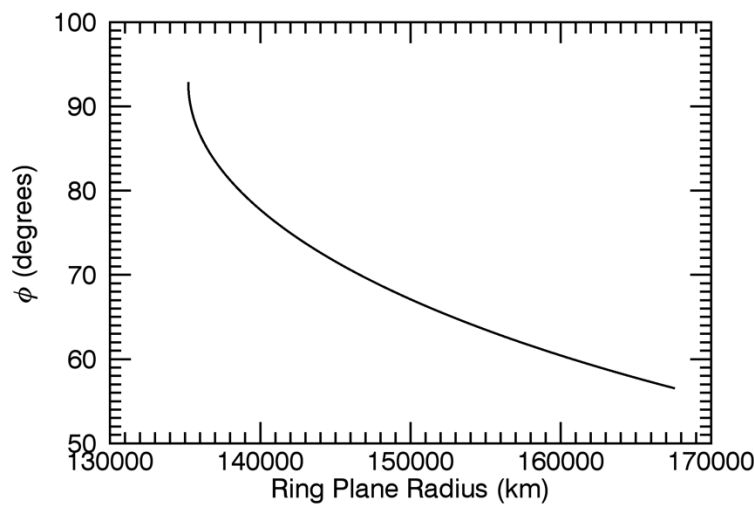
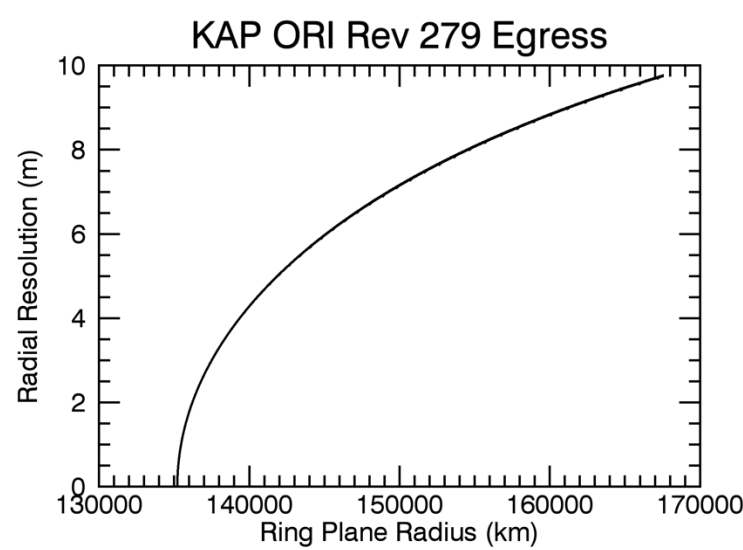
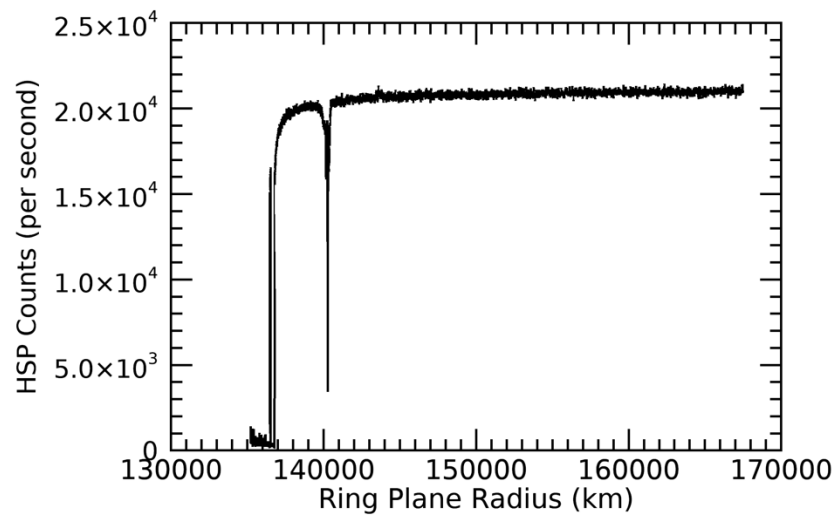
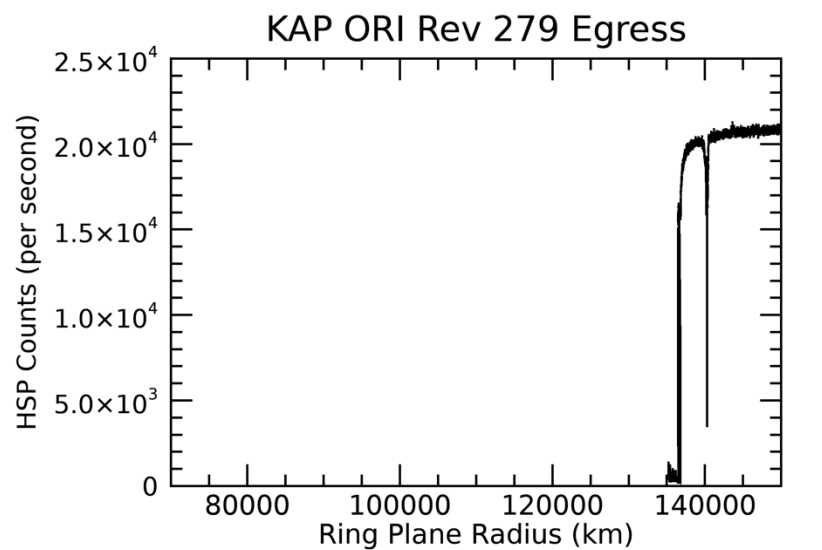
+

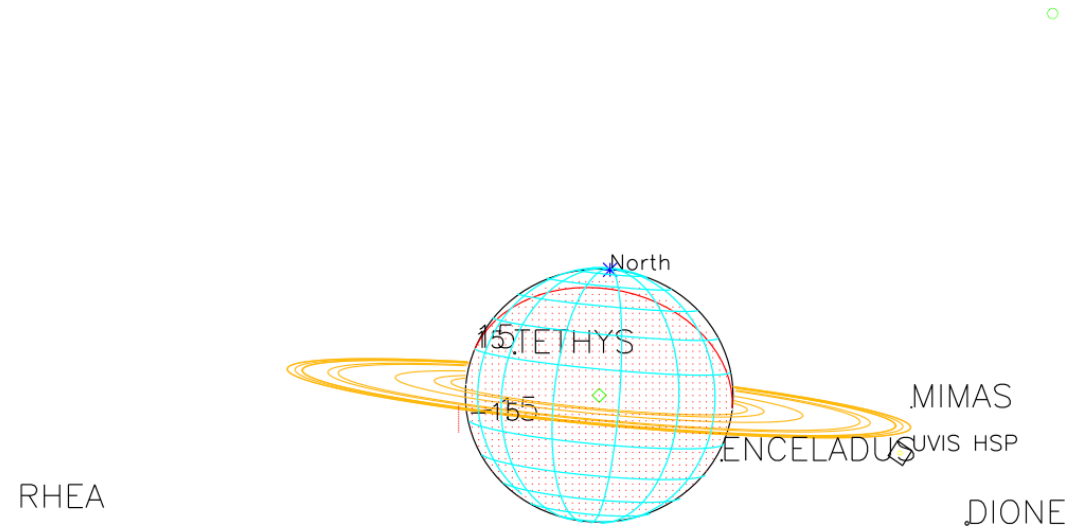
2017-171T01:20:00.000 1267636.8 km

Target RA/dec: 92.86, -8.21

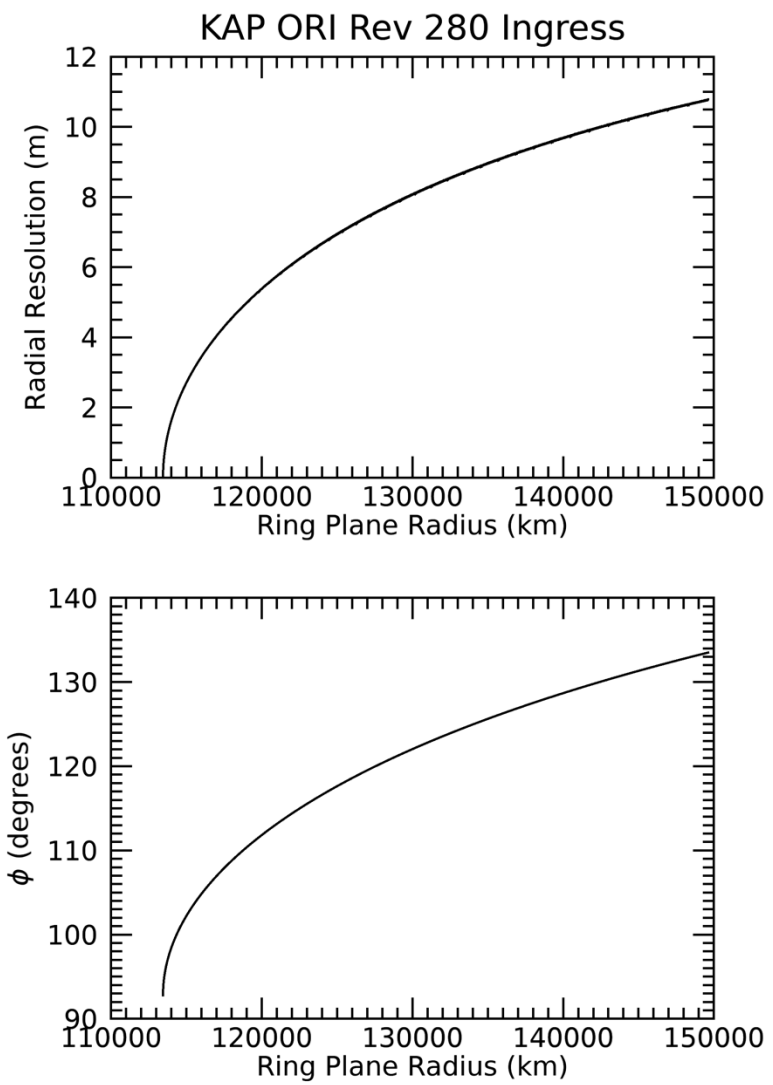
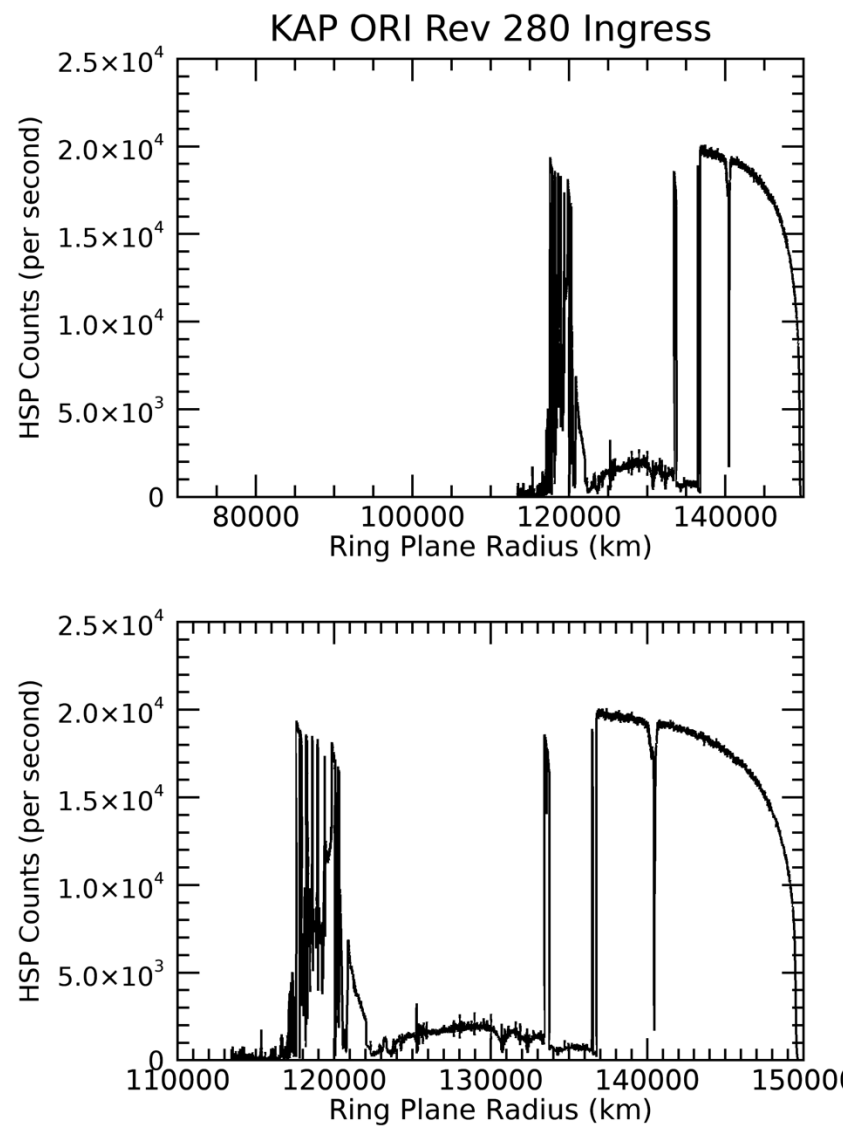
Subsolar lat/lon: 22.28, -108.82

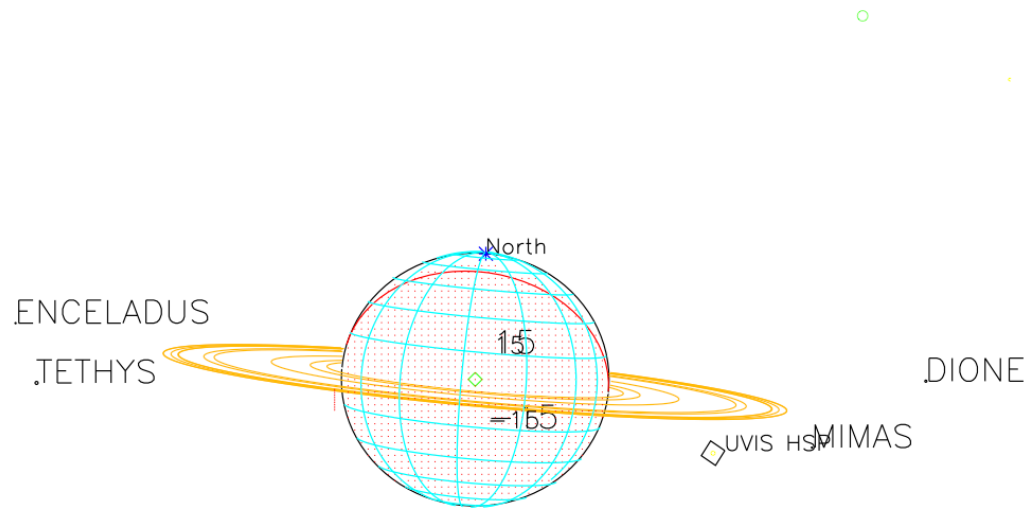
Sub-s/c lat/lon: 3.48, 77.47





2017-171T03:01:00.000 1270770.4 km
Target RA/dec: 93.12, -8.60
Subsolar lat/lon: 22.28, -165.68
Sub-s/c lat/lon: 3.81, 20.83



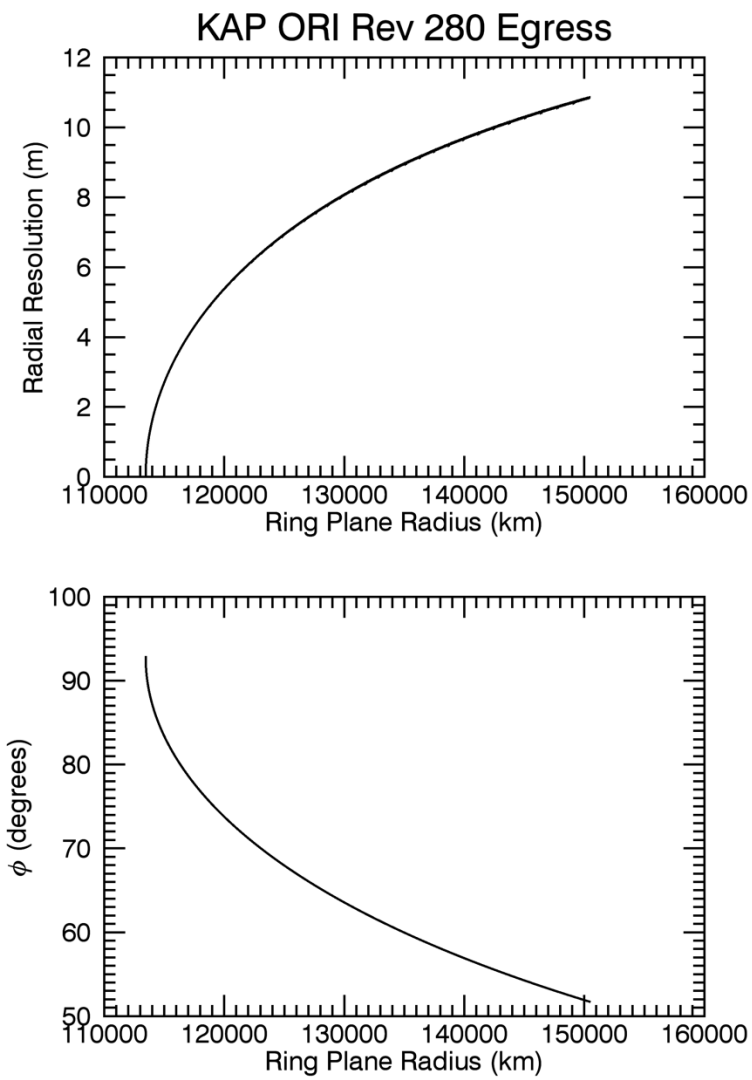
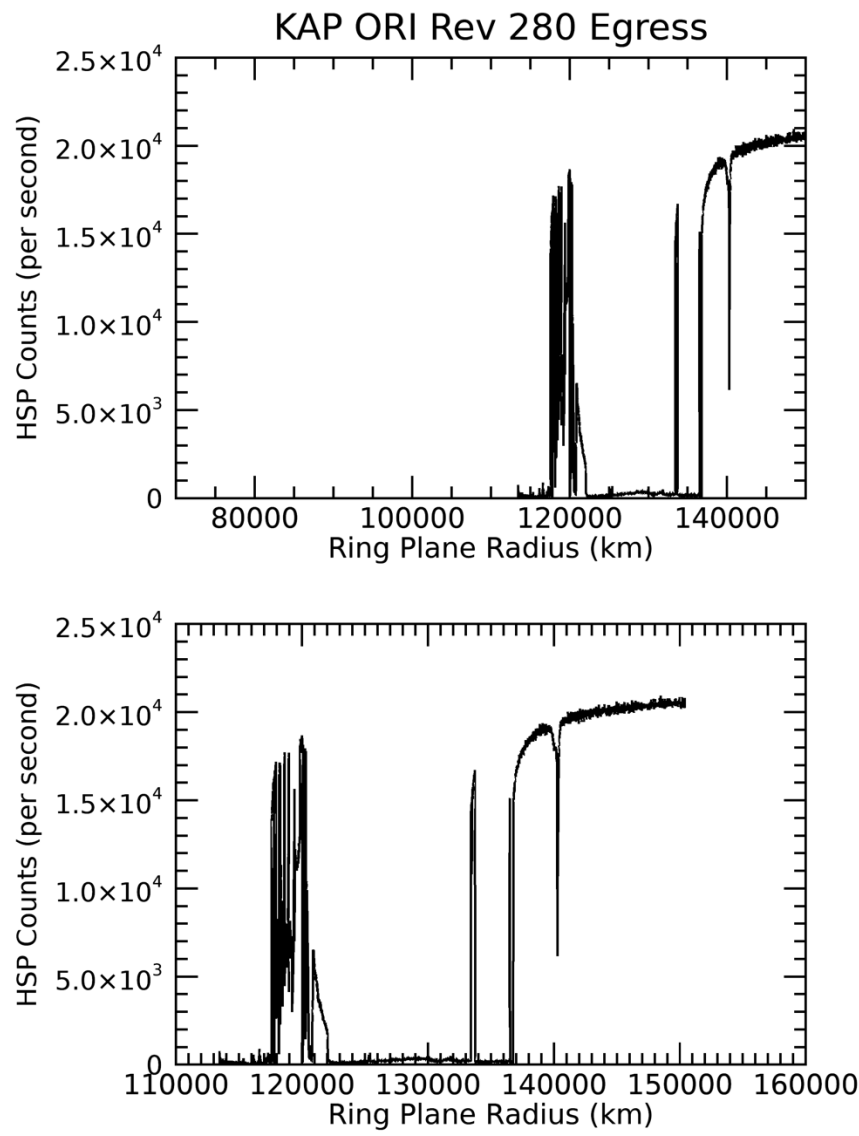


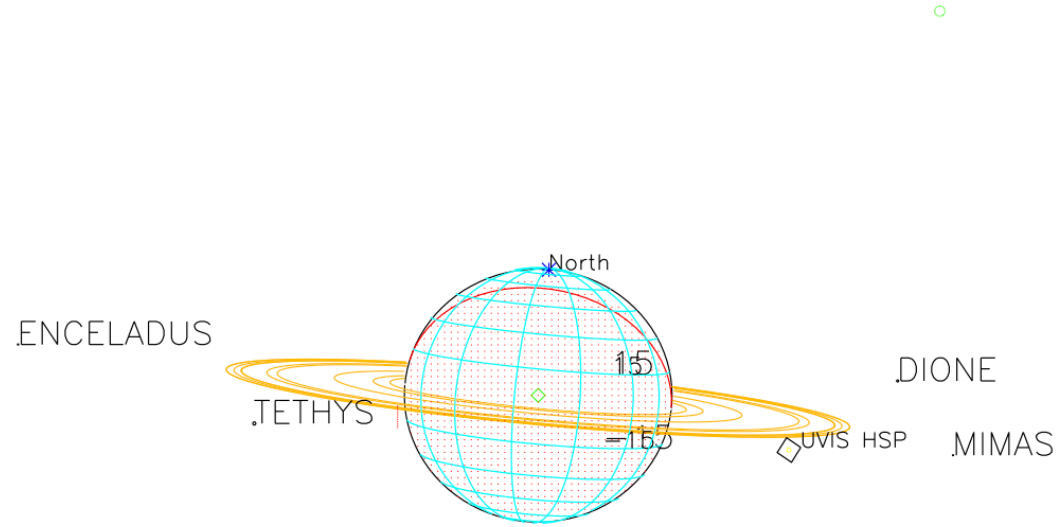
2017-177T12:09:00.000 1267324.5 km

Target RA/dec: 91.84, -8.26

Subsolar lat/lon: 22.28, 61.21

Sub-s/c lat/lon: 3.45, -113.72





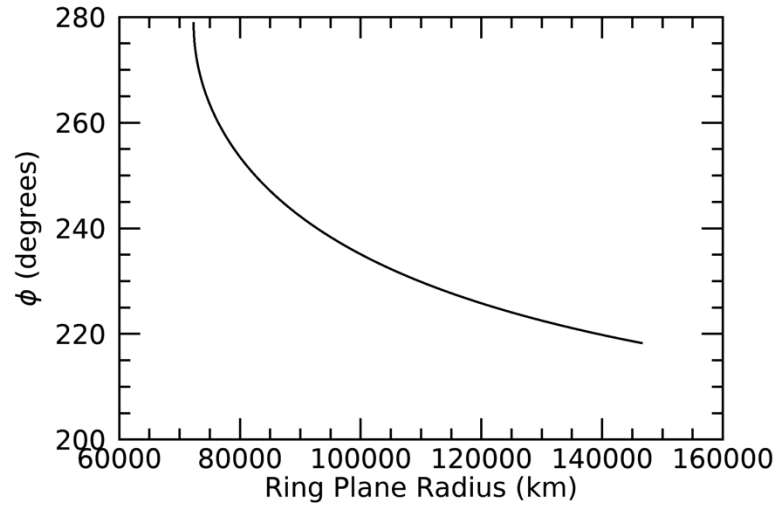
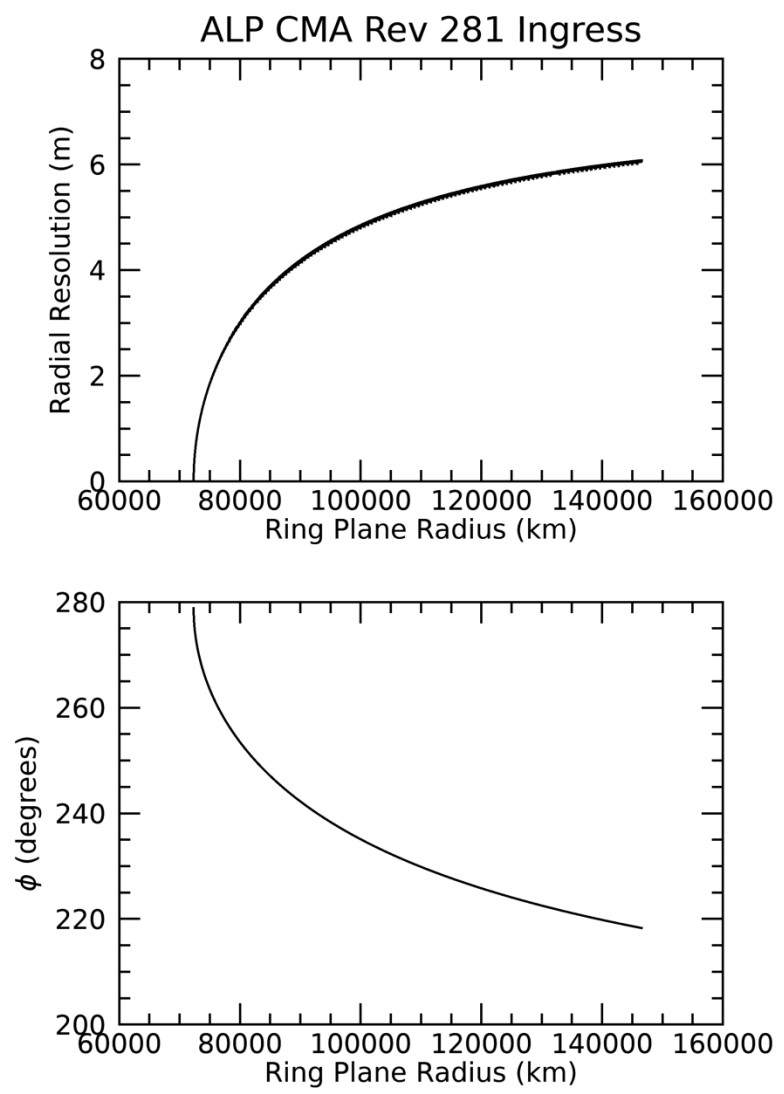
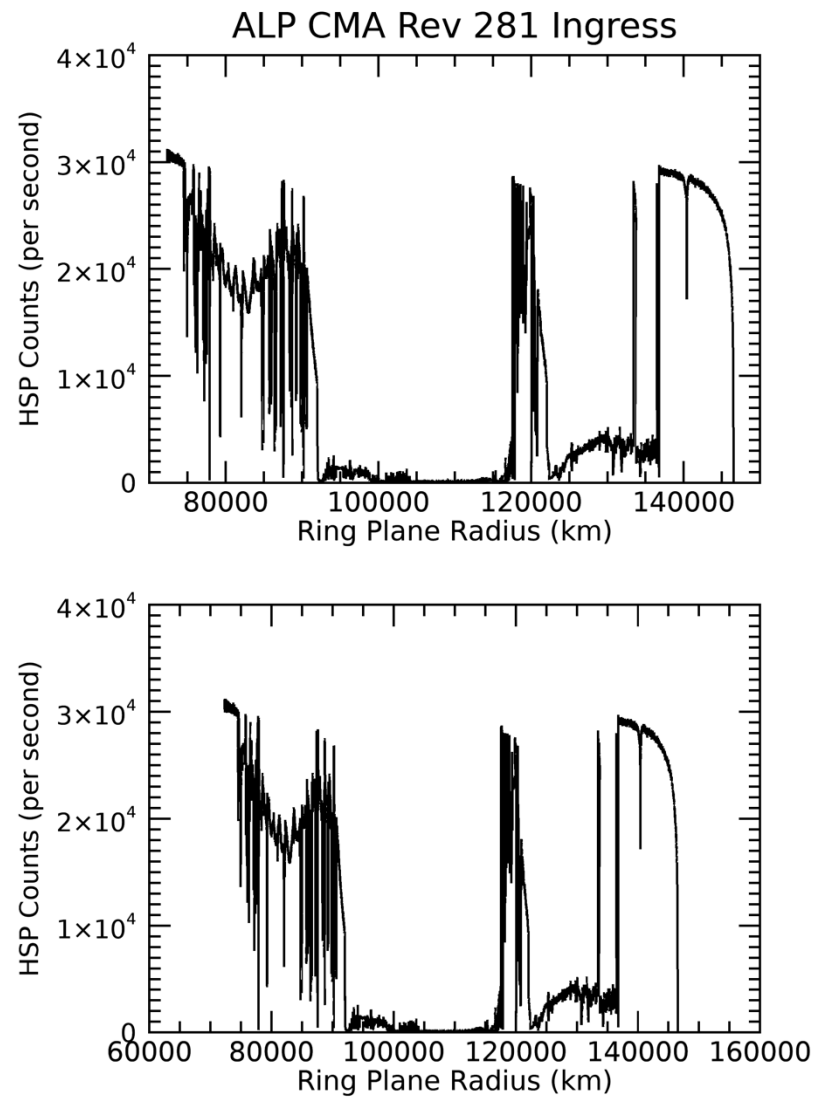
+

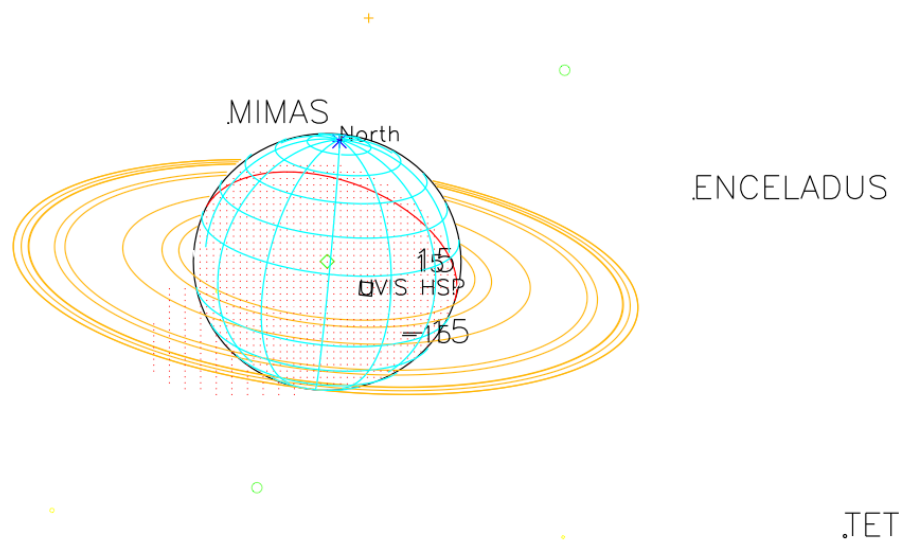
2017-177T13:48:00.000 1270667.6 km

Target RA/dec: 92.10, -8.64

Subsolar lat/lon: 22.28, 5.47

Sub-s/c lat/lon: 3.77, -169.25



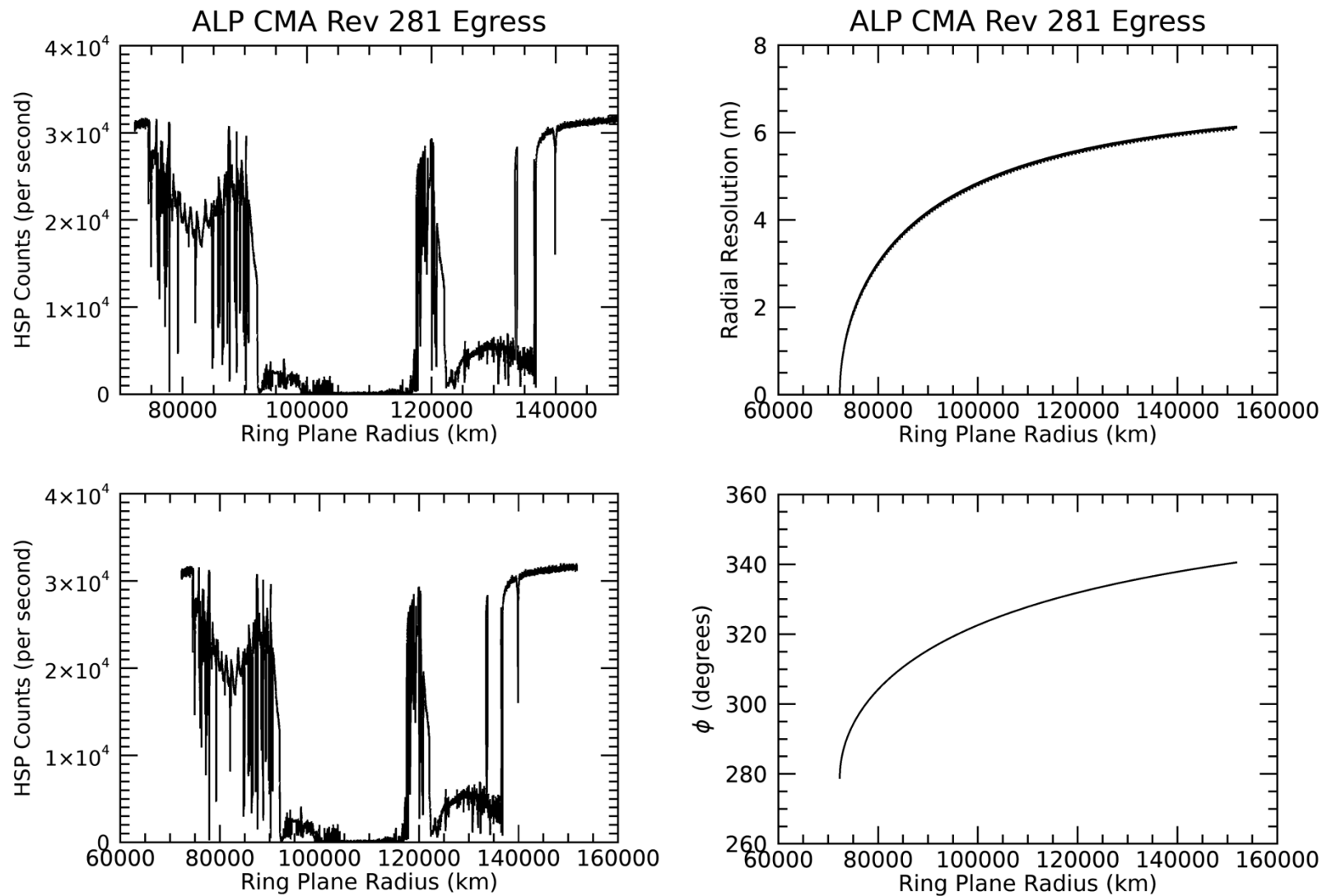


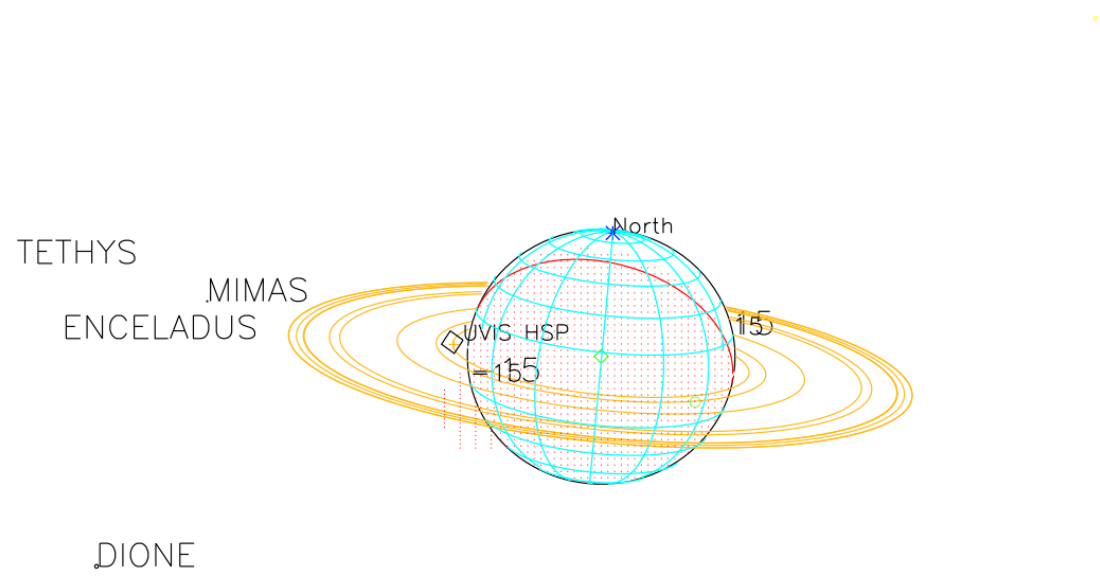
2017-179T19:42:00.000 942919.47 km

Target RA/dec: 102.47, -23.07

Subsolar lat/lon: 22.28, -15.37

Sub-s/c lat/lon: 16.61, 178.57



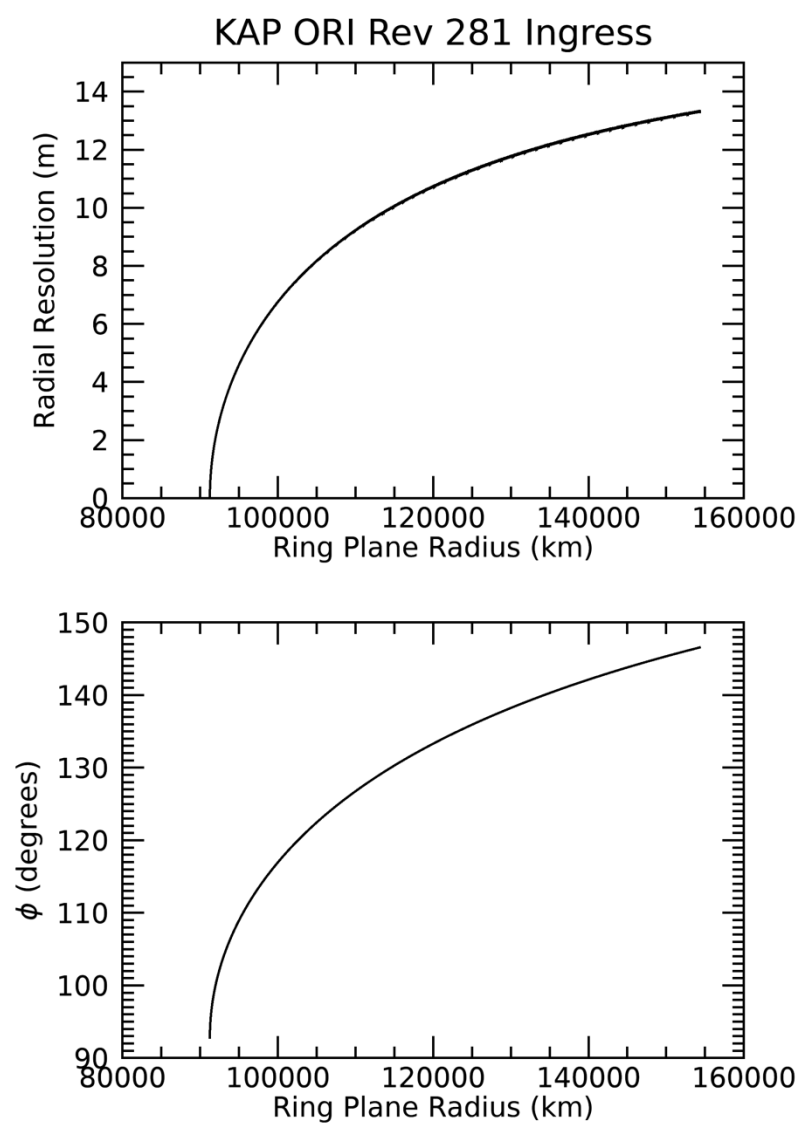
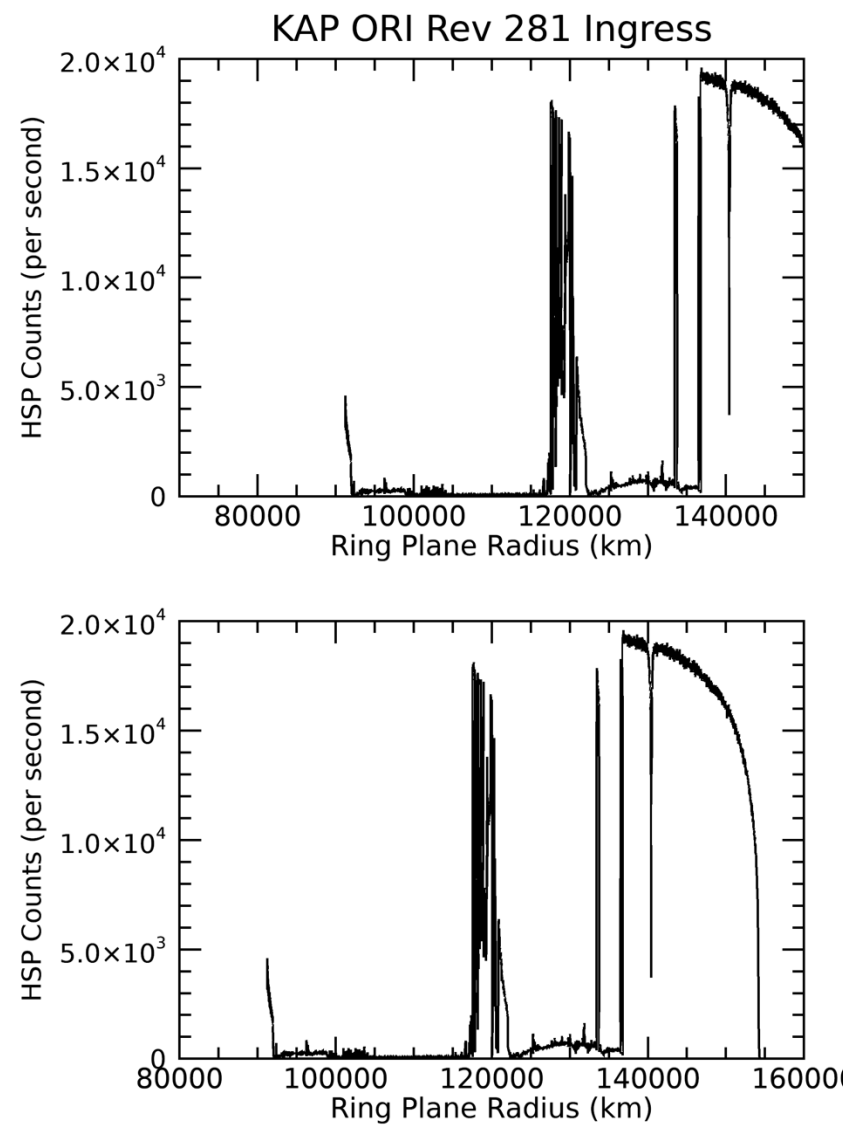


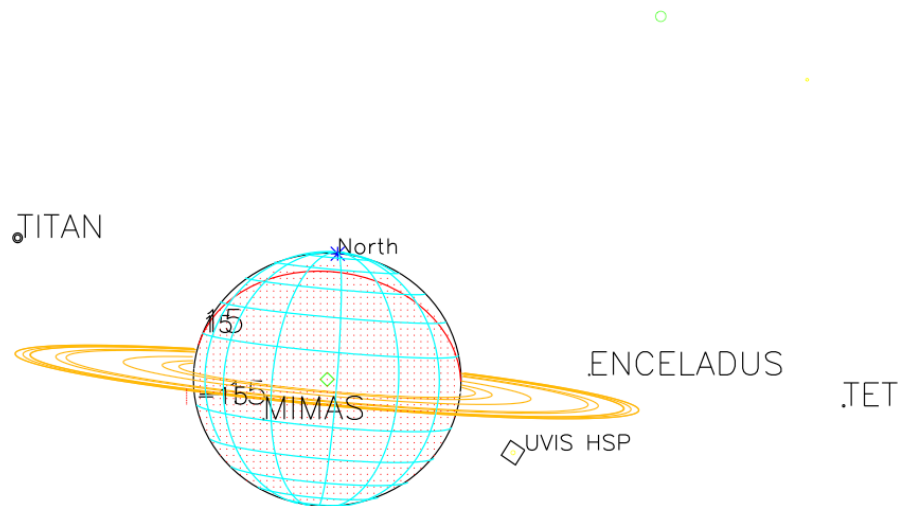
2017-179T00:54:00.000 1162268.5 km

Target RA/dec: 97.87, -17.00

Subsolar lat/lon: 22.28, -100.27

Sub-s/c lat/lon: 11.10, 89.85



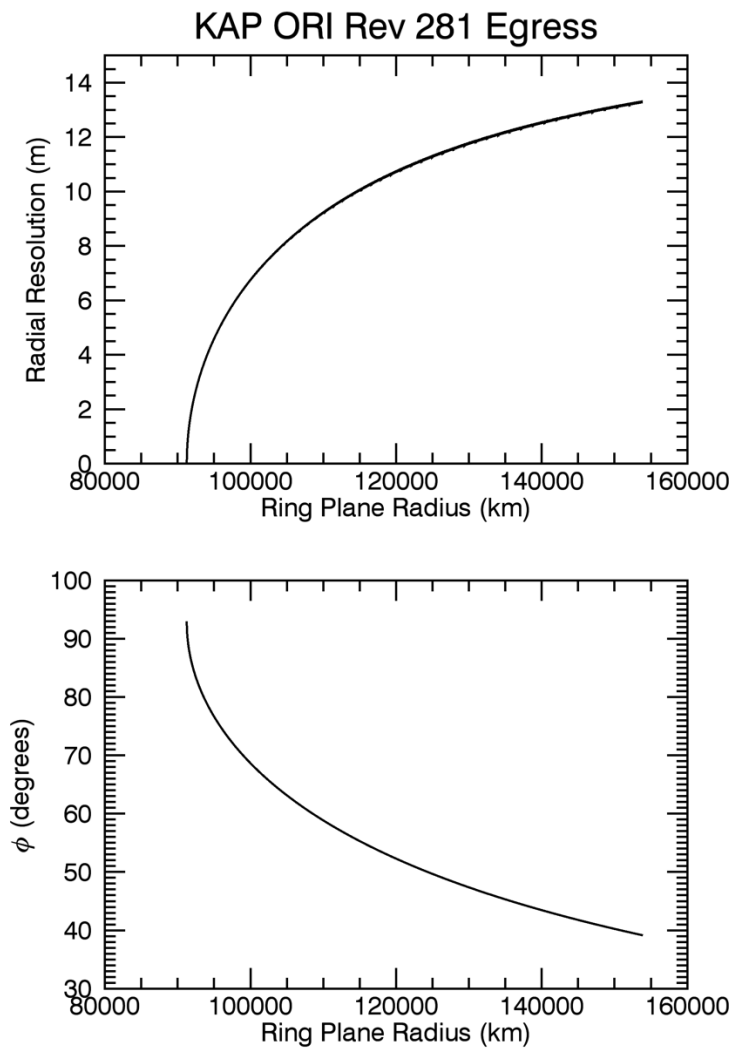
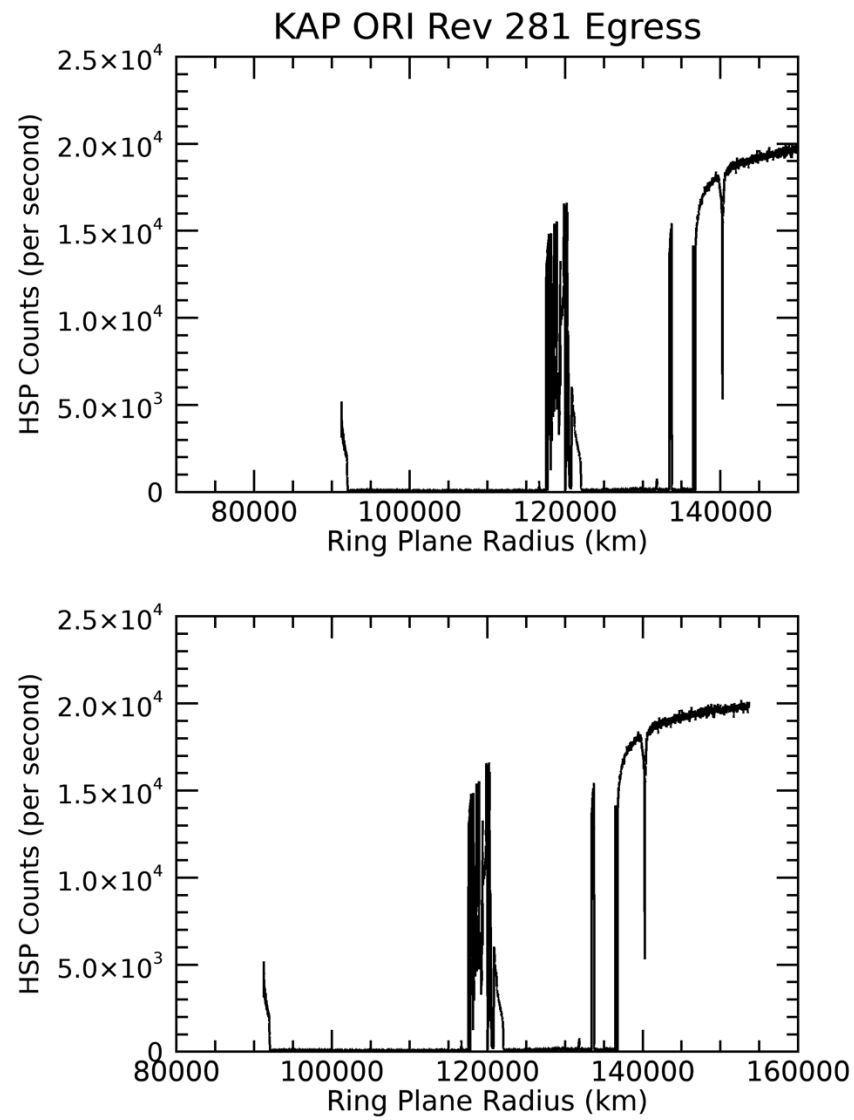


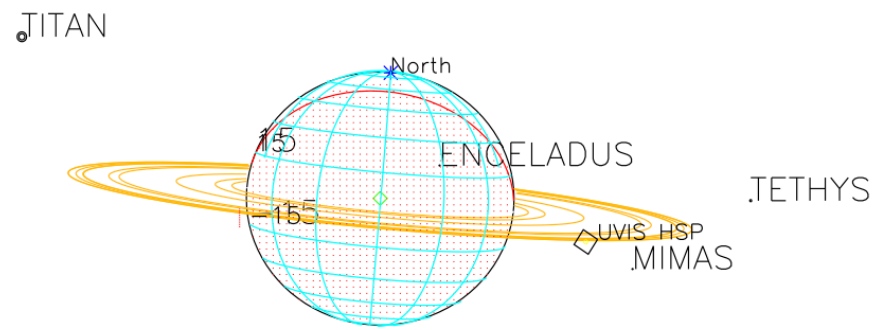
2017-183T22:57:00.000 1265813.5 km

Target RA/dec: 90.78, -8.26

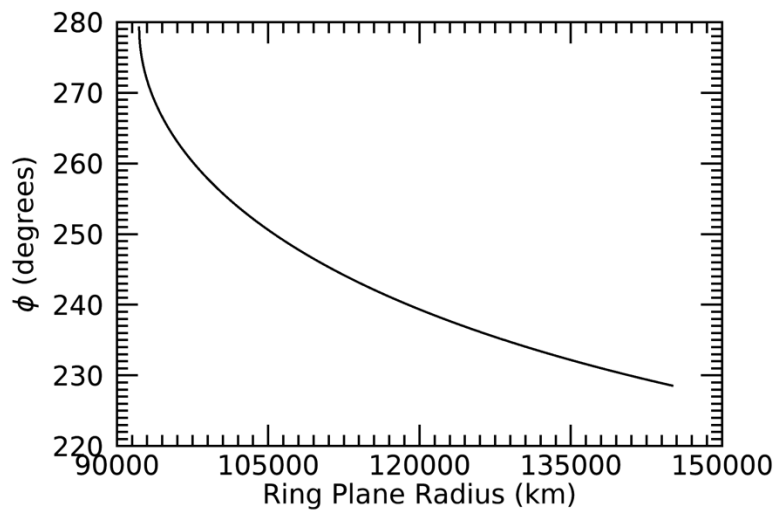
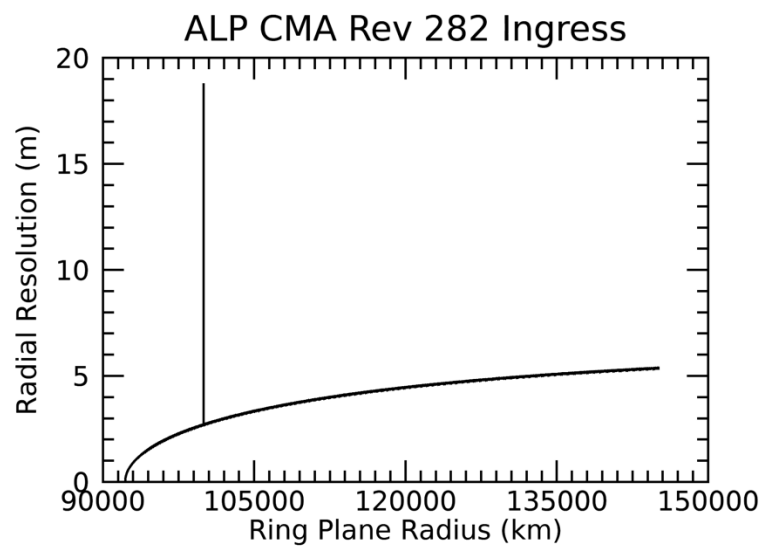
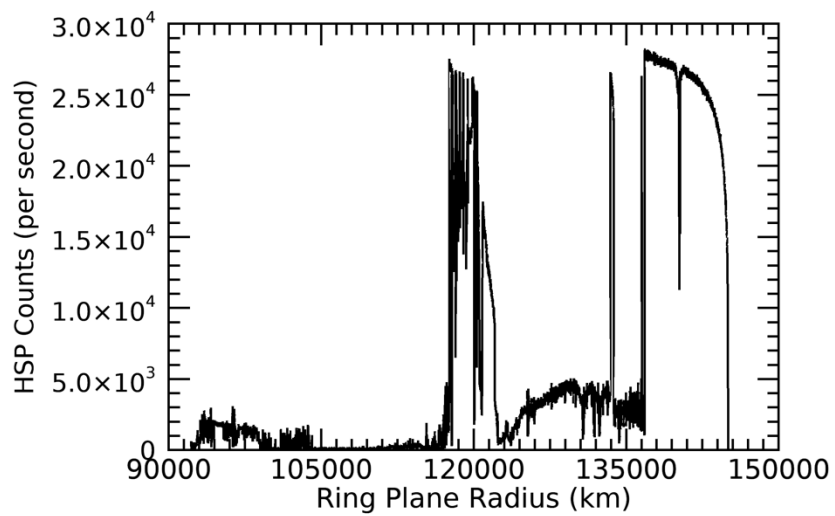
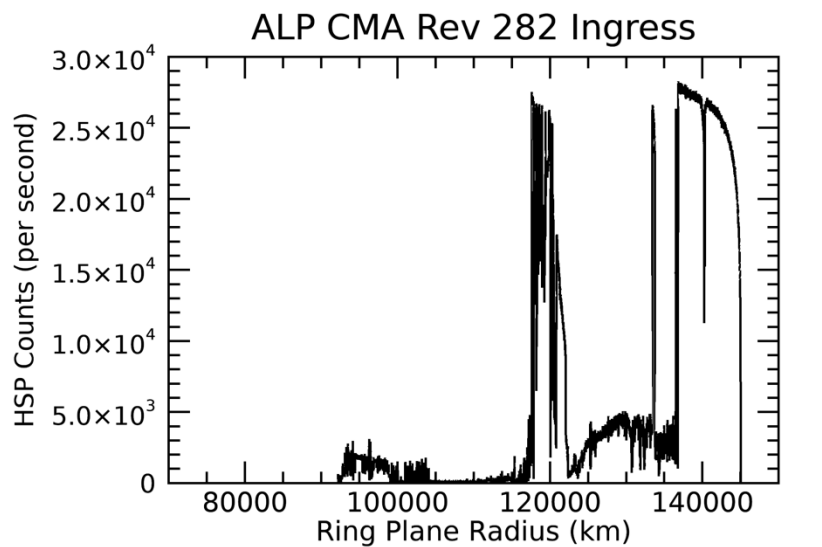
Subsolar lat/lon: 22.28, -128.19

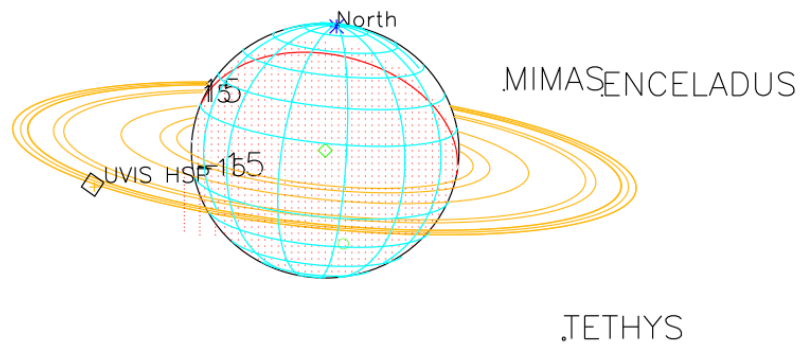
Sub-s/c lat/lon: 3.37, 55.61





2017-184T01:30:00.000 1271189.6 km
Target RA/dec: 91.17, -8.85
Subsolar lat/lon: 22.28, 145.67
Sub-s/c lat/lon: 3.88, -30.21



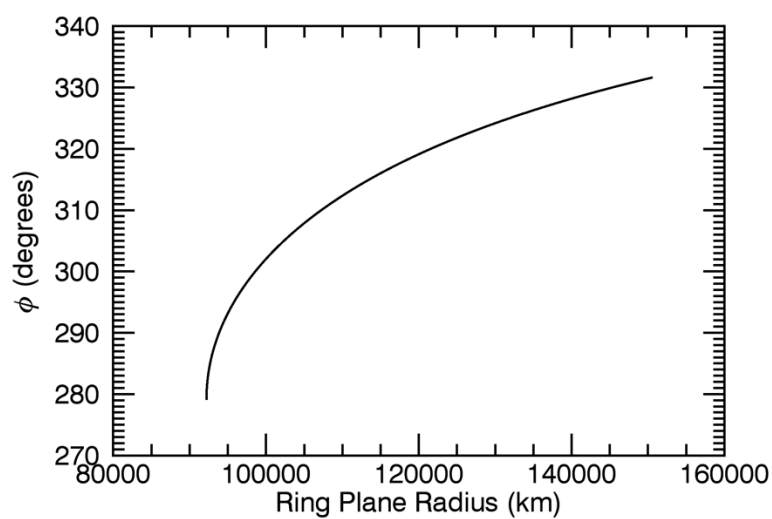
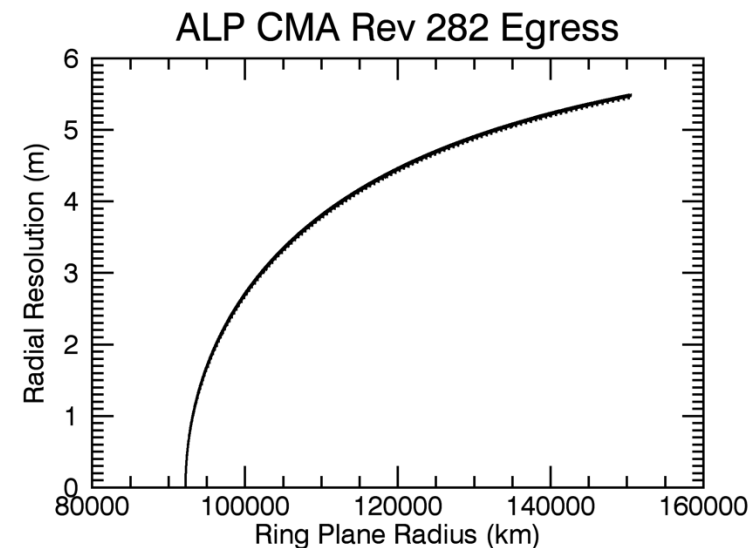
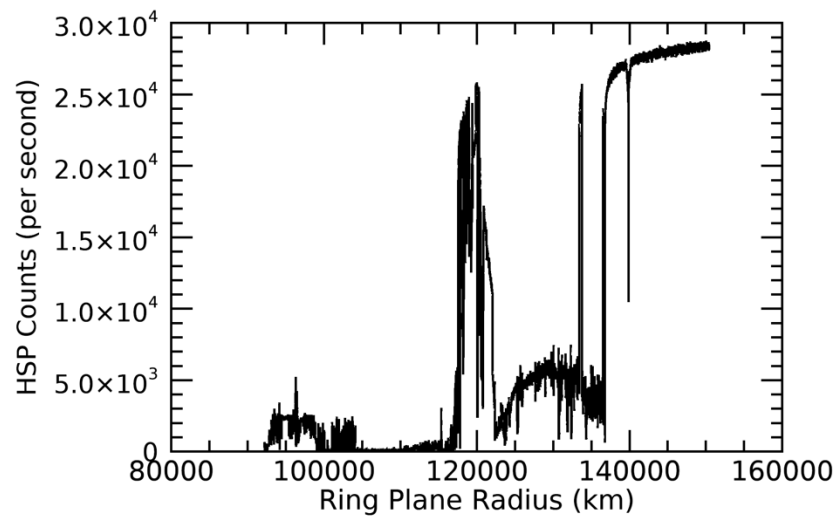
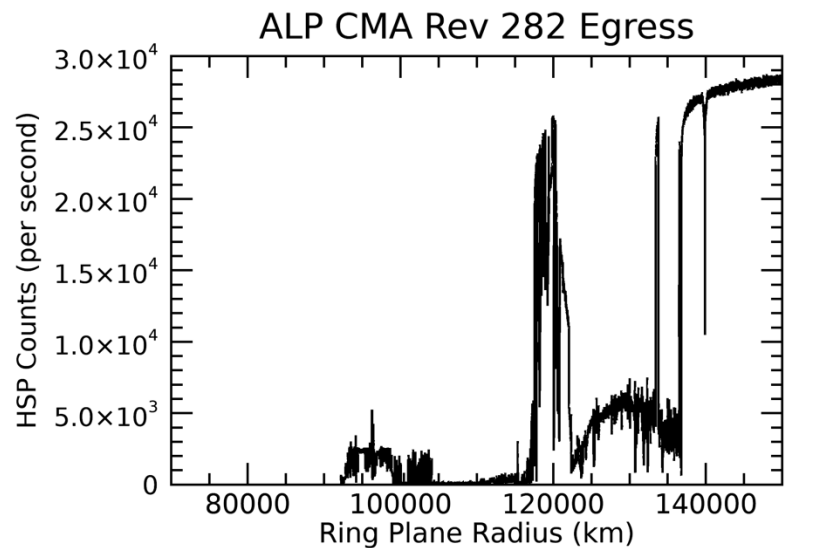


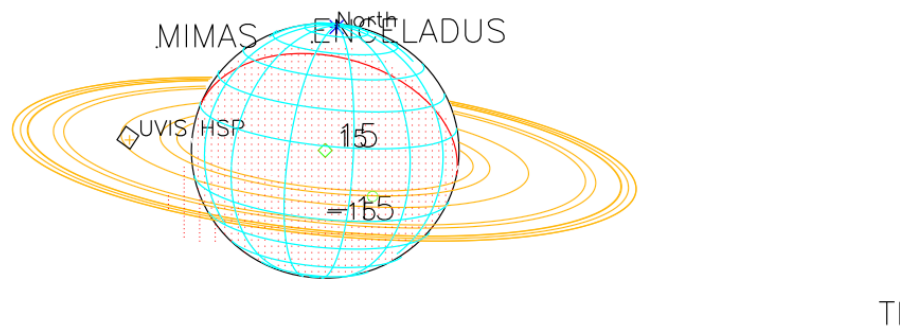
2017-185T08:06:00.000 1195508.1 km

Target RA/dec: 96.09, -16.02

Subsolar lat/lon: 22.28, -168.05

Sub-s/c lat/lon: 10.15, 20.21



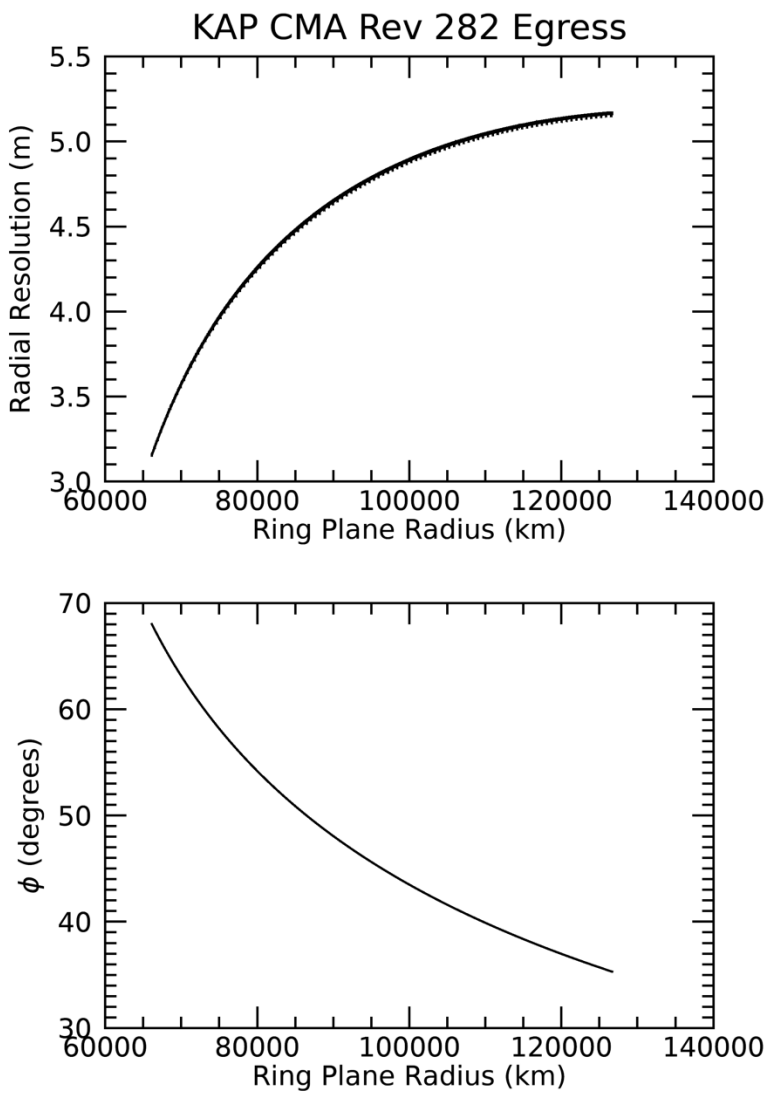
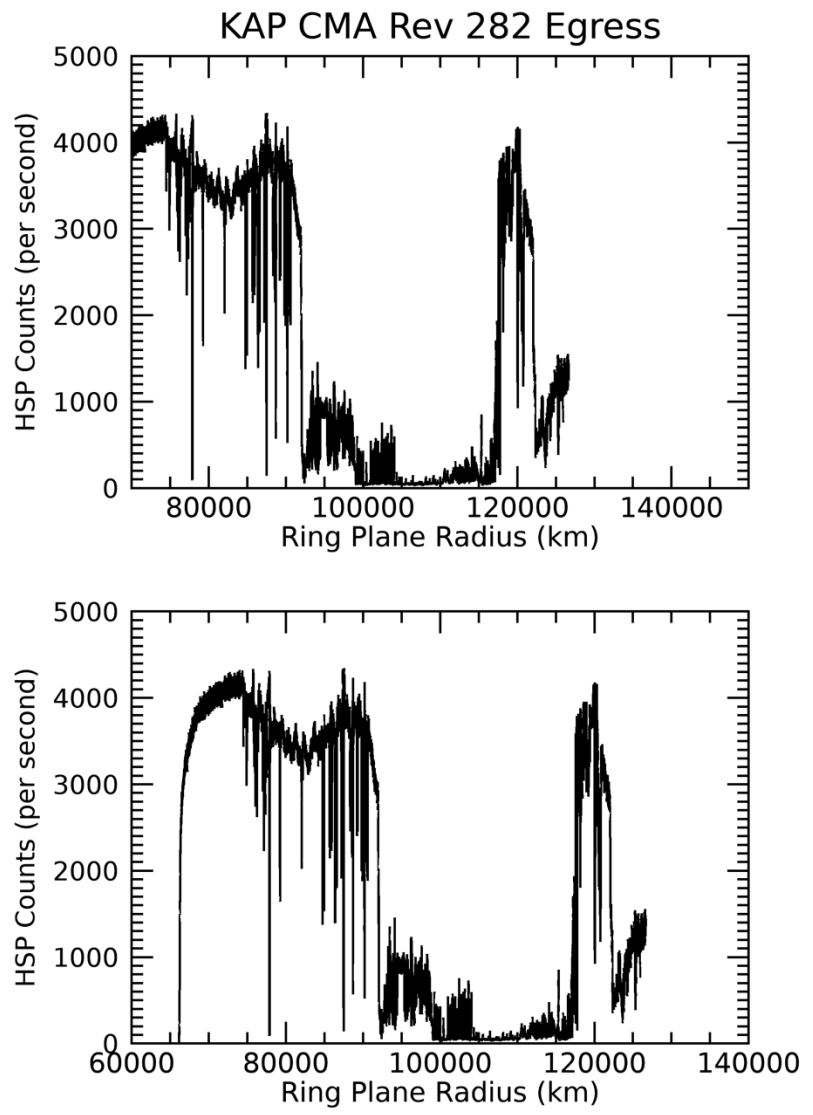


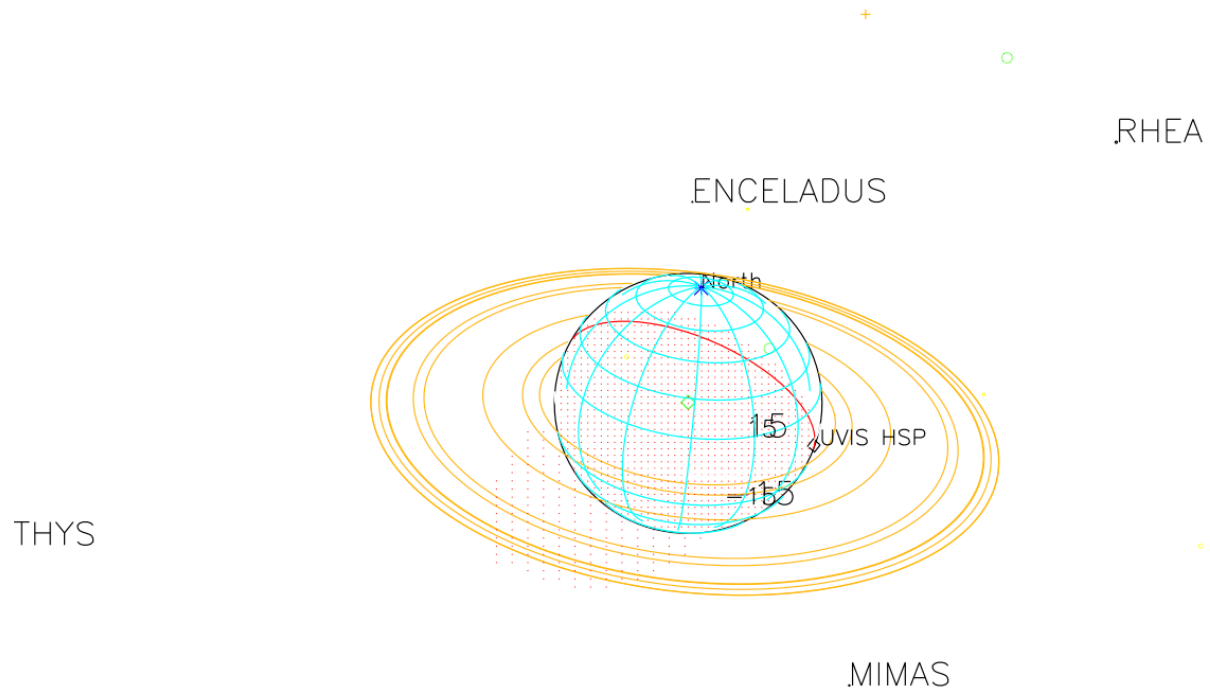
2017-185T11:46:00.000 1168213.8 km

Target RA/dec: 96.78, -16.98

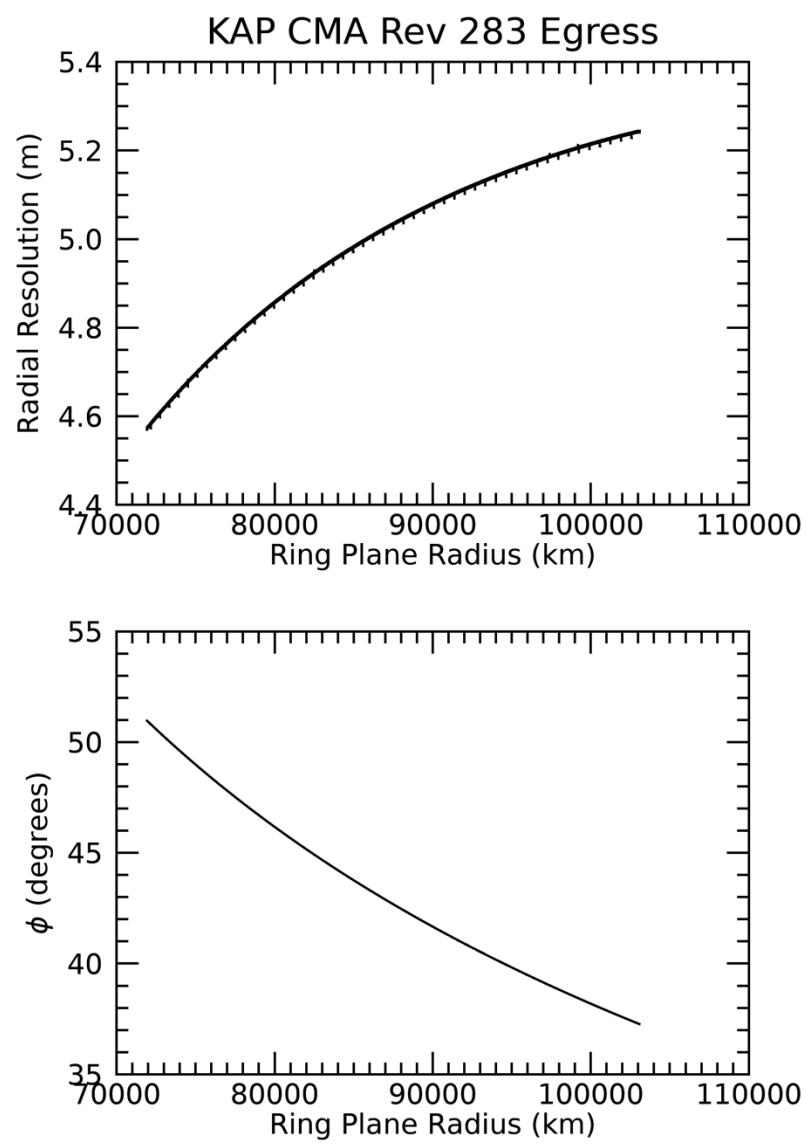
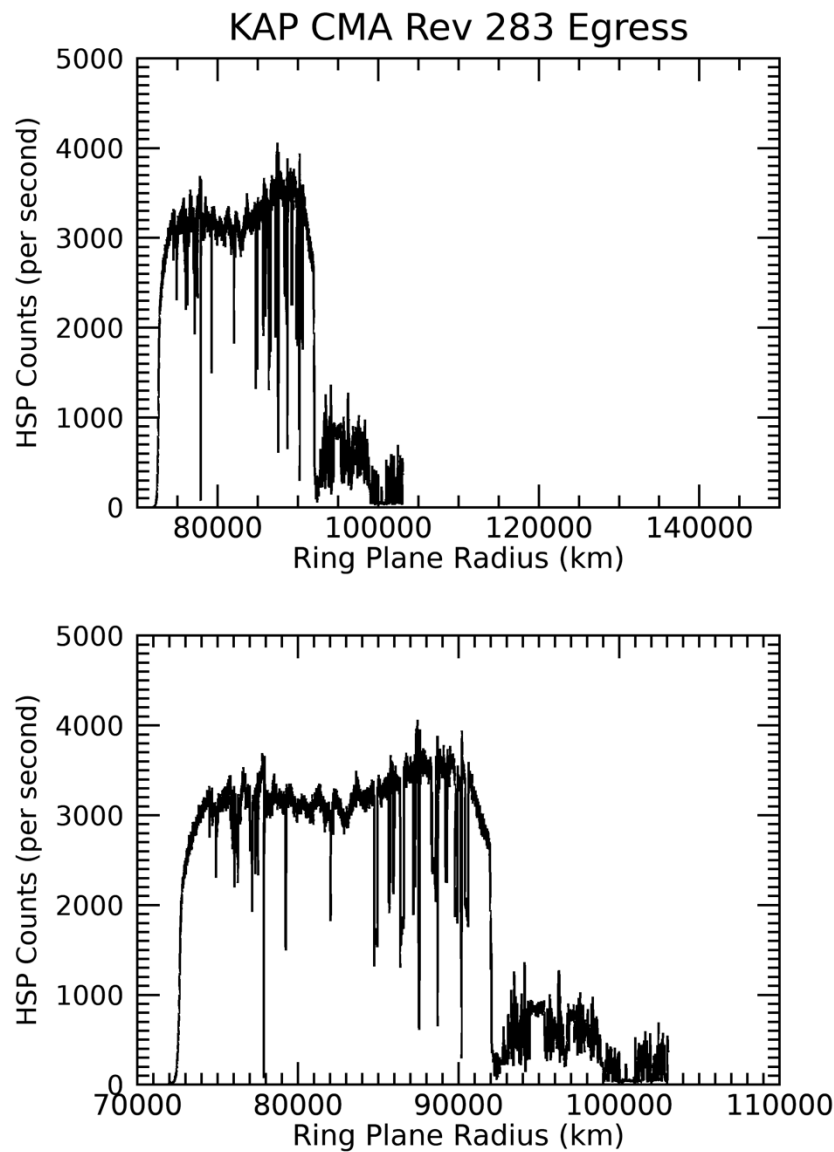
Subsolar lat/lon: 22.28, 68.08

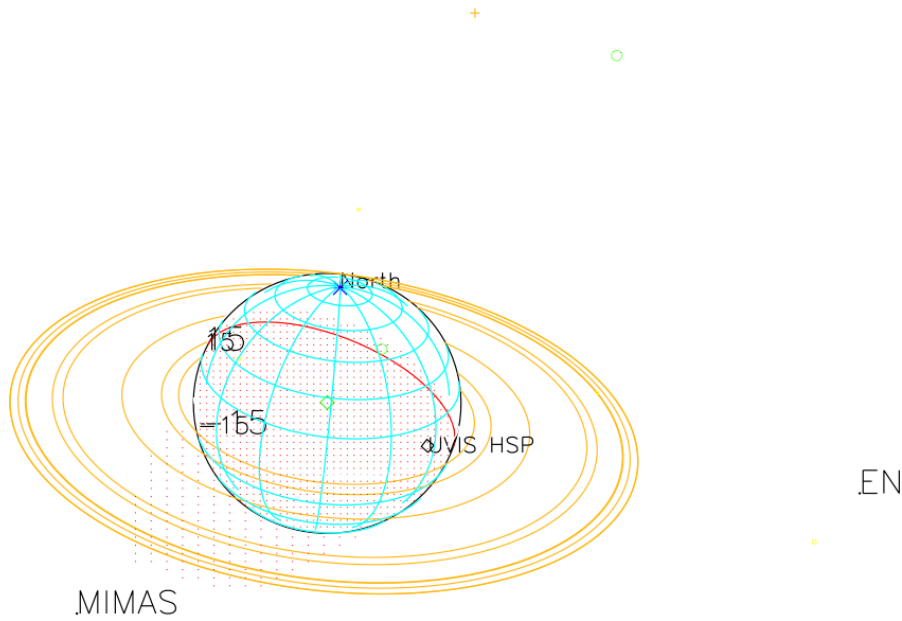
Sub-s/c lat/lon: 11.01, -103.09



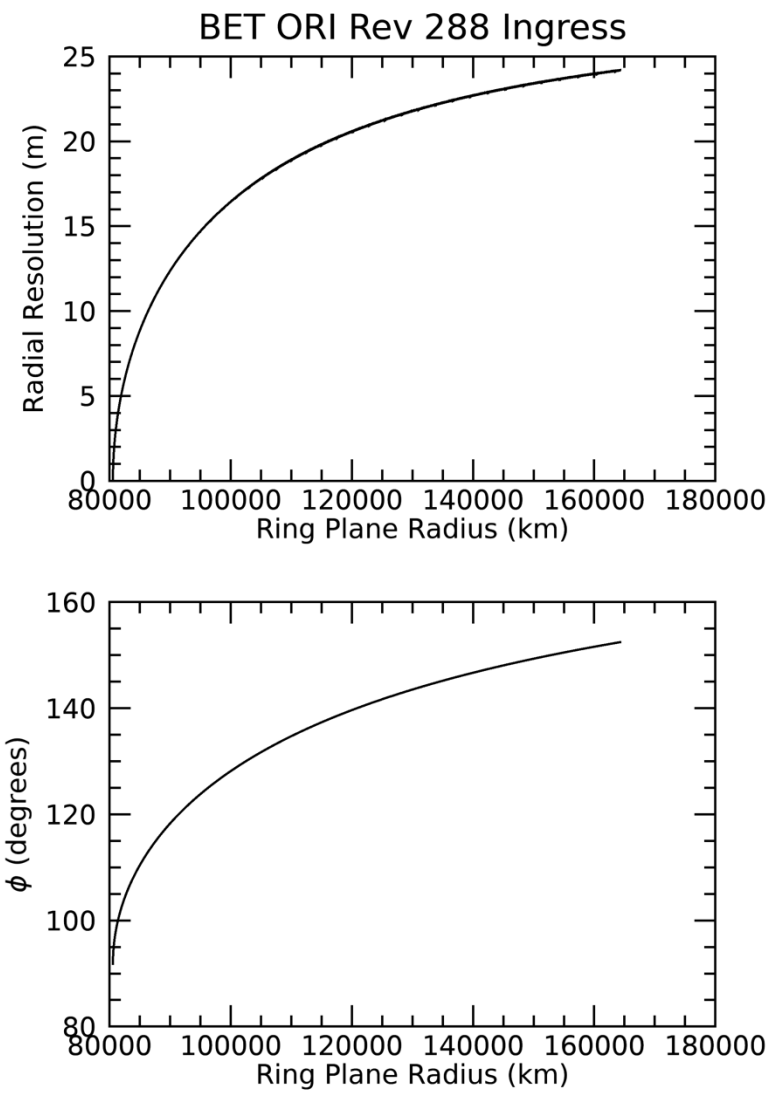
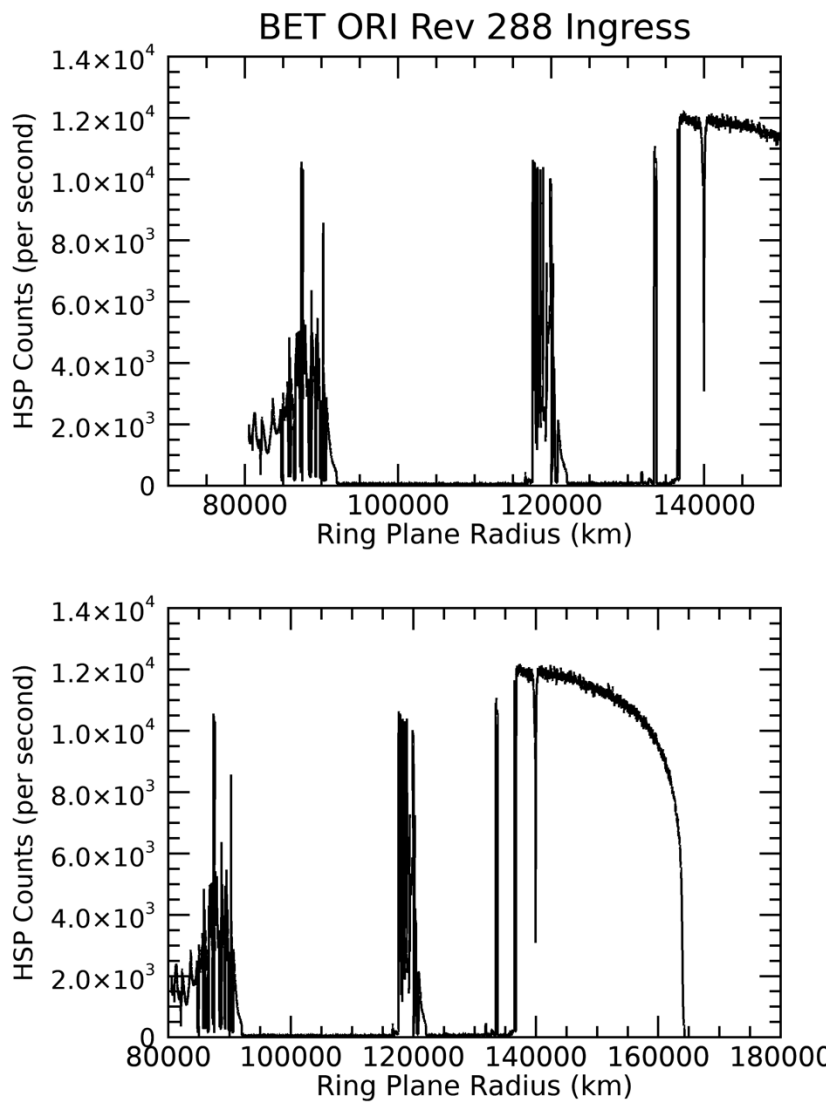


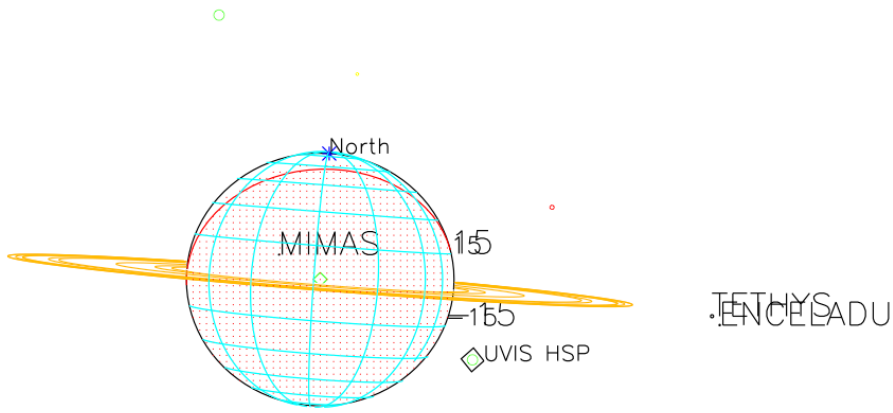
2017-186T21:30:00.000 663457.43 km
Target RA/dec: 108.27, -31.03
Subsolar lat/lon: 22.28, 8.50
Sub-s/c lat/lon: 24.11, -153.16





2017-193T08:50:00.000 666569.86 km
Target RA/dec: 107.08, -30.97
Subsolar lat/lon: 22.28, 161.08
Sub-s/c lat/lon: 23.96, -1.94



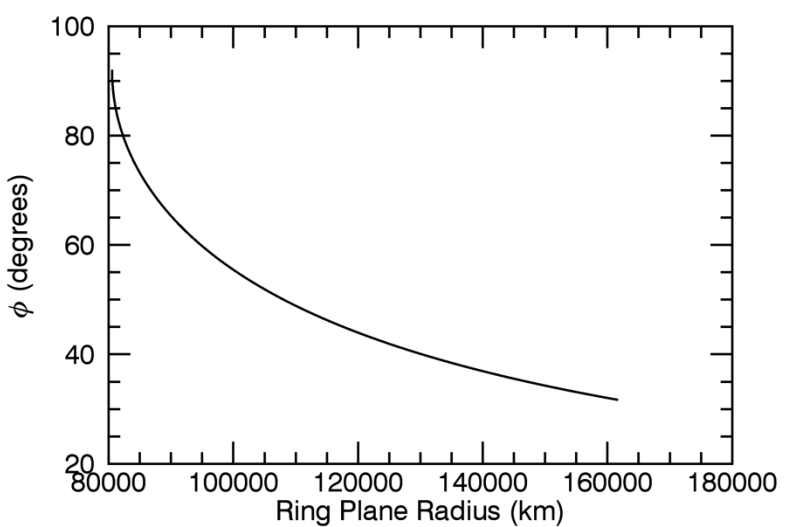
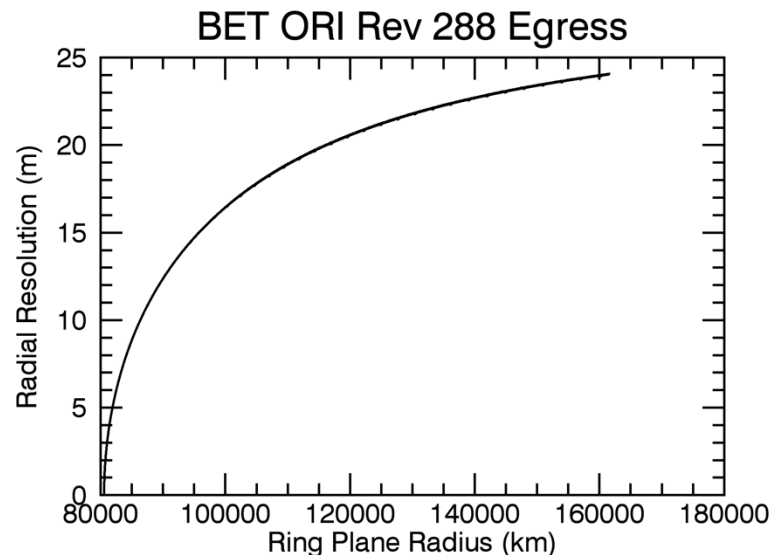
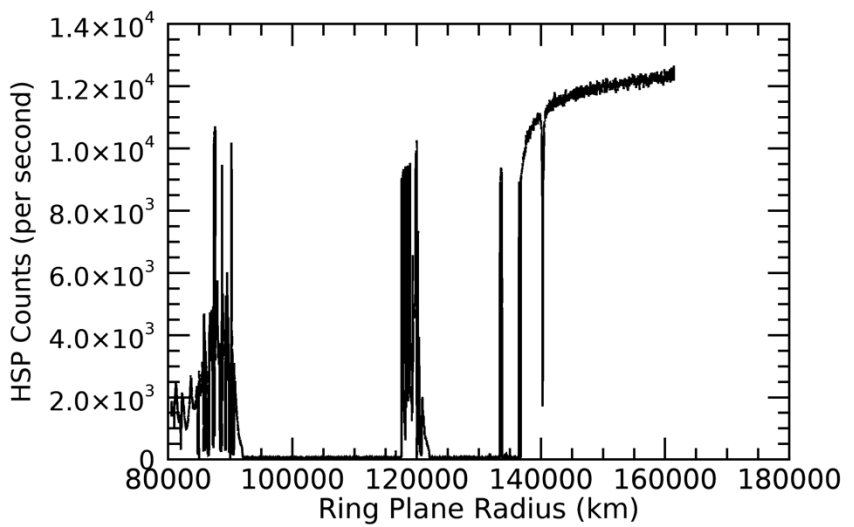
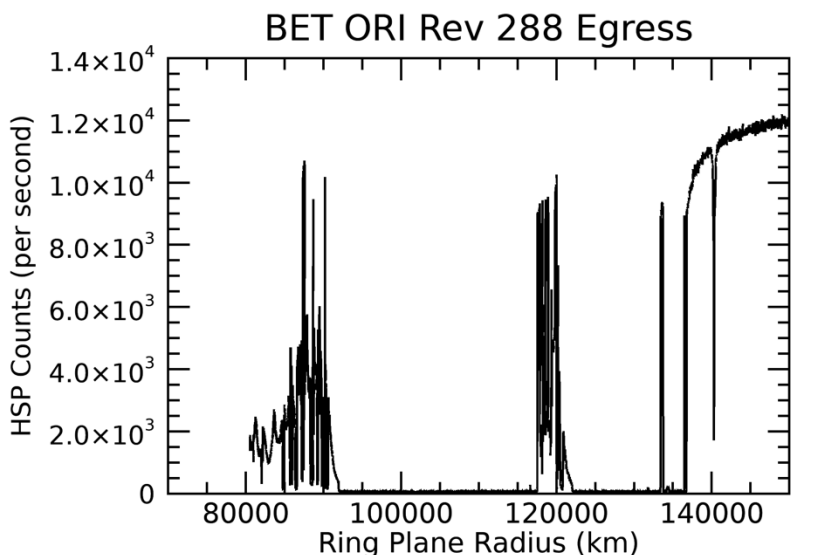


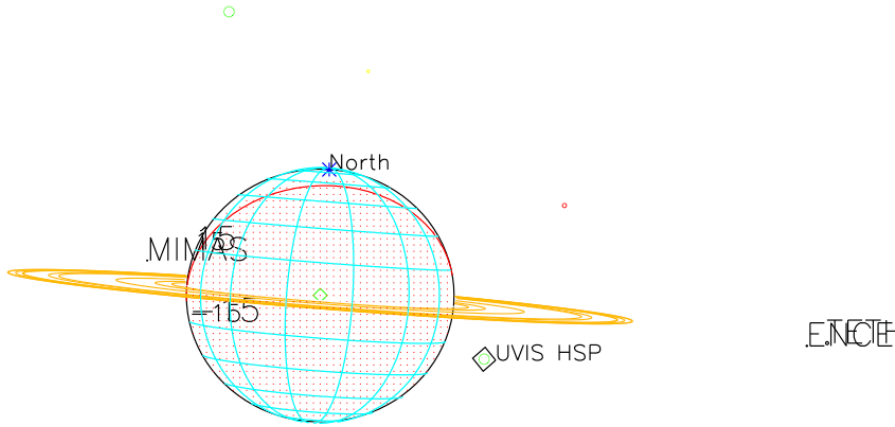
2017-228T17:52:00.000 1212492.1 km

Target RA/dec: 81.91, -6.57

Subsolar lat/lon: 22.26, -80.68

Sub-s/c lat/lon: 1.40, 92.97



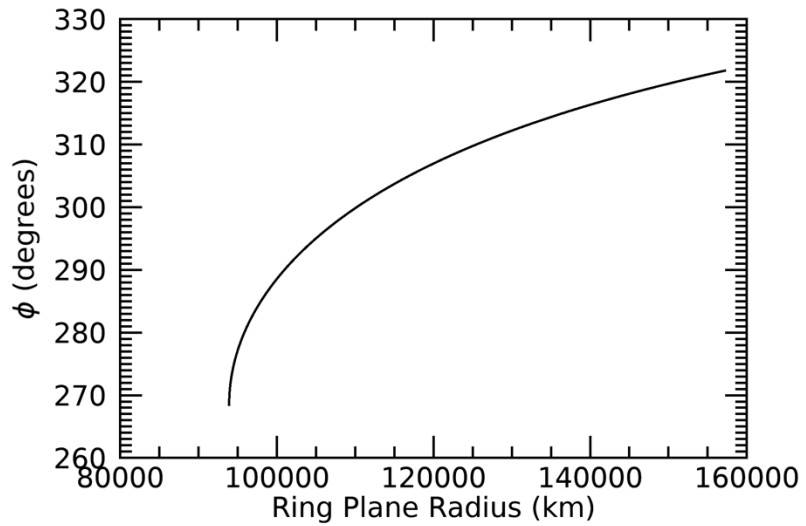
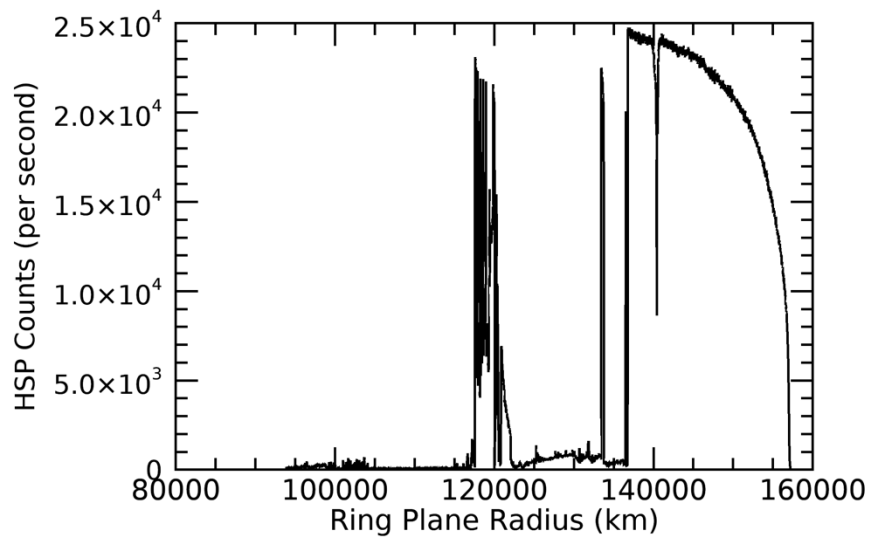
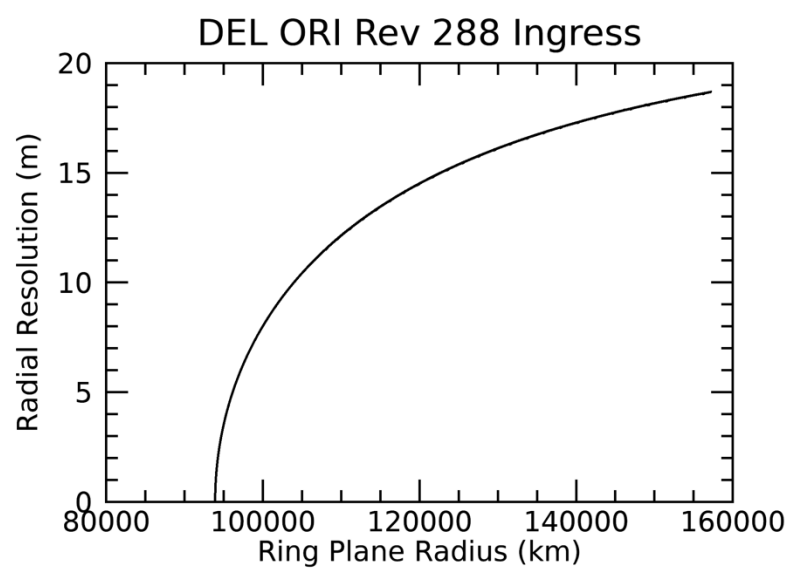
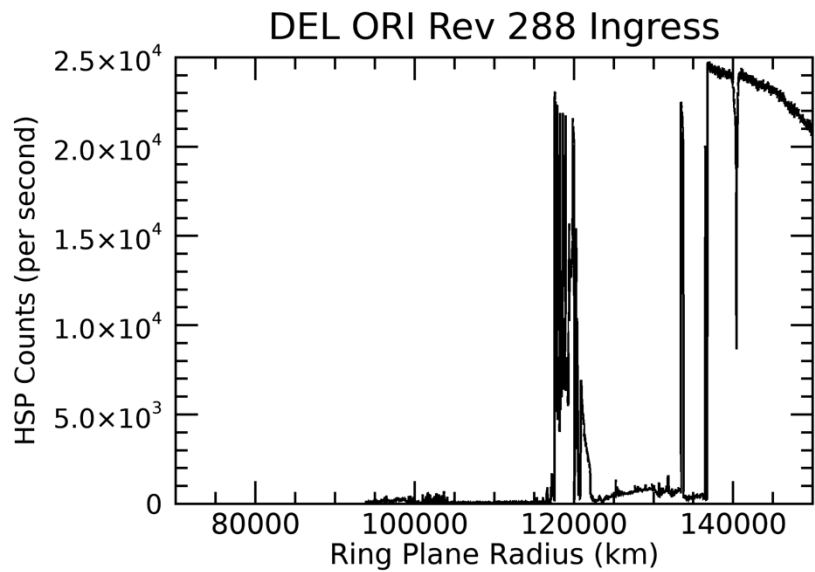


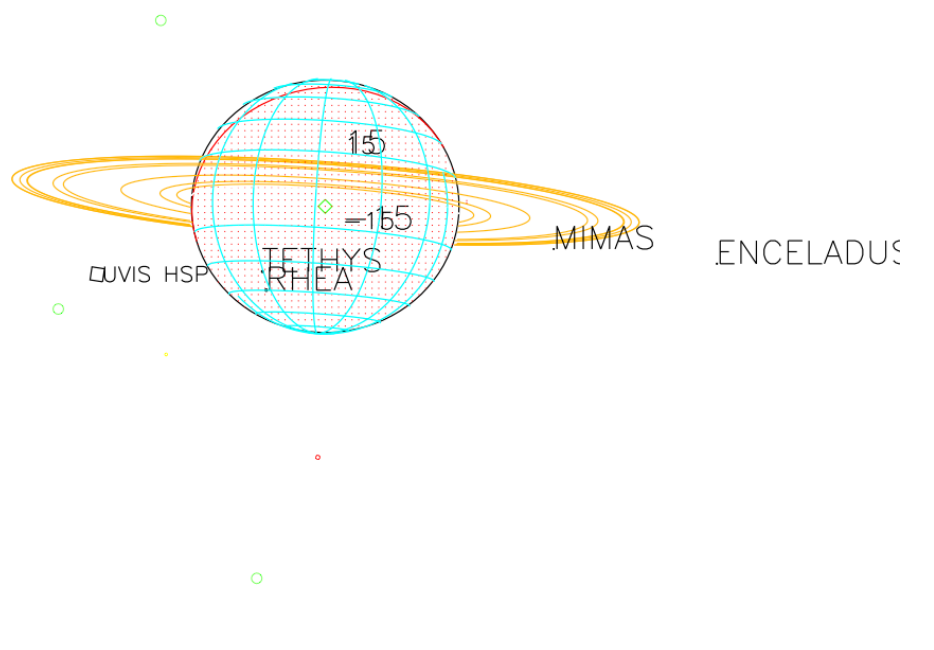
2017-228T19:17:00.000 1220815.4 km

Target RA/dec: 82.13, -6.93

Subsolar lat/lon: 22.26, -128.53

Sub-s/c lat/lon: 1.70, 45.31



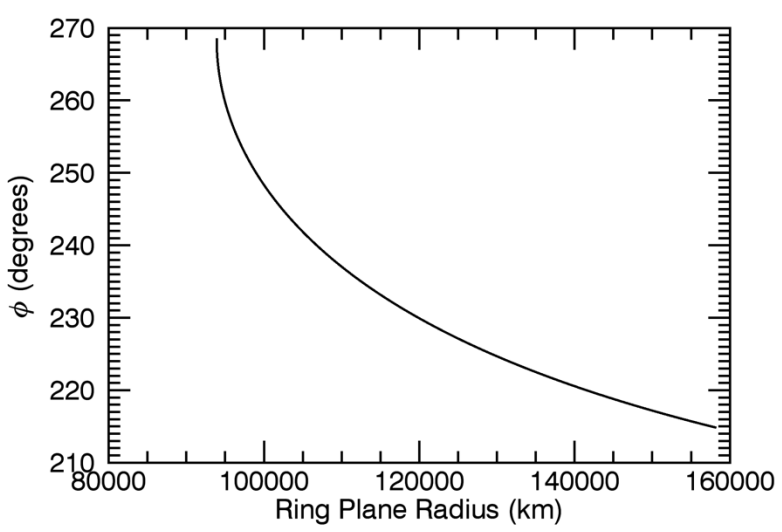
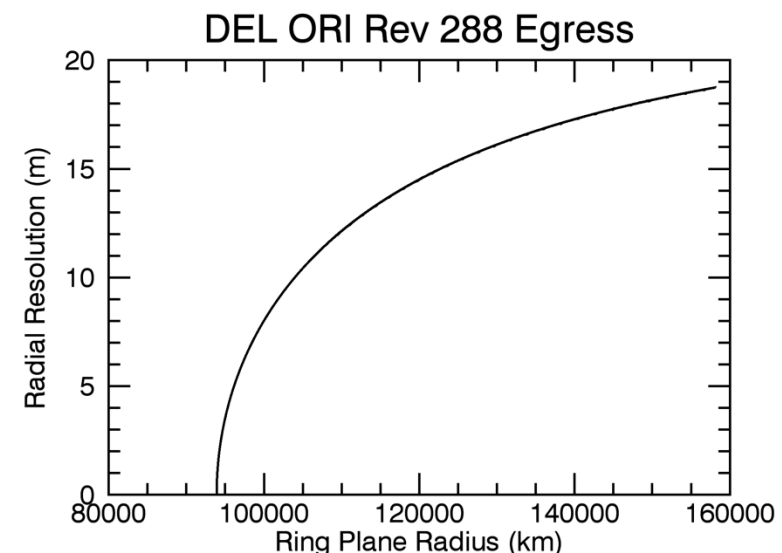
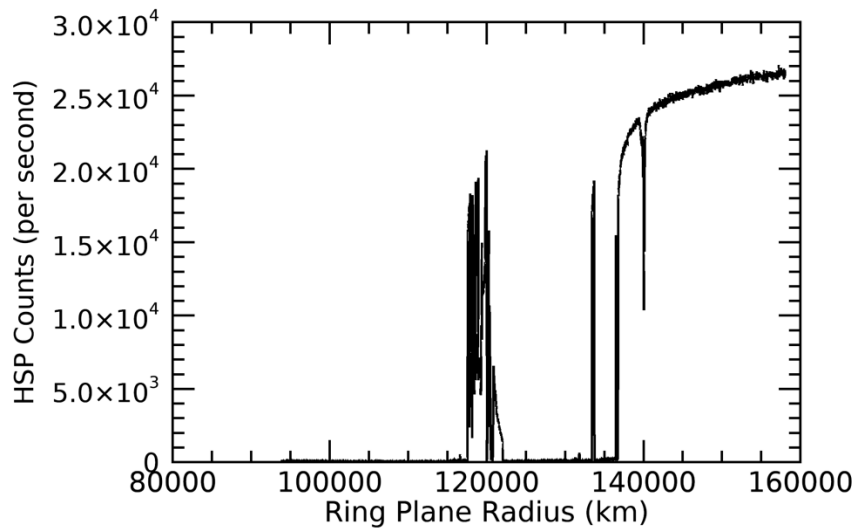
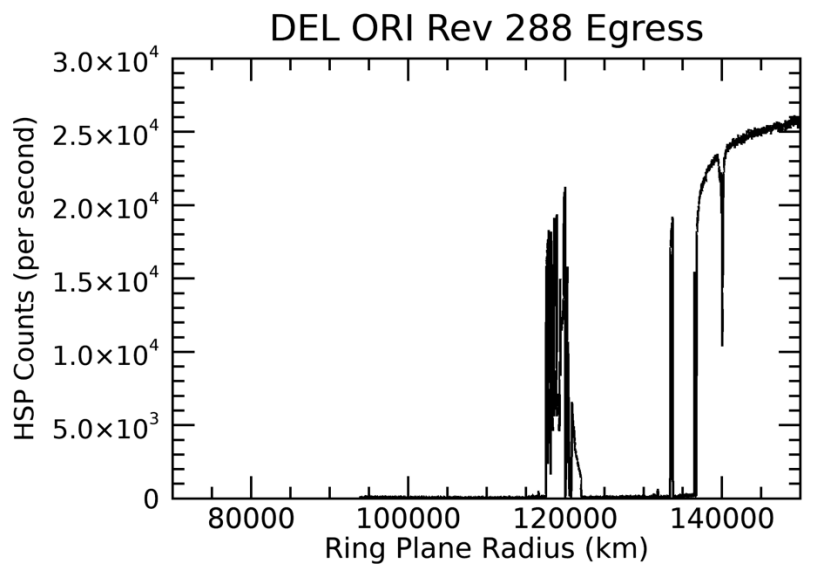


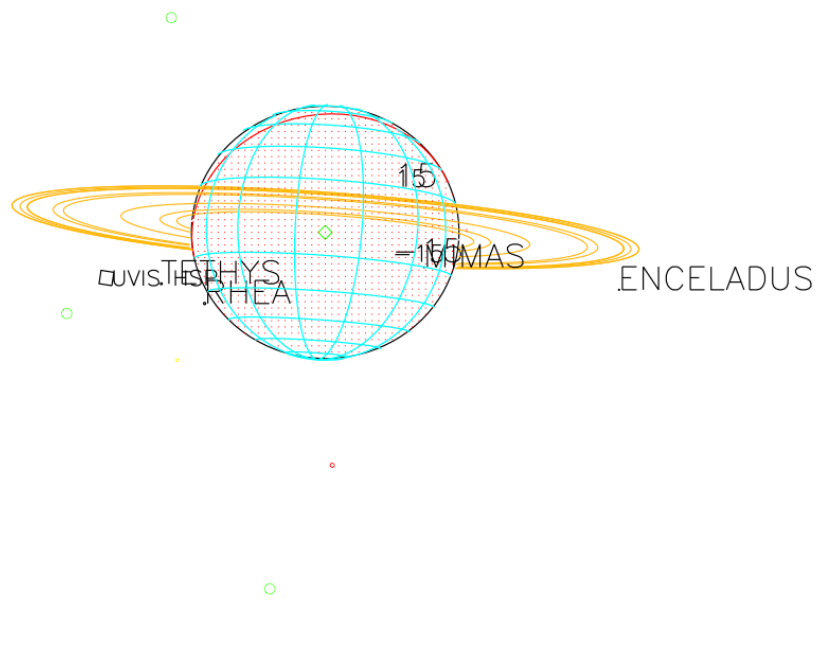
2017-227T15:56:00.000 940067.41 km

Target RA/dec: 76.76, 1.49

Subsolar lat/lon: 22.26, 75.39

Sub-s/c lat/lon: -5.52, -115.50





2017-227T17:27:00.000 963298.40 km

Target RA/dec: 77.15, 0.87

Subsolar lat/lon: 22.26, 24.15

Sub-s/c lat/lon: -4.99, -166.38